DISSERTATION

STATISTICAL PROPERTIES OF DUNE PROFILES

Submitted by

Carl F. Nordin, Jr.

In partial fulfillment of the requirements

for the Degree of Doctor of Philosophy

in Civil Engineering

Colorado State University

Fort Collins, Colorado

February 1968

COLORADO STATE UNIVERSITY

February 16 1968

WE HEREBY RECOMMEND THAT THE DISSERTATION PREPARED UNDER OUR SUPERVISION BY

CARL F. NORDIN, JR.

ENTITLED STATISTICAL PROPERTIES OF DUNE PROFILES

BE ACCEPTED AS FULFILLING THIS PART OF THE REQUIREMENTS FOR THE DEGREE OF DOCTOR OF PHILOSOPHY

Committee on Graduate Work

D. B. Simons
Major Professor

M. M. Siddiqui

E. V. Richardson

Scott Creely

J. Crawford
Head of Department

Examination Satisfactory

Committee on Final Examination

E. V. Richardson

M. M. Siddiqui

William F. Schulz

Scott Creely

B. F. Dilligaff

D. B. Simons
Chairman

Permission to publish this dissertation or any part of it must be obtained from the Dean of the Graduate School.

ABSTRACT OF DISSERTATION

STATISTICAL PROPERTIES OF DUNE PROFILES

Properties of sand waves formed by subcritical unidirectional water currents are investigated by statistical analyses of records of streambed profiles. Records of bed elevation y as a function of distance x along the channel, $y = y(x)$, and time records at a fixed point of the channel, $y = y(t)$, were collected in three laboratory flumes that were 8 inches, 2 ft and 8 ft wide and in a straight alluvial channel that was 55 ft wide. For all cases, the bed material was fine sand. The continuous analogue records were converted to discrete data points and were analyzed by digital computer.

The analyses show that both types of records, $y(x)$ and $y(t)$, can be approximately represented as stationary Gaussian processes. When the data are standardized and the length or distance are expressed as ratios of the mean duration between zero-crossings of y, the statistical properties of all the flume data are similar, with no distinguishing characteristics that can be attributed to size of flume or to whether the bed forms were ripples or dunes. The field data, however, reflect the influence of large alternate bars that were not present in the flumes.

The Gaussian assumption, together with the spectral properties of the records as expressed by a dimensionless parameter, δ, permit predicting the distributions of maximum and minimum

values of y between successive zeros of y. These distributions represent the probability distributions of the depth of local scour and fill due to the formation and migration of sand waves, and the parameters that specify the distributions relate approximately to flow velocity and depth.

Observed values of the number of zero and h-level crossings, the mean duration between zero crossings, and the mean duration of upward excursions of the process y(t) above the fixed level h compared reasonably well with theoretical values for the Gaussian model. The distribution of the duration of upward excursions is the conditional probability distribution of the rest period of a particle, given that it is deposited on the downstream face of a ripple or dune at the level h. Observed distributions of these durations can be approximated by a gamma distribution with parameters that relate to h, where h is measured in units of standard deviation from the mean bed level. These distributions and other probability distributions that enter into stochastic models of sediment transport can be determined either from the theoretical model or empirically from the observed data. The results of the study show that even though the bed elevation deviates somewhat from the postulated normal distribution, reasonable estimates of many properties of the bed profiles can be derived from fairly simple statistical models.

Carl F. Nordin, Jr.
Civil Engineering Department
Colorado State University
Fort Collins, Colorado

ACKNOWLEDGMENTS

The writer expresses his appreciation for the counsel and encouragement of his major professor, Dr. D. B. Simons, and of his committee members, Dr. E. V. Richardson, Dr. E. J. Plate, Dr. M. M. Siddiqui and Dr. S. Creely.

Special thanks are due J. K. Culbertson, R. E. Rathbun, and H. P. Guy, U.S. Geological Survey, and T. Yang, Colorado State University, for permitting use of their unpublished data, and to W. W. Sayre and I. Rodriguez-Iturbe for many useful suggestions and stimulating discussions.

Dr. V. M. Yevjevich assisted in the initial planning of this work, and Mrs. Lois Niemann did the programing and computing. The entire study was a part of the U.S. Geological Survey Water Resources Division research program on mechanics of flow and sediment transport in alluvial channels.

TABLE OF CONTENTS

LIST OF TABLES

LIST OF FIGURES

LIST OF SYMBOLS

Symbol	Definition	Units
$A(\omega)$	Gain function	0
a	Dune amplitude, the maximum ordinate of y between zero crossings	0
c	Wave celerity	ft/min
$c(\omega)$	Co-spectrum	0
D	Mean flow depth	ft
E	Expected value	0
F	Froude number	0
f	Frequency number	cycles/unit time
f'	Dimensionless frequency	0
$G_{yy}(\omega)$	Spectral density function	$\left(\text{cycles/unit time}\right)^{-1}$
$G_{yz}(\omega)$	Cross spectrum	$\left(\text{cycles/unit time}\right)^{-1}$
G(x)	Spectral density function for the process y = y(x)	$\left(\text{cycles/unit time}\right)^{-1}$
G(t)	Spectral density function for the process y = y(t)	$\left(\text{cycles/unit time}\right)^{-1}$
G'	Dimensionless spectra	0
g	Acceleration due to gravity	ft/sec^2
h	A fixed level of the bed, measured in units of standard deviation of y from the mean bed level	0
H	Dune height, from crest to trough	ft

Symbol	Definition	Units
$H(\omega)$	Frequency response function	0
ℓ_h^+	Duration or length of the upward excursion of the process y above the fixed level h	min or ft
L	Dune length, from trough to trough	ft
m_n	The n^{th} moment of the spectrum	0
N_o	Number of zero crossings	0
N_h	Number of h-level crossings	0
P	Probability distribution function	0
p	Probability density function	0
$q(\omega)$	Quadrature spectrum	0
s	A time or distance lag	min or ft
t	Time	minutes
T	Wave period	minutes
V	Mean flow velocity	ft/sec
x	Distance along channel in flow direction	ft
y	Bed elevation, measured from y = 0	ft
α	Height of local maximum of y(t)	ft
$\gamma^2_{yz}(\omega)$	Coherence function	0
δ^2	A parameter	0
ε	Wave number	cycles/ft
ε'	Dimensionless wave number	0

Symbol	Definition	Page
η	A dimensionless wave height	0
$\Theta(\omega)$	Phase angle	0
μ	Mean number of upcrossings per unit time	$(\text{min})^{-1}$
$\rho_{yy}(s)$	Autocorrelation function	0
$\rho_{yz}(s)$	Cross-correlation function	0
σ^2_y	Variance of the process y	ft^2
$\phi_{yy}(s)$	Covariance function	0
$\phi_{yz}(s)$	Cross-covariance function	0
ω	Angular frequency, $\omega = 2\pi f$	radians/unit time

Chapter I

INTRODUCTION

Background

A distinguishing characteristic of sand waves formed by unidirectional subcritical water currents is their tendency to form "en echelon" with gently sloping upstream faces and more steeply sloping downstream faces that meet the horizontal at approximately the natural repose angle of the sand. These features migrate slowly in the mean flow direction as material is eroded from their upstream faces and deposited on their downstream faces.

Generally, these features are described as simple triangular forms, in profile, somewhat as sketched in Figure 1, with a mean length from crest to crest or trough to trough, $\overline{L}$, a mean height from crest to trough, $\overline{H}$, and a constant angle of downstream face, β. If the waves are long-crested, or two-dimensional, their geometric properties then are considered completely specified by $\overline{L}$, $\overline{H}$, β. The ratio of mean length to mean height, $\overline{L}/\overline{H}$, called the ripple index, is a measure of the wave steepness.

In reality, the sample wave forms of Figure 1 rarely exist. Long-crested sand waves occur apparently only under rather restricted flow conditions which will not be considered here. In the general

case of flow in a wide channel with a bed of fine sand, the ripples and dunes that form are three-dimensional and highly irregular in size, shape and spacing.

The three-dimensional properties of these features are completely described by a contour map of the bed, and with modern sounding, navigation and computing equipment, large areas of a streambed can be mapped with ease and dispatch. However, the expense involved in obtaining detailed contour maps is prohibitive for most practical cases, and more generally, one has available only profiles of the streambed, obtained either by sounding along the channel from a boat or by sounding at some fixed point in the flow and recording changes in the bed elevation as the dunes and other bed features migrate past the sounding point.

Although the profiles give only a two-dimensional picture of the streambed, they still provide a great amount of useful information. From longitudinal records, one can determine directly the distributions of lengths and heights associated with a particular ensemble of wave forms. From time records, the average wave period is easily found, which, together with mean wave height, provides a very good estimate of the bed load transport (Simons and others, 1965). The distribution of troughs and crests indicates the amount of local scour and fill associated with the migrating sand waves; information that may be important in such practical

problems as designing and maintaining navigation channels or in estimating the depth to which a structure such as a pipeline or siphon should be buried beneath the mean bed level to minimize the probability of local scour exposing the structure to the current.

From a comparison of the properties of different streambed profiles, it may be possible to establish whether or not there are any essential differences, other than scale, between ripples and dunes, and whether or not there are statistical properties of the dune profiles other than scale that can be attributed to the size of the channel. Both questions have important implications in modeling alluvial channel processes.

Perhaps the potentially most useful information to be derived from streambed profiles is information that relates to stochastic models of sediment transport. For example, in their two-dimensional stochastic model for the transport and dispersion of bed-material sediment particles, Sayre and Conover (1967) require the probability that a sediment particle will be deposited at a given level in the bed and the conditional probability for the length of time a particle will remain buried in the bed (i.e., that it will experience a rest period of a certain duration), given that it is deposited at a particular level. These probabilities, together with some other distributions of interest, are easily found from the bed profiles.

To be more specific, consider the short segment of profile sketched in Figure 2. Assume a straight, uniform channel with equilibrium flow conditions, as defined by Simons and Richardson (1966, p. J3). If y is the bed elevation, measured from the mean bed level so that $\bar{y} = 0$, and x is distance along the channel in the direction of flow, the bed profile then can be represented in the form $y = y(x,t)$, $x \epsilon X$, $t \epsilon T$. At any given position $x = x_0$ along the channel, one may record the change with time of bed elevation y to produce the record, $y = y(t)$. Similarly, at any given instant of time, $t = t_0$, one can sound along the channel to obtain a record of the bed profile, $y = y(x)$. In reality, of course, it is impossible to obtain instantaneously a longitudinal profile, but practically the time required to obtain a profile is small compared to the time required for a dune to shift appreciably downstream, so the assumption that $y = y(x)$ is quite reasonable.

In either case, $y = y(x)$ or $y = y(t)$, the bed elevation y, measured about the mean bed level, is a random variable that depends on a parameter (t or x) defined on an arbitrary parameter set (T or X, respectively). By definition, then, $y = y(x,t)$ is a stochastic process (Cramer, 1964, p. 137).

In all cases, y is a continuous function; obviously, there can be no discontinuities in the sand bed of a stream. Intuitively, one also would expect that if the mean properties of the flow, of

the sediment and of the sediment transport do not change with time or with distance along the channel, then y will represent a stochastic process which meets the requirements both of stationarity and of ergodicity.

Consider next, in Figure 2, some simple definitions that will be used later. The points where the processes y(x) or y(t) cross the zero axis are zero crossings, and the average distance between successive upcrossings (values of y going from negative to positive) is an average wave length or wave period, somewhat analagous to $\overline{L}$ shown in Figure 1. The maximum ordinate between zero crossings, in absolute values, is defined as the amplitude, (a), and is roughly comparable to one-half the wave height of Figure 1.

Crossings of the level h are defined in a similar manner. Note that the average duration of the upward excursion of the process y(t) above the fixed level h is the average rest period experienced by a particle after it is deposited on the downstream faces of the sand waves at the level h.

The probability that a particle will be deposited at the level h also can be determined from the bed profiles for at least some simple postulated depositional patterns. If a particle is equally likely to be deposited at any place on the bed, the distribution is simply the frequency distribution of the y values. If deposition occurs only on the downstream faces of the ripples

or dunes, the distribution can be determined from the distribution of y values where the process y(x) has a negative slope or y(t) has a positive slope. If nothing is known of the previous history of a particle, that is, if it is equally likely to be found any place in the bed above the lowest point of particle motion, then the probability that it will be found at the level h can be determined approximately as the ratio of the area bounded by the fixed level h and the upward excursions of the process y(x) above h to the total area of the bed profile above the minimum y value.

Many properties of the processes y(x) and y(t) that are of interest can be determined empirically if suitable records of streambed profiles are available. Usually, though, it is difficult to obtain both types of records. In the laboratory, where flows can be controlled, it is possible to obtain long records of y(t), but longitudinal profiles of the process y(x) are limited by the effective length of the flume. On the other hand, in field studies, it may be possible to obtain suitable longitudinal profiles, but the sand waves generally move so slowly that satisfactory samples of the process y(t) cannot be obtained under constant flow conditions. It has not been established that the statistical properties of the processes y(x) and y(t) are comparable, although some similarities have been noted (Nordin and Algert, 1966). Thus, it is extremely important to determine in

what respects the two types of records are similar and to develop methods of correlating the properties of the two types of records.

Ultimately, of course, one will wish to predict something about the streambed profiles, given only information on the characteristics of the flow and the bed sediment. In order to do this, it is necessary first to determine if there are any consistent or recognizable patterns in the properties of interest, and then to attempt to relate these properties to flow and sediment parameters.

There is little theoretical or empirical basis upon which to postulate the statistical properties of $y(x)$ or $y(t)$. However, during the course of preliminary studies of the bed profiles, several facts emerged that led to the approach adopted for this investigation. First, it was noted that the y values were distributed about their mean values approximately as normal distributions, which was to be expected as most natural processes that develop under the influence of many random factors exhibit approximate Gaussian distributions. Second, many of the properties of a Gaussian process with known covariance functions are well established, particularly the mean values of duration between zero and h-level crossings and the maximum between zero crossings, from previous work on the statistical properties of random noise (Rice, 1954) and on ocean waves (Longuet-Higgins, 1958, 1962, 1963). Finally, it has been shown that properties of the covariance function near the

origin relate to a simple flow parameter, at least for a limited range of flow conditions (Nordin and Algert, 1966), so in looking to the prediction problem, the assumption of a known covariance function may be rather simple to satisfy.

Therefore, the approach adopted for this study was to compare the observed properties of the bed profiles with the theoretical properties of a Gaussian process of known covariance function. In the following section, the scope and specific objectives of the study are given in more detail.

Purpose and Scope

In broad terms, this study was designed to investigate the statistical properties of streambed profiles. Data were collected both in laboratory and in field investigations, and in all cases, attention was restricted to equilibrium flow over a bed of fine sand in a straight uniform channel with either a ripple or dune bed configuration. The classification of bed configurations as either ripples or dunes is according to Simons and Richardson (1966, p. J5-J7). Details of the hydraulic and sediment data are given in a later section.

Specifically, we are interested in the mean values and the distributions of the durations between zero and h-level crossings, of the durations of upward excursions of the process y(t) above the fixed level h, and of the positive and negative maximums of y(x)

or y(t) between zero crossings. In addition, it is of interest to consider whether or not the statistical properties of y(x) and y(t) are similar, whether or not there are any significant differences other than scale in the statistical properties of ripple and dune profiles, and whether or not or to what extent the statistical properties of dune profiles depend on the scale of the flow system.

Particular attention is paid to the spectral representations of the process y because the distributions of the amplitudes (a) for a Gaussian process depend to a large extent on the properties of the spectra (Cartwright and Longuet-Higgins, 1956). Some applications of cross-correlation and of cross-spectral analysis are examined briefly.

As indicated above, the approach used in this study is to compare the observed properties of the bed profiles to the theoretical properties of a Gaussian process of known covariance function. Similarities and differences between the observed and the theoretical processes are noted, and some of the statistical parameters that describe the observed processes are related empirically to properties of the flow.

In the following chapter, a review of the properties of a Gaussian process is given, and some of the mathematical relations for spectral analysis are listed. Chapter III describes the data and presents the results of the analysis. Chapter IV discusses

the implication of the results, summarizes the conclusions drawn, and lists some recommendations for future research along these same lines.

Chapter II

SOME PROPERTIES OF A GAUSSIAN PROCESS

Zero and H-level Crossings

Suppose that $y(t)$ is a real stationary, Gaussian random function of the continuous parameter t, $0 < t < \infty$, with zero mean and covariance function $\phi_{yy}(s)$ and possessing a spectral density function $G_{yy}(\omega)$. The covariance function is the expected value of the lagged product of $y(t)$ and $y(t+s)$

$$\phi_{yy}(s) = E\{y(t)y(t+s)\} \; . \tag{1}$$

The process $y(t)$ is assumed to be ergodic, so the covariance function is given by

$$\phi_{yy}(s) = \lim_{T\to\infty} \frac{1}{T}\int_0^T y(t)\; y(t+s)\; dt \tag{2}$$

which by stationarity is a function only of s.

The covariance function is related to the spectral density function by the equation

$$\phi_{yy}(s) = \int_0^\infty G_{yy}(\omega)\; \text{Cos}\; \omega s d\omega \tag{3}$$

where ω is the angular frequency.

The covariance and spectral density are Fourier transform pairs

$$G_{yy}(\omega) = \frac{2}{\pi} \int_0^\infty \phi_{yy}(s) \cos \omega s \, ds \quad . \tag{4}$$

The variance of y(t) is

$$\text{var } y(t) = \phi_{yy}(0) = \int_0^\infty G_{yy}(\omega) \, d\omega \quad . \tag{5}$$

The first moment of the spectrum about the origin is given by

$$m_1 = \int_0^\infty \omega \, G_{yy}(\omega) \, d\omega \tag{6}$$

and, in general, the r $\frac{\text{th}}{}$ moment, r = 0, 1, 2, ..., is defined as

$$m_r = \int_0^\infty \omega^r \, G_{yy}(\omega) \, d\omega \quad . \tag{7}$$

The mean frequency of the spectrum is then

$$\bar{\omega} = m_1/m_0 \tag{8}$$

and the derivatives of the covariance function at the origin , if they exist, are

$$\begin{aligned} \phi^r(0) &= (-1)^{1/2\,r} \, m_r \quad , \; r \text{ even} \\ &= 0 \quad , \quad r \quad \text{odd} \end{aligned} \quad . \tag{9}$$

Apparently, there is no general solution for determining the probability distribution of the interval between zero crossings, $p\{\ell_0\}$, but its mean value is the reciprocal of the average number of zero crossings per unit time, $E\{N_0\}$, which was given by Rice (1954), as

$$E\{N_0\} = \frac{1}{\pi}\left[\frac{-\phi^{11}(0)}{\phi(0)}\right]^{\frac{1}{2}} \tag{10}$$

The expected number of h-level crossings is

$$E\{N_h\} = \frac{1}{\pi}\exp\{-h^2/2\}\left[\frac{-\phi^{11}(0)}{\phi(0)}\right]^{\frac{1}{2}} \tag{11}$$

The ratio of the average number of h-level crossings to the average number of zero crossings from Equations 10 and 11 is

$$E\{N_h\}/E\{N_0\} = e^{-h^2/2} \quad . \tag{12}$$

The expected duration of an upward excursion above the level h is given by Cramer and Leadbetter (1967),

$$E\{\ell_h^{+}\} = \mu^{-1} \quad pr\{y(0) > h\} \tag{13}$$

where μ is the mean number of upcrossings per unit time and pr denotes probability. The mean number of upcrossings is one-half

the mean number of crossings per unit time, so, combining Equations 10 and 12, the ratio of expected duration of upward excursions above the level h to expected duration of upward excursions above the zero level is

$$E\{\ell_h^+\}/E\{\ell_0^+\} = 2\ \mathrm{pr}\{y(0) > h\}\ e^{h^2/2} . \qquad (14)$$

An interesting alternative to Rice's approach is given by Tick and Shaman (1966) for a straight line interpolation of an underlying continuous Gaussian process determined by sampling the underlying process at equi-spaced intervals. Again, it is assumed that $y(t)$ is a stationary Gaussian process with continuous parameter t, $-\infty < t < \infty$, and with zero mean and covariance function $\phi_{yy}(s)$, and possessing a spectral density function $G_{yy}(\omega)$, defined by Equation 3. Assume that $\phi(0) = 1$ and that $y(t)$ is sampled discretely at the time points $\ldots -2\Delta t, -\Delta t, 0, \Delta t, 2\Delta t, \ldots$. The sampled process also is Gaussian with covariance sequence $\phi(n\Delta t)$, $n = 0, \pm 1, \pm 2, \ldots$. Connecting successively the observed ordinates of the sampled sequence with straight line segments yields the interpolation process mentioned above.

The expected number of zero crossings in a record of length $k\Delta t$ is found to be

$$E\{N_0\} = k\left[\frac{1}{2} - \frac{1}{\pi}\arcsin\ \phi(\Delta t)\right] . \qquad (15)$$

To determine the expected number of h-level crossings, choose two adjacent values, $y(n\Delta t)$ and $y(\{n+1\}\Delta t)$ and denote them by Y_1 and Y_2. The joint distribution of Y_1 and Y_2 is bivariate normal with correlation $\phi(\Delta t)$. Then, the expected number of h-level crossings is

$$E\{N_h\} = k\left[pr(Y_1 > h,\ Y_2 < h) + pr(Y_1 < h,\ Y_2 > h)\right]$$

$$= 2k\left[pr(Y_1 > h,\ Y_2 > \infty) - pr(Y_1 > h,\ Y_2 > h\right] . \quad (16)$$

From Equations 15 and 16, the value of the ratio of the expected number of h-level to the expected number of zero crossings is seen to depend on the covariance function at one lag, $\phi(\Delta t)$. Values were computed for $\phi(\Delta t) = 0.7$ and 0.9, and the curve for $\phi(\Delta t) = 0.7$ is plotted in Figure 3 along with Equation 12 for the continuous process. There is so little difference in the two curves for values of $\phi(\Delta t)$ greater than 0.7 that the simpler expression of Equation 14 is to be preferred.

Although the probability distribution of the ℓ values cannot be precisely determined in the general case, Longuet-Higgins (1962, 1963) gives some approximations for upper and lower bounds of $p\{\ell_0\}$, with particular attention to certain ideal forms of the spectra of $y(t)$, and Cramer and Leadbetter (1967) give equations for the moments of the distribution functions of the duration of upward excursions

above the level h. From a practical point of view, the mean values of ℓ_h^+ are of most interest, and particularly the mean in an interval $h_2 - h_1$, which is the mean rest period of a particle deposited on the downstream face of a sand wave between the elevations h_1 and h_2, and which can be determined easily by integrating Equation 13 between appropriate limits.

Wave Heights and Amplitudes

The wave height H was defined as the difference in elevation between a crest (maximum) and the following trough (minimum) in Figure 1. The statistical distribution of H generally is not known, but for the case where y(t) has a narrow spectrum, it has been established that H/2 is distributed according to a Rayleigh distribution (see Cartwright and Longuet-Higgins, 1956).

$$p(H/2) = \frac{H}{(m_0)^{\frac{1}{2}}} \; e^{-\left(\frac{H}{2}\right)^2 / (m_0)^{\frac{1}{2}}} \tag{17}$$

where m_0, the variance of y(t), is determined by Equation 5 or Equation 7. If the process y has unit variance, the equation simplifies to

$$p(H/2) = He^{-(H/2)^2} \tag{18}$$

and the cumulative probability distribution of H/2 is given by

$$p\left(H/2 \leq \S\right) = 1 - e^{-\S^2} \quad . \tag{19}$$

Although the probability distribution of H is not established, the statistical distribution of the local maxima of y(t) is known. If y(t) is a strictly stationary process possessing a continuous sample derivative y'(t), a local maximum or crest is said to occur at $t = t_0$ if y'(t) has a downcrossing of zero at t (Cramer and Leadbetter, 1967, p. 242). Define α as the difference in height between the crest and the mean level of y(t). Then, for the Gaussian process considered here, the probability distribution of α depends only on $(m_0)^{1/2}$ and on a parameter δ that represents the relative width of the frequency spectrum,

$$\delta^2 = \frac{m_0 m_4 - m_2^2}{m_0\, m_4} \quad , \; 0 < \delta < 1 \quad . \tag{20}$$

For $\delta \to 0$, the spectrum becomes infinitely narrow and the dimensionless maxima, η, tend to a Rayleigh distribution

$$\begin{aligned} p(\eta) &= \eta e^{-\frac{\eta^2}{2}} \quad , \; \eta > 0 \\ &= 0 \qquad\qquad , \; \eta < 0 \quad , \end{aligned} \tag{21}$$

where η is defined by the relation

$$\eta = \alpha/(m_0)^{1/2} \quad . \tag{22}$$

When δ approaches its maximum value of 1, the distribution of η is Gaussian,

$$p(\eta) = \frac{1}{(2\pi)^{1/2}} e^{-\eta^2/2} \quad , \; -\infty < \eta < +\infty \quad . \tag{23}$$

Derivations of the above distributions are given by Rice (1954) and are discussed in detail by Cartwright and Longuet-Higgins (1956). The cumulative probability distributions of η for various values of δ are shown in Figure 4.

In Figure 2, (a) was defined as the maximum y value between zero crossings, and it can assume either positive or negative values. From a practical point of view, it may be advantageous to consider separately the distributions of positive (a+) and negative (a-) values, in the event that y(t) is not symmetric about its mean level. The theoretical Gaussian model is assumed symmetric, so in this case it is permissible to consider only the positive (a) values, keeping in mind the symmetry of the distribution about zero when negative values are of concern.

Clearly, for narrow-band random noise, the distribution of (a+) would approach the distribution of local maxima, the Rayleigh

distribution (see, for example, Bendat and Piersol, 1966, p. 17). For the general case, however, there apparently is no theoretical derivation for the probability distribution of the (a) values. For purposes of this study, therefore, the observed distributions of (a) simply will be compared with the theoretical distributions of local maxima shown in Figure 4. Intuitively, at least, one would expect the (a) values for a process with a broad spectrum to approach a form of the normal distribution, but there is no reason to expect the distribution to depend only on δ and m.

Theory of Time Series Analysis

In the preceding section, the covariance function, $\phi(s)$, or alternatively, the spectral density function, $G(\omega)$, was assumed known. Values of these functions are required to predict mean durations between zero and h-level crossings and to estimate probability distributions of maxima for the Gaussian model. For the actual streambed profiles analyzed in this study, values of $\phi(s)$ and $G(\omega)$ were computed and the observed properties of the profiles were then compared with properties of a Gaussian process having the same covariance and spectral density functions.

Apart from the problem of predicting the zero and h-level crossings, the covariance functions and spectra together with the probability distributions of the y values provide a great deal of

information about the process y(t), and these functions will be found particularly useful in later sections when considering the similarities and the differences of the streambed profiles that can be attributed to scale of the flow system or to channel size. Therefore, it is appropriate at this point to review briefly the theory of time series analysis and to mention some of the properties of the covariance functions and spectral density functions that were found useful in analyzing the dune profiles.

For this purpose, consider y(t) to be a real continuous random function of time t, $-\infty < t < \infty$. The process y(t) is assumed to be stationary and ergodic. Stationarity implies time invariance of the general statistical properties of the process y(t), and ergodicity insures that averages across an ensemble are equivalent to averages over time along a single sample function or realization of infinite extent (for a more detailed discussion of these concepts, see Yaglom, 1962 or Cramer and Leadbetter, 1967).

By stationarity, both the mean value, $\overline{y}$, and the variance, σ^2_y, are constants, so it is always possible to form a new time series, $\left(y(t) - \overline{y}\right)/\sigma_y$, that has zero mean and unit variance. Unless otherwise specified, it will be assumed in the following discussion that this transformation has been made. Then the correlation function, defined as

$$\rho_{yy}(s) = \phi_{yy}(s)/\phi_{yy}(0) \ , \tag{24}$$

is identical to the covariance function.

Both $\phi(s)$ and $G(\omega)$ are even functions of their respective arguments, and the usual equations for these functions are

$$G_{yy}(\omega) = \frac{1}{\pi}\int_0^\infty \phi_{yy}(s)\ e^{-i\omega s}\ ds \tag{25}$$

$$\phi_{yy}(s) = \int_0^\infty G_{yy}(\omega)\ e^{i\omega s}\ d\omega \tag{26}$$

where negative values of both time and frequency are considered. Because $y(t)$ is a real function, the correlation and spectral density functions often are given as a cosine transform pair, Equations 3 and 4, where the G and ϕ values are modified by the necessary constants to apply only to positive t and ω values. Bendat and Piersol (1966, p. 77-84) give a complete discussion of the "one-sided" correlation and spectral density functions that generally are used in practical computations.

The autocovariance function measures the degree of dependence between the observed quantity y at one time and at another time s units later. It is especially useful in defining periodicities in the process $y(t)$.

The power spectrum or spectral density function describes the general frequency composition of the data in terms of the density of its mean square value, that is, $G_{yy}(\omega)d\omega$ represents the contribution to the variance of the process from the frequencies

between ω and $(\omega + d\omega)$. Thus, the spectra show directly similarities and differences in the streambed profiles and provide a quantitative basis for comparing the ripple bed forms with the dune forms or for evaluating the effect of scale on the statistical properties of the streambed profiles.

The treatment is extended to two stochastic processes as follows. The cross correlation between two series $y(t)$ and $z(t)$ is given by

$$\rho_{yz}(s) = \frac{\phi_{yz}(s)}{\sqrt{\phi_{yy}(0)\,\phi_{zz}(0)}} \tag{27}$$

where $\phi_{yz}(s)$ is the cross covariance between the series and is defined as the expected value of the product $y(t)\ z(t+s)$. Both $y(t)$ and $z(t)$ are ergodic, so the cross covariance is

$$\phi_{yz}(s) = E\{y(t)\ z(t+s)\} = \lim_{T\to\infty} \frac{1}{T} \int_{-T/2}^{T/2} y(t)\ z(t+s)\ dt. \tag{28}$$

The cross-spectrum is defined as the Fourier transform of the cross-covariance function

$$G_{yz}(\omega) = \frac{1}{\pi} \int_{-\infty}^{\infty} \phi_{yz}(s)\ e^{-i\omega s}\ ds = c(\omega) + iq(\omega) \tag{29}$$

where ω represents the angular frequency, $c(\omega)$ is the co-spectrum, a measure of the in-phase covariance, and $q(\omega)$ is the quadrature

spectrum, a measure of the out-of-phase covariance. The co-spectrum measures the contributions of oscillations at the lag zero between two time series. The quadrature spectrum measures the contribution of the different harmonics to the total cross covariance between the series when all the harmonics of the series y(t) are delayed by a quarter period but the series z(t) remains unchanged.

The real quantity defined as coherence, $\gamma^2_{yz}(\omega)$, is a direct measure of the square of the correlation of the amplitudes of frequency ω of the processes y(t) and z(t)

$$\gamma^2_{yz}(\omega) = \frac{c^2_{yz}(\omega) + q^2_{yz}(\omega)}{G_y(\omega)\, G_z(\omega)} \quad , \; 0 \leq \gamma(\omega) \leq 1 \tag{30}$$

where $G_y(\omega)$ and $G_z(\omega)$ represent the spectra of y(t) and z(t), respectively.

Even if the amplitudes are fully correlated, it is possible that the corresponding frequency components will have different phases. The phase lag at each frequency is given by

$$\Theta(\omega) = \arctan \frac{q(\omega)}{c(\omega)} \tag{31}$$

where $\Theta(\omega)$ is called the phase function.

Another quantity sometimes useful in cross spectral analysis if the frequency response function, $H(\omega)$, calculated from the

relation

$$H(\omega) = \frac{G_{zy}(\omega)}{G_z(\omega)} = A(\omega)\, e^{i\Theta(\omega)} \quad . \tag{32}$$

The quantity $A(\omega)$ is the gain function or amplitude gain of the system and measures the ratio of the amplitude of the frequency components of the series $y(t)$ and $z(t)$ at each frequency ω.

The cross covariance measures the dependence between two time series at the given lag, s, and for this study, it was applied to investigate the three-dimensional properties of the sand waves, their mean rate of shifting and the time or distance required for the waves effectively to lose their identity. The cross spectral functions, Equations 29-32, were used in conjunction with the cross covariance.

The above theory is presented for a continuous process with the parameter t representing time. The frequency $f = \omega/2\pi$ is then given in cycles per unit time. The parameter t is simply a member of an arbitrarily specified parameter set, and it can be any quantity that permits the set of y or z values to be ordered linearly. If time t is replaced by distance x, the frequency f is replaced by wave number ε and the wave period $T = 1/f$ is replaced by wave length $L = 1/\varepsilon$.

Chapter III

DATA AND ANALYSIS

Basic Data

Profiles from four different channels were selected for these analyses. Table 1 in the Appendix gives a summary of the records. Three of the channels were recirculating laboratory flumes located at the Research Center Hydraulics Laboratory, Colorado State University, Fort Collins, Colorado. The other channel was Atrisco Lateral near Bernalillo, New Mexico, a conveyance channel with a sand bed and with banks stabilized by clay and vegetation. The dimensions of the flumes were: 0.67 ft wide by 30 ft long, 2 ft wide by 60 ft long, and 8 ft wide by 200 ft long. Atrisco Lateral was approximately 55 ft wide, and the profiles were obtained about midway in a straight reach 12,000 feet long. The median diameters of bed material and flow parameters are shown in Table 1.

A total of 54 records representing six different flow conditions were selected for analysis. Runs 1, 2, and 3 were data collected from Atrisco Lateral on three different days, but with similar flows. Records 4 through 19 and 20 through 39 are from the 8 ft flume for two different flow conditions, and

like the field data for the first three runs, the bed configuration was dunes. The records for runs 40-43 are for a ripple bed in the 2 ft flume, and runs 44-47 are for identical flow conditions. Runs 48-51 are for a dune-bed flow in the 2 ft flume, and runs 52-54 are for a ripple bed in the 0.67-ft flume, corresponding to the experiments reported by Rathbun and Guy (1967). Run 54 subsequently was discarded because of suspected errors in the basic data, so analysis eventually was carried out on 53 profiles from the six different flow conditions.

Profiles of the bed elevations were obtained with the sonic depth sounder described by Karaki and others (1961) except for the smallest flume where the profiles were traced on a stripchart from the plastic side-walls of the flume. All data were digitized with an analogue to digital converter at the intervals shown in Table 1. The flume data, runs 4 through 54, were standardized with zero mean and unit variance after removing a straight line trend to account for the possibility that the sand bed in the flume was not parallel to the instrument carriage rails supporting the sonic sounder.

At first, the trend was not removed from the Atrisco Lateral data because the sounder was mounted on a boat at a constant depth below the water surface. However, initial analyses showed some long-term trends in the data, so parts of records from run 2 were selected for trend removal. These shorter records from Atrisco

Lateral are shown as runs 55 through 57 in Table 1 and are discussed in detail in a later section.

Only longitudinal profiles were available for Atrisco Lateral and the smallest flume; for the 2-ft and 8-ft wide flumes, time records, $y = y(t)$ were available along with the longitudinal profiles. All the computations described in this and subsequent sections were accomplished on the CDC 6400 computer at Colorado State University.

For the discrete data used in this study, the values in Equations 25 through 32 were approximated by the estimates presented by Granger and Hatanaka (1964), using the Blackman and Tukey spectral estimates with a Hanning window (Blackman and Tukey, 1958, page 34). Formulas for the digital calculations of the covariance functions and spectra, and some guidelines for estimating the length of record required for the various calculations are given in Appendix III. A detailed discussion of the calculations and an excellent review of spectral theory are given in the above references and in a recent book by Bendat and Piersol (1966). Rodriguez-Iturbe (1967) investigated the application of cross-spectral analysis to hydrologic data and gave a thorough discussion of the computational procedures for discrete data. The procedures used in this study are identical to those listed by him (Rodriguez-Iturbe, 1967, p. 5-7).

Zero and H-Level Crossing Analyses

In this section, mean values of the durations between zero and h-level crossings, the mean durations of upward excursions above the level h and some of the probability distributions of interest in the two-dimensional stochastic model of particle movement (Sayre and Conover, 1967) will be considered.

First, it is noted that the bed elevation y, measured from the mean bed level, follows approximately a Gaussian distribution, Figure 5. Intuitively, an approximate normal distribution is expected, because physical phenomena governed by the complex interaction of many factors often exhibit such a distribution. Logically, the distribution can be only approximate; in a finite flow depth, the variation of the bed elevation about the mean can never assume infinite values. In addition, the preferred orientation of the dune forms, with the characteristic steeply sloping downstream faces, suggests a pattern more regular than normal distribution. Figure 5 shows examples of the distributions from each of the four channels and although the sets of values plot around the straight line of a normal distribution, each shows some departures from normality.

The cumulative distribution curves of Figure 5 tend to smooth out irregularities of the data and are not really a good indication of the normality or lack of normality of the data. A better criterion, perhaps, is to compare the skewness of the data

with the skewness of a normal distribution, which is zero. Table 2 lists the properties of the raw data and shows that the skewness varied from -0.3 to about 1.7, with a preponderance of values on the positive side. Both the skewness and kurtosis show a considerable range of values with no recognizable pattern.

Even though the distributions of the data depart from normality, the relation of Equation 10 provides a good estimate of the mean duration or the mean distance between zero crossings, ℓ_0, as shown in Figure 6. Although there is considerable scatter, the data group around the line of perfect agreement. No consistent trends in the scatter could be attributed to flume size or type of bed form, so it is assumed that most of the scatter is due to the shortness of the records of the flume data.

The ratio of the expected number of h-level crossings to the expected number of zero crossings was given for both the continuous process and the discrete approximation to the continuous process in Figure 3. Because the two curves are so similar, the simpler expression of Equation 12 will be used. Observed values of the ratio N_h/N_0 are plotted on Figure 7, along with the curve representing Equation 12. Values for thirteen profiles were plotted. Six of the profiles, runs 4, 19, 33, 40, 44 and 48 are of the process $y = y(t)$, and seven of the profiles, runs 16, 32, 41, 45, 53 and 56, are of the process $y = y(x)$. For positive values of h, the

points scatter symetrically about the curve of Equation 12, but for negative values of h, most of the points fall above the curve for values of h from 0 to -1 and below the curve for values of h from -1 to -2.

Figure 7 shows clearly that there are more crossings below the mean bed elevation than above, which would be expected from consideration of flow conditions over a dune. Below the mean bed elevation, the reverse flow in the trough and the flow impinging on the back of the dune results in lower velocities to promote the growth of small-scale features. Above the mean bed elevation, the converging flow up the back of the dune results in a higher-than-average velocity and shear stress near the bed, and small-scale features cannot form.

Figure 8 shows the average of all observations, with the points connected by dashed lines to give an indication of the shape of the distribution of N_h/N_0 values, and with averages of $y(t)$ and $y(x)$ differentiated. The figure indicates that records of both $y(t)$ and $y(x)$ yield values of N_h/N_0 that agree very well with the theoretical curve for $h > 0$, but that deviate appreciably from the curve of Equation 12 for $h \leq 0$, with the values from the process $y = y(t)$ showing the greatest deviation. Figure 8 suggests that there may be some slight differences in the properties of $y(x)$ and $y(t)$. However, distributions of the raw data and the

spectral analyses of the processes, discussed in a later section, indicate that there are no appreciable differences, so the greater deviation of the values for the process $y = y(t)$ probably are fortuitous.

No consistent differences in the deviations of the values from the curve in Figure 7 could be attributed either to flume size or to bed forms, where both ripples and dunes are represented.

The mean duration of an upward excursion of the process $y(t)$ above the level h, $E\{\ell_h^+\}$, was given by Equation 13, and Equation 14 is the ratio of mean duration of upward excursions at the level h to mean duration of upward excursions at the zero level. Equation 14 is plotted on Figure 9 along with observed values of the ratio ℓ_h^+ / ℓ_0^+ . Again, as in Figure 7, there is systematic deviation from the curve for values of h from 0 to -1, and there is considerable scatter at the higher values of h. However, this is not too disturbing because the number of upward excursions that are observed in the relatively short flume records probably are too small to get reliable average values of ℓ_h^+ .

The average rest period of a particle deposited between the levels h_1 and h_2 can be computed from Equation 14 or estimated graphically from Figure 9. Theoretically, there are no limitations to Equation 14; it is applicable between any two levels of the bed, $-\infty < h < +\infty$. The ratio ℓ_h^+/ℓ_0^+ approaches zero as h assumes large

positive values and approaches an infinite value as h assumes large negative values. From a practical point of view, these extremes rarely would be of interest. The major transport of bed material occurs in the actively shifting part of the bed, and it is unlikely that one would need to consider anything beyond two standard deviations of the mean bed level to account for the bulk of the sediment movement. Within these limits, a reasonable estimate of an average rest period can be determined from Figure 9 or Equation 14.

Equation 13 gives the mean rest period, ℓ_h^+, of a particle deposited on the downstream face of a dune at the level h. We are interested in not only the mean value but also the distribution of ℓ_h^+, the conditional probability distribution of rest periods, given that a particle is deposited at the level h. As indicated previously, there is no theoretical basis for predicting a distribution of the ℓ_h^+ values, and, unfortunately, the records of y(t) were not long enough to establish the rest period distributions.

However, it may be useful to establish some of the properties of the distributions for ℓ_h^+ values of the process y(x), even though these values do not represent rest periods, because if the statistical properties of y(x) and y(t) are similar, the distribution of crossings and other features of

interest should be the same. (For Gaussian processes with zero means, similar covariance functions insure similarity of all other properties.) For this purpose, the Atrisco Lateral records were selected because they were the longest available.

Figure 10, a bar graph of ℓ_h^+ distributions for run 1, shows that shapes of the distributions vary with h and suggests that at the level h = 0, the lengths of upward excursions follow an exponential distribution. Figure 11 shows as solid lines exponential distributions with the same means as observed mean values of ℓ_0^+ for runs 1, 2 and 3. The plotted points represent the observed values. Obviously, the exponential distribution is only a rough approximation.

W. W. Sayre (personal communication, 1967) suggested that perhaps a gamma distribution would serve as a model for the distribution of ℓ_h^+ values over any practical range of bed elevations that are of interest. To investigate this possibility, consider the gamma distribution with parameters $b > 0$, $\lambda > 0$,

$$\begin{aligned} p(\ell) &= \frac{\lambda}{\Gamma(b)} (\lambda x)^{b-1} e^{-\lambda x} \quad \text{for } x > 0 \\ &= 0 \qquad\qquad\qquad\quad \text{for } x \leq 0 \ . \end{aligned} \tag{33}$$

When b = 1, this is the negative exponential distribution shown in Figure 11, with $\lambda = 1/\ell_0$. The variance of the gamma distribution

is b/λ^2, and its coefficient of variation, C_v, the standard deviation divided by the mean, is $1/\sqrt{b}$.

Figure 12 shows observed values of C_v for the distributions of ℓ_h^+ values plotted as functions of h. The trend line sketched through the plotted points is positioned with $C_v = 1$ at $h = 0$, corresponding to the exponential distribution of Figure 11. Thus, the postulated gamma distributions of the lengths or durations of positive excursions above the level h can be determined directly from Figures 12 and 9, with λ and b computed from the following equations:

$$b = 1/C_v^2 \tag{34}$$

$$\lambda = 1/C_v^2\{\text{ave } \ell_h^+\} \ . \tag{35}$$

Figure 13 shows bar graphs of the observed ℓ_h^+ distributions for run 1, with points plotted at the midpoint of each class interval representing the frequency for that class from a gamma distribution with parameters given by Equations 34 and 35. The observed mean value of ℓ_0^+ was used to compute λ for $h = 0$, and all other parameters were determined from Figures 9 and 12. The results of this example certainly are encouraging but not conclusive.

It should be noted that the data from one time record, run 19, are plotted on Figure 12. These data deviate more from the trend

line of the C_v values than do the data from the longitudinal profiles, but the number of crossings observed in the time records was too small to provide reliable statistical estimates of the distribution of the ℓ_h^+ values. Thus, the approach outlined above appears to be equally applicable to records of $y(x)$ or $y(t)$, but confidence levels for estimating the distributions of rest periods cannot be established until longer records of the process $y = y(t)$ become available.

One other distribution of interest that will be considered in this section is the probability that a particle is residing in the bed at the level h. This is not the same as the probability that a particle is deposited at the level h, for deposition occurs on the downstream faces and in the troughs of the sand waves; this later probability no doubt depends on flow conditions. The distributions derived empirically by investigating the area bounded by the curve $y = y(t)$ or $y = y(x)$ above a level h give the percent of particles found in the bed above the level h and represent the probability of finding a particle at the level h if nothing is known of its previous history. Figure 14 shows the computed values for $y(x)$ and $y(t)$ records from the 2-ft flume, with a smooth curve drawn by eye to indicate the trend of the distributions. An approximate equation for P(h), the probability that a particle is residing in the bed above the level h, is given by

$$P(h) = 1 - e^{=0.157(h + 1.75)} \quad . \tag{36}$$

Equation 36 is a good approximation in the range $0.1 < P < 0.9$, but it is not applicable for extreme values of h.

Distribution of Wave Heights and Amplitudes

The absolute maximum value of y between zero crossings was defined in Figure 2 as the wave amplitude, (a), and it was noted that the distribution of positive amplitudes, (a+), represented the probability distribution of local deposition and that the distribution of negative values, (a-), represented the probability distribution of local depth of scour associated with the formation and migration of sand waves. If the processes y(x) and y(t) were symmetric about their mean values, the distribution of positive and negative (a) values would be identical, and for a Gaussian process, it was postulated that the distributions of (a) values would approximate the distribution of crest heights, η, shown on Figure 4.

All of the records analyzed exhibited relatively broad spectra, with values of δ^2 from Equation 20 varying from 0.83 to 0.99, see Table 7, and with most of the values greater than 0.9. Figures 15 through 17 show distributions of positive and negative (a) values for runs 1 through 3. The solid curves on the figures represent the Gaussian distribution from Figure 4 of crest heights for a process with a broad-band spectrum ($\delta^2 = 1.0$). Two points of interest should

be noted: (1) the distributions are not symmetric; and (2) the negative values, (a-), follow more closely the normal distribution than do the positive values.

The positive amplitudes, (a+), followed approximately an exponential distribution, as shown in Figure 18. In this figure, P(a) is the cumulative probability distribution of (a), and for this form of plotting, a Rayleigh distribution (Equation 21) would have a slope of two and an exponential distribution the slope of one. Clearly, except for very small values of (a), the slope is one, indicating an approximate exponential distribution.

As discussed previously, there is no basis for estimating the probability distribution of wave heights, H, the trough-to-crest height, and there is no reason to expect similarities in the distribution of H and (a) values. Figure 19 shows the distribution of wave heights to approach the Rayleigh distribution, rather than the exponential distribution. The same data were used to prepare Figures 18 and 19, but in Figure 19, the raw data were not standardized and the wave heights are given in feet rather than in units of standard deviations.

Even though the distributions are different, the mean values of (a+) and H relate reasonably well, Figure 20, as do the mean values of distances between successive upcrossings of y and mean dune lengths, L, (trough-to-trough distance) Figure 21. Note,

however, that values of 2a and of the distance between successive upcrossings are not strictly comparable to H and L because entire wave forms occur above or below the mean bed level, and their lengths and heights are not reflected in the average distance or average of maximum ordinates between zero crossings.

An interesting correlation was found to exist between the average of maximum ordinates between zero crossings and the standard deviation of the bed elevation, Figure 22. For the smaller features, a direct linear relation applies, with the standard deviation of the bed elevation approximately equal to the average amplitude of the sand waves. This is precisely the relation predicted for the mean value of local maxima given by Equation 23 and shown in Figure 4 as the curve corresponding to $\delta^2 = 1.0$. The relation of Figure 22, then, supports the assumption that the distribution of (a) values should be similar to the distribution of the local maxima. The deviation from the line of agreement at the larger (a) values might be attributed to the fact that some of the details of the record are lost in digitizing the continuous trace of bed elevation. The larger dunes are not more regular than the smaller features; in fact, the reverse is true. If the bed profile were represented as a succession of identical triangles, similar to the idealized dune form of Figure 1, with ripple index, $\overline{L}/\overline{H}$, of 15 and $\tan \beta = 0.6$, the relation of mean amplitude to standard deviation of y is given

by $a = 0.64\ \sigma_y$. For this condition to hold for the larger dunes represented in Figure 22, the plotted points would fall to the left of the line of agreement.

Summarizing, the average amplitude (a) is approximately equal to the standard deviation of the bed elevation, and the distributions of (a) values predicted by the relations in Figure 4 appear to give reasonable agreement with the observed distributions. However, the bed profile is not symmetric about its mean level, and the distribution of negative values (a-) agrees more closely with the predicted normal distribution than do the positive values (a+). For the positive values, an exponential distribution can be shown to apply (Figure 18).

Spectral Analysis

In the previous discussion, the autocovariance functions or the spectral density functions for the processes y(x) and y(t) were assumed known. These functions were required to predict the number of zero and h-level crossings for the model Gaussian process, and for the experimental data, the functions were known because they were computed. In the following sections, the properties of the covariance functions and spectra will be considered in somewhat more detail.

Stationarity and Equilibrium Flow - A critical assumption in spectral analysis is that the processes under consideration are

stationary, at least to the second order. At the initiation of this study, it seemed intuitively obvious that stationarity of the processes $y(t)$ and $y(x)$ would be a direct consequence of equilibrium flow conditions. If the mean characteristics of the flow, the sediment, and the transport do not change with time or with distance along the channel, then surely the statistical properties of records of the bed profile should be invariant with respect to shifts in the origin of the records.

For the longer field records, it can be demonstrated that the assumption of weak stationarity is justified. Figure 23a shows mean values and standard deviations for 8 short segments from the record of run number 3 plotted with their respective 90 percent significance levels. The standard deviations do not vary significantly. The rather large variations in the mean values resulted from large alternate bars and a meandering thalweg that existed in the channel, which introduced apparent trends in the short segments of the record. The bed profiles were obtained by sounding from a boat with the water surface as a datum, and the depth of flow varied somewhat systematically along the channels. However, when the bed elevations were measured from the mean bed level established by a linear trend line through short segments of the reach, the assumption of second-order stationarity for these short segments of record was satisfactory. For longer

segments of the record, say on the order of 40 to 50 times the mean channel width, no significant differences were noted in the means and variances.

The flume records presented a somewhat different problem. It was assumed that for equilibrium flow conditions, any two records of the bed profile would show approximately the same statistical properties. However, this was not found to be the case. Figure 23b shows that the standard deviations for runs 8 through 15, all of which were taken during apparent equilibrium flow conditions over an identical reach of the flume (see Table 1), vary significantly.

Two factors appear responsible for the large variations in the flume records. First, the flume records for $y(x)$ are short, relative to the number of dunes that are observed, and the short records introduce inherently large variations in the statistics from one observation to the next. Second, the concept of equilibrium flow implies a time-averaged stability that may not necessarily apply to any single observation. Simons and Richardson (1966, p. J3) indicate that equilibrium flow obtains when the time-averaged water-surface slope and bed slope are parallel and constant and the time-averaged sediment discharge is constant. Rathbun and Guy (1967, p. 111) have shown that extremely large variations in sediment transport rates are to be expected in

recirculating flumes, and probably these variations are reflected in changes in the properties of the bed profiles from one observation to the next.

Despite the rather large variations in the flume records due to the fact that equilibrium flow conditions do not prevail over short time intervals, the spectral properties of the individual records are remarkably similar for a given flow condition, provided the data are standardized to zero mean and unit variance. Figure 24 shows as plotted points the spectral ordinates for runs 8, 10, 12 and 14 plotted against a dimensionless wave number, $\varepsilon/\varepsilon_{max}$, where ε_{max} is the maximum wave number for which the computations were carried out, with the solid line representing an average curve for the spectra and with the dashed lines representing a 90 percent confidence band based on the procedure given by Blackman and Tukey (1958, p. 21-23). Only two of the 80 points fall outside the confidence band, indicating that the general shape of the spectra are quite reproduceable from one observation to the next. The approximation used in this study, therefore, was to treat each individual record as if it were weakly stationary. The moments of the spectra for the individual records could then be used to estimate the number of zero crossings by Equation 10 to compare with observed values. However, in attempting to relate the statistical properties, especially the variance, of the bed profiles

to flow parameters, it will be found convenient to work with average values over a consistent set of flow conditions.

The Markov Model for Dune Profiles - A major question with regard to the spectral analysis is whether or not the properties of the covariance functions or the spectra can be predicted from only the characteristics of the flow and the sediment. Some work already has been accomplished along these lines. Algert (1965) observed that the general shapes of the autocorrelation functions and of the spectra for the process $y = y(x)$ were similar to that of a second-order Markov process, and he developed a model for the spectra based on previous work of Siddiqui (1962). Nordin and Algert (1966) presented essentially the same development, based on Algert's 1965 study, but added some observations on the process $y = y(t)$. Ashida and Tanaka (1967) noted that a second-order Markov process fits the observed spectra only for dunes, and postulated a higher-order linear regressive scheme for other bed forms but did not develop a model or apply the higher order scheme to any of their data.

In the studies by Algert (1965) and Nordin and Algert (1966), the parameters upon which the model of the spectra is based are the values of the covariance function at zero, one and two lag intervals, and these values were shown to relate roughly to the flow parameter, unit discharge, Figure 25. We can use Figure 25 and Equation 15 to predict the average length between zero crossings

of the process y(x) by noting that the spacing of the discrete data points used by Nordin and Algert (1966) in Figure 25 was approximately given by

$$\Delta x \simeq 4\sigma_y = 4C_0^{1/2} \quad . \tag{37}$$

For this case, Δx is equivalent to Δt in Equation 15, C_1/C_0 is $\phi(\Delta t)$, and C_i is $\sigma_y \phi(i\Delta t)$. Substituting these relations in Equation 15 and reading values of C_0 and C_1 from Figure 25 for values of unit discharge given in Table 1, the average distances between zero crossings were computed and are compared with observed values in Figure 26. For the dune bed configuration, the observed values of ℓ_0 fall between plus and minus 40 percent of the expected value, $E\{\ell_0\}$. For the ripple bed configuration, the variations are considerably greater, probably because the size of ripples is more dependent on grain size than flow conditions, so Figure 25 perhaps is not applicable. In view of the gross assumptions that went into estimating $E\{\ell_0\}$, the results of Figure 26 are considered quite good.

There are a number of problems involved in using the second-order Markov model and the relations of Figure 25 for predictive purposes. Both the model and the relations of Figure 25 are strongly dependent on the lag interval at which the continuous

records are digitized. In addition, spectral analyses by the writer and by D. R. Dawdy and N. C. Matalas (personal communication, 1966) have shown that the Markov model does not apply for many of the dune profiles examined. Finally, Plate (1967) has raised some serious questions with regard to the lack of physical basis of this model. It is desirable, therefore, to consider an alternative approach to describe the properties of the spectra and to relate their properties to characteristics of the flow.

Dimensionless Spectra - Autocovariance functions and spectra were computed for all the data listed in Table 1. Figure 27 shows spectra for the process $y = y(x)$ for runs 17, 32, 43, 46 and 49. Spectra of the process $y = y(t)$ for identical flow conditions, runs 19, 33, 40, 44 and 48, are shown in Figure 28. The data include dune flows in the 8-ft flume and both ripples and dunes in the 2-ft flume. The abscissa in both figures is dimensionless, with each value of frequency or wave number divided by the maximum value. All the spectra are remarkably similar in general shape, and there is little difference in the two figures to differentiate the processes $y(t)$ and $y(x)$, suggesting that the statistical properties of the two types of records are similar.

Figure 29 shows a comparison of spectra for ripples and dunes for the 2-ft flume, with a 90 percent confidence band

estimated according to the method given by Blackman and Tukey (1954). Here, as in Figures 27 and 28, the similarity in the spectra is apparent. For both ripples and dunes, the major part of the variance is contributed by the longer wave length components, say greater than two feet. Both spectra show peaks at about 0.3 cycles per foot and again at about 0.8 cycles per foot. Both show additional peaks in the range from 2 to 4 cycles per foot, but within the confidence limits, the peaks on the dune spectra in this range probably are not significant, whereas, those for the ripples are. The rather wide band of the confidence limits leaves open to question the significance of most of the peaks at the lower wave numbers, but there is no question as to the general shape of the spectra.

The similarity of shape of the spectra in Figures 27 and 28 suggests that a model incorporating flow parameters might be developed from dimensional considerations. For a first approximation, consider the major part of the spectra, that part which contributes all but a small percent of the variance, to be a function of only four variables

$$G(t) = \psi(f,g,D,V) \tag{38}$$

$$G(x) = \psi(\varepsilon,g,D,V) \quad . \tag{39}$$

where D is mean flow depth, V is mean flow velocity, g is the acceleration due to gravity and other symbols are as defined

previously. Dimensionless spectra G' are then given in terms of a dimensionless frequency f' or wave number ε' and the square of the Froude number, F, as follows:

$$G'(t) = \psi'(f', F^2) \tag{40}$$

$$G'(x) = \psi'(\varepsilon', F^2) \tag{41}$$

where

$$G'(t) = Gg/V \tag{42}$$

$$f' = fV/g \tag{43}$$

$$G'(x) = Gg/V^2 \tag{44}$$

$$\varepsilon' = \varepsilon V^2/g \tag{45}$$

$$F^2 = V^2/gD \quad . \tag{46}$$

Neither fluid nor sediment properties enter into Equations 38 and 39 on the assumption that water temperature and particle size for the data analyzed were approximately constant. Then, the sediment transport rate and the bed forms are primarily functions of velocity and depth (Colby, 1964, Nordin and others, 1965). The mean flow depth enters Equations 40 and 41 only through the Froude number. It is assumed that the equilibrium height of the bed configurations depends on flow depth, and it was shown in the previous section that the mean height of the bed irregularities and the variance of the process y(x) are closely related. Thus, because all the records were previously standardized in terms of the variance, the Froude number should be a parameter of only

minor importance in the spectra, and for the first approximation, G' should be a function only of the dimensionless frequency or wave number.

Figure 30 shows the relation between G' and ε' for the same data given in Figure 26. For values of dimensionless wave numbers greater than 0.03, all data follow the relation

$$G' = 0.0012(\varepsilon')^{-3.2} \quad . \tag{47}$$

For lower wave numbers, each set of data follow a separate curve without a consistent pattern. It does not appear possible to collapse the family of curves into a single curve on the basis of Froude number. The dashed curve on the figure is intended only to show the general trend of the data, which seems always to show a maximum value for values of ε' less than 0.025.

The dimensionless spectra for the process y = y(t) are shown on Figure 31, where the general relation for dimensionless frequencies less than 0.001 is given by

$$G' = 0.013(f')^{-2.1} \quad . \tag{48}$$

In Figure 31 as in Figure 30, there is considerable scatter, with each set of data defining a general trend which tends to parallel Equation 48. Again, it was not possible to sort the curves

in terms of the third parameter, Froude number, which supports the assumption that depth should be a variable of minor importance in this analysis.

In both Figures 30 and 31, the data for the 8-ft flume, runs 17, 19, 32 and 33 differ slightly in trend from the data of the 2-ft flume, with the set of data from each flume deviating consistently from the average line shown on the figures. It is important to determine whether this is a result of a scale effect or of the difference in particle size of the bed material. Figure 32, which shows the dimensionless spectrum for run 53 in the 8-inch flume, strongly suggests that the difference is not a scale effect, since the data for this flume deviate from the line of Equation 48 in the same direction as the data for the 8-ft flume. It is assumed, then, that the difference is due to differences in the particle size distribution of bed material not accounted for in Equations 38 and 39.

Equation 47 by no means characterizes the entire spectrum, but if the maximum values of G' and the dimensionless wave numbers at which they occur were either constant or functions of the flow and sediment, the spectra would be reasonably well-described. Table 3 summarizes pertinent data for such an analysis for the process $y = y(x)$. The maximum spectral ordinate relates to flow velocity, as shown in Figure 33. The straight line represents

the relationship between the maximum G'(x) and the square of the velocity

$$G'(x)_{max} = 440\ V^{-2} . \qquad (49)$$

No apparent relation was found between values of ε' corresponding to maximum values of G'(x) and any of the flow or sediment characteristics, but it simply may be that there was an insufficient number of observations to establish any trends.

From Equations 47 and 48, the spectral density function G is approximately proportional to the square of the wave period, $T = 1/f$, or to the third power of the wave length, $L = 1/\varepsilon$. The wave celerity c is defined as $L/T = f/\varepsilon$, so from the equations for the dimensionless spectra, we can conclude that wave celerity is directly proportional to $\varepsilon^{1/2}$. Thus, for constant flow conditions, the small waves move faster than the large waves. This conclusion is supported by Simons and others (1961), who state, "Smaller dunes with their higher velocities overtake the larger dunes."

One arrives at the same conclusion by considering a simple model for sediment transport based on continuity principles, such as the one given by Simons and others (1965), which states that for ripples or dunes, the unit transport rate of bedload, q_b, is directly proportional to wave height, H, and wave celerity, c.

Suppose that the bed forms are dunes with ripples superposed, and that the dune movement is due entirely to the ripples overtaking the dune crest and depositing material on its downstream face. Then, continuity requires that $q_b \sim c_1 H_1 \sim c_2 H_2$, which states simply that the larger features move at a smaller velocity.

Note, however, that Equations 47 and 48 say nothing about how the mean wave celerity might vary with varying flow conditions. This matter is considered in the next section in connection with mean frequencies and wave numbers of the spectra computed from Equation 8.

Other Properties of the Spectra - The probability distributions of the y values, the characteristics of the zero and h-level crossings, and the consistent shapes of the dimensionless spectra all point to some remarkable similarities of the bed profiles, irrespective of the size of the channel or of whether the bed forms were ripples or dunes. Indeed, the analysis to this point has been directed primarily toward exposing such similarities, and the procedures for standardizing the raw data to zero mean and unit variance and for non-dimensionalizing the spectra really are nothing more than procedures for applying appropriate scale factors to the data to facilitate comparison. Quite often, however, one is more interested in the differences than in the similarities of the bed profiles, and if this is

the case, it is more appropriate to compare the spectra of the records directly in terms of the actual frequency or wave number components. Figure 34 is an example of such a comparison. Spectra of longitudinal profiles, $y = y(x)$, from each of the four channels, are plotted against wave numbers in cycles per foot. The spectra were computed from the standardized data, so that the area under each curve is equal to unity. The standard deviation, σ_y, for each record is shown on the figure. The effects of channel size on the distribution of the variance over the various wave number components is obvious.

Several features of Figure 34 are particularly interesting. First, note that the flow conditions for run 56 and run 24 are quite similar (Table 1), yet there are appreciable differences in the spectra of the dune profiles. Run 56 is a 200-ft reach of Atrisco Lateral, and the major differences in fluid and flow characteristics between the field data and flume data are that in the field case, the velocity is about 5 percent higher and the temperature is lower by 4 degrees Centigrade. In addition, a fine sediment load was associated with the field data that was not present in the flume. For Atrisco Lateral, the observed sediment concentration from suspended sediment samples was 1440 parts per million (ppm) of which 220 ppm were in the sand sizes, greater than 0.062 mm. For the flume data, the sediment concentration was 164 ppm, all of which was sand. It is rather surprising that the

dune profiles would be so markedly different with only the minor differences in mean flow properties. However, the effects of channel width, of the 4 degrees Centigrade difference in temperature, of the 1,200 ppm fine suspended sediment and of the minor velocity variations are all undefined. Their combined effect on the bed forms, though, is appreciable, and comparison of the spectra indicates that even if the mean velocity, depth and slope are similar in the laboratory and the field, there may exist important differences in bed forms.

A second point of interest concerns the comparison of run 46 and run 49. Here, the difference in the distribution of variance is due strictly to bed configuration and not to channel size. The only difference in the flows for these two runs is the increase in velocity, slope and sediment transport rate associated with the dune bed configuration; all other factors, depth, width, water temperature and particle size of bed material were constant. For the dune bed configuration, values of the standard deviation of the bed elevation, the mean wave amplitude, and the mean length between zero crossings are approximately double the values observed for the ripples. Surprisingly, the flow resistance as measured by the dimensionless Chezy coefficient is very similar for these two runs.

Finally, a third interesting feature of Figure 34 is the indication that for all the dune records, the variance is distributed

generally over components of wave length greater than two feet, whereas for the ripple bed configuration, the variance is distributed more-or-less uniformly over a greater range of wave numbers. The higher wave-number, or shorter wave-length, components contribute an appreciable part to the total variance of the profiles of the ripple bed configurations, but their contribution to the variance of the dune profiles is almost negligible. The question of whether the transition from ripples to dunes is gradual or abrupt cannot be answered from these data, but if additional experimentation were to show the transition to be abrupt, then the distribution of variance over the wave number components would serve as a reliable criterion for distinguishing between ripples and dunes.

Spectral analyses of the longer records from Atrisco Lateral also are of particular interest because they permit better definition of the spectra at the lower wave numbers. An example of these analyses is shown for run number 3 in Figure 35. In part a, the autocovariance function shows an apparent cyclic trend with a wave length approximating the maximum lag of 600 or 200 feet. Inspection of cross sections of the channel every 50 feet along the length of the reach revealed the existance of a meandering thalweg and of alternate bars spaced approximately three to five times the channel width through the entire 4,000-ft reach. The trend in

the autocovariance function, Figure 35a, is almost certainly due to the presence of these alternate bars. The spectra for these longer records show the general decreasing values of G(x) with increasing wave numbers, Figure 35b, which are very similar in shape to the spectra shown in Figures 27 and 28, but which afford much greater detail at the lower wave numbers. Figure 35c shows the spectrum for wave numbers less than 0.1, corresponding to wave lengths of 10 feet or greater, with the wave lengths of the spectral peaks noted. The chi-square test with 20 degrees of freedom to establish a 90 percent confidence band on the spectral estimates indicates that the average ordinate should fall between 1.85 G(x) and 0.66 G(x). The peak at 200 feet may or may not be related to the meandering thalweg, but there is clearly a significant peak in the spectrum at wave numbers less than 0.01. All other peaks shown on the spectrum of Figure 35c are considered significant with the exception of the one at 13 feet, but the wave lengths at which these significant peaks occur were not found to correlate with any recognizable features of the bed profile. There is, of course, no reason to suspect that these peaks in the spectrum should relate to the lengths of the physical waves on which the analysis is being performed, although it has been observed that for dune records, there sometimes is a correlation between the wave length corresponding to the peak in the spectra and the average dune length (Nordin and Algert, 1966; Ashida and Tanaka, 1967).

As a final consideration of the properties of the spectra, it might be worthwhile to explore further the relation between the characteristics of the spectra and the physical characteristics of sand waves. It was previously shown, Figure 22, that a correlation exists between the average amplitude, a, and the standard deviation of the bed elevation, σ_y, which is related to the spectrum of y through Equation 5. The reciprocal of the mean frequency or wave number from Equation 8 is the mean period or wave length of the spectrum, and this value relates reasonably well to the mean period or wave length defined from the zero crossing analysis, as shown in Figure 36. Thus, it is possible to relate empirically the spectral properties and the observed properties of the sand waves.

Ashida and Tanaka (1967) used spectral analyses for determining the propogation velocity of sand waves by plotting the wave length of the maximum spectral ordinate for the process y(x) against the wave period for the maximum spectral ordinate of the process y(t). For the records analyzed in this study, some of the corresponding records of y(x) and y(t) possessed maximum ordinate values of their spectra at the origin, so this method could not be used. In addition, no consistent relations were found between the peaks in the spectra and the average wave lengths or periods of the ripples and dunes. Consequently, the procedure used by Ashida and Tanaka (1967) is not recommended. However,

from the relation of Figure 36, it should be possible to determine the mean wave celerity either from the mean length and period found in the zero crossing analysis or from the mean wave number or frequency of the spectra using Equation 8. Table 4, which shows a comparison of mean wave celerities computed by these two methods, indicates that values of $\overline{c}$ by the two methods are comparable.

The data in Table 4 also give an indication of how the mean wave celerity varies with mean wave number for different flow conditions. In the previous section, it was established that for a constant flow condition, the wave celerity of the different wave-number components varied directly as the square root of the wave numbers. This relation is shown schematically in Figure 37a. In Figure 37b, the mean wave celerities computed from Equation 8 are plotted against mean wave number from the spectral moments. Here we see that with increasing flow velocity, the average wave celerity varies inversely with wave number or directly with wave length. This implies that the mean wave celerity is independent of frequency; or on the average, for these data it took just as long for a ripple to move past a given point as it did for a dune.

The importance of the relations in Figure 37 is in the fact that these relations permit determining the properties of the process, y(t), from the properties of only the longitudinal

profiles, y(x). If the spectral properties of y(x) are known, then the spectral properties of y(t) can be determined from the relation in Figure 37a and Equations 47 and 48. If the mean wave number for the process y(x) is known, then the mean frequency or wave period of y(t) can be established by the relation of Figure 37b, and the mean particle rest period at any level h and the conditional probability distributions for the rest periods at any level h can be determined directly from the relations in Figure 12 and Equations 14 and 33. Note, however, that the relation in Figure 37b is no doubt a consequence of the sediment transport rates associated with the particular flow conditions examined here, and it is not known if the relation is generally applicable for greater flow depths.

O'Loughlin and Squarer (1967) and Squarer (1968) have urged that the standard deviation of the bed elevation and some characteristic wave length from the spectrum of the bed profiles be used to describe the geometric properties of sand waves, rather than simply the mean lengths and heights. Because no consistent terminology for describing bed configurations or methods for computing average wave lengths and heights exist in the literature, it is very difficult to evaluate the results of different investigators. Certainly, then, it is desirable to develop some standard and rigorous method for describing the porperties of the bed profiles that will permit comparison of different studies, and

perhaps the standard deviation of the bed elevation and the reciprocal of the mean wave number of the spectrum from Equation 8 would serve that purpose. In addition, it might be useful to specify the value of δ (Equation 20) which generally may be interpreted as a measure of the root-mean-square width of the variance spectrum (Cartwright and Longuet-Higgins, 1956, p. 216). Values of these parameters and of other measures of wave lengths and heights are given in Tables 6 and 7 in the appendix.

Cross-Correlation and Cross-Spectral Analysis - Several interesting properties of the sand waves can be investigated using the techniques of cross-correlation and cross-spectral analysis. Cross-correlation is the simpler to use and admits to direct physical interpretations. Figure 38 shows the cross-correlograms for correlations of run 8 with each of the runs 9 through 15. The profiles are all for the same reach of flume (see Table 1) and were obtained five minutes apart. If the distance of the peak of the correlogram from the origin is plotted against time, Figure 39a, the slope of the trend line, 7 feet per hour, may be taken as the mean speed of movement of the dunes. An independent check on this figure is provided by the zero crossing analysis, where the mean dune length for runs 8 through 15 is 5.7 feet and the mean period of runs 4 and 19 is 0.72 hours, giving a dune velocity of about 8 feet per hour.

The general trend for the attenuation of the peak value of the correlation with time, Figure 39b, gives an indication of the rate of change in shape of the dune profiles. The dune profiles are assumed to be uncorrelated when the maximum value of the correlation function is 0.3 or less. The value of 0.3 is chosen because cross-correlation of any two profiles taken at random from a group collected during approximate equilibrium flow conditions shows a maximum correlation generally less than 0.3. Then, from Figure 39b, it is inferred that the profile essentially loses its identity in about 90 minutes, or in about the same time for the average size dune to migrate twice its own length.

From Figure 38, it is seen that the maximum value of the cross-correlation function for runs 8 through 15 is approximately the same as the maximum value for runs 8 and 9. Even though the maximum cross correlations are about the same, it is assumed that the distributions of variance over the wave number components should be appreciably different for the two cases because the waves change shape somewhat as they shift downstream. In other words, the general shapes of the cross correlograms are not the same even though their maximums are equal. Plots of the coherence function, γ^2, and the gain function, A, in Figure 40, support this assumption. The general decrease in both coherence and gain from the cross spectral analysis of runs 8 and 15, as opposed to the values for runs 8 and 9, shows that the wave number components of the two records 8 and 15 are essentially uncorrelated.

The cross-correlation and cross-spectral analysis also proved useful in investigating the three-dimensional properties of the dunes. Run 17 was a profile y(x) taken down the centerline of the 8-ft flume. Runs 16 and 18 were profiles taken two feet on either side of the centerline. The correlograms and the spectra for the individual profiles, Figure 41, do not suggest any appreciable differences in the profiles. A major part of the variance in all cases is contributed by the shorter wave-number components corresponding to wave lengths generally greater than 4 feet.

The cross-correlogram for runs 16 and 17, Figure 42a, shows that the two profiles, taken two feet apart along the same reach of flume, are practically uncorrelated, indicating that the sand waves certainly are not long-crested. However, the cross-correlogram for runs 17 and 18 (Figure 42) shows a somewhat better correlation, suggesting that the dunes along the centerline of the flume extend to or at least influence the dunes along the right side of the flume. The coherence diagrams for the spectral analyses of the two sets of data, Figure 43, show the same effect, with values of the coherence function γ^2 for runs 17 and 18 (Figure 43) approximately twice that for runs 16 and 17.

Prediction

In previous sections, the problem of predicting the properties of the bed profile from only the characteristics of the flow and the sediment was considered briefly in terms of the Markov model

and the dimensionless spectra. Neither of these approaches was found to be completely satisfactory. At this point, some additional aspects of predicting the properties of the bed profiles will be considered.

Under the assumption that the bed profiles can be approximated by a random Gaussian process, only three factors are needed to predict the mean values of durations between zero and h-level crossings and the distribution of maximum and minimum y values between zero crossings. These factors are the variance of the bed profile, σ^2_y, the second derivative of the covariance function at the origin, $\phi^{11}(0)$, and the parameter δ^2. The parameter $\phi^{11}(0)$ enters only in calculations of the mean duration between zero crossings, so it could be replaced by $E\{\ell_0\}$. Values of δ^2 approached unity, so as a first approximation, it can be considered equal to one and the prediction problem reduces to determining σ_y and $\phi^{11}(0)$ or $E\{\ell_0\}$.

Definition of the dimensionless spectra in terms of flow parameters would permit determination of $\phi^{11}(0)$ and $E\{\ell_0\}$, and this approach is favored by the writer. Some simple alternatives are to relate ℓ_0 directly to flow parameters or to find a relation between ℓ_0 and the standard deviation of the bed profile, which would be analogous to the ripple index commonly used in geologic literature. In either event, it would still be necessary to determine σ_y, because the dimensionless spectra are based on the standardized data.

As we might expect, the standard deviation of the bed elevation, σ_y, relates roughly to flow depth, Figure 44a, or to the unit water discharge, Figure 44b. Data for these figures are summarized in Table 5 and include average values from this study and values reported by Nordin and Algert (1966). It was not possible to reduce the scatter in these relations by consideration of other hydraulic or fluid variables. The point falling farthest to the left on the figures may be unrepresentative, because the bed profiles (runs 52 and 53) were collected after cessation of sediment motion and probably represent residual features from higher velocity flow (see Rathbun and Guy, 1967, for details of this experiment).

All things considered, the scatter of the points in Figure 44 is neither unexpected nor discouraging. The data represent observations from five different flumes and two field channels. Two of the flumes used a sand feed system and three were of the recirculating type. In all of the experiments except those performed by Algert (1965) in the 0.4 ft flume, information on the bed configurations was a consideration peripheral to the main objectives of the study. A number of unknown factors may contribute to the scatter in the data, such as flume entrance and exit characteristics, operating procedures in the experiment, imposed fine sediment load (in the field case) and particle size distribution of the bed material.

The one other property of the bed profiles that is of most interest is the probability distribution of the durations of upward excursions of the process $y(t)$ above the fixed level h, which is the conditional probability distribution of the rest period of a particle, given that it is deposited on the downstream face of a dune at the level h. The gamma distribution with parameters that relate to h, as shown in Figures 12 and 13, is an attractive possibility. However, before this approach can be recommended, it is necessary to verify both the gamma distribution and the relation of Figure 12 with additional observations of the process $y = y(t)$. Experiments to collect data for such verification have been designed and will be undertaken by the writer and others of the U.S. Geological Survey sometime in 1968.

In summary, the problem of predicting the properties of interest of the bed profiles is still not solved, but the results of this study have suggested several promising approaches. Some crude empirical relations, such as those of Figures 12, 13, 26, 37 and 44, permit approximations to be made of most of the properties of interest, but the need for both refined theoretical models and additional experimental data is obvious.

Chapter IV

SUMMARY AND CONCLUSIONS

Discussion of Results

The application of statistical techniques to analyze the properties of sand waves is a relatively recent undertaking, so perhaps it is difficult to evaluate objectively some of the ramifications of this investigation. Nonetheless, three implications of the results seem to the writer to be of particular importance and to merit further discussion.

The first important conclusion drawn from these investigations is that the properties of the profiles obtained in the laboratory flumes are all very similar, regardless of the size of the flume or of whether the bed configurations are ripples or dunes, provided that scale effects are properly taken into consideration. The scale effects seem to be completely accounted for by standardizing the raw data to zero mean and unit variance and by expressing the length of h-level crossings as a ratio of the mean length between zero crossings, or by forming dimensionless parameters in terms of the flow properties, as in the case of the spectra. This means that certain simple properties, such as the average values of the conditional probability-density functions of rest periods, can be

modeled in a ripple bed configuration or in a very small flow system, and the results can be extrapolated to dune configurations of much larger flow systems.

Similarity of the properties of the ripple and dune profiles does not imply that there are no differences in these features, but only that their general shape and method of movement are similar, as noted by Taylor and Brooks (1961). In fact, the comparisons of distributions of variance over the wave-number components shown in Figure 34 support very strongly the notion that there are appreciable differences. The major differences between ripples and dunes are described in detail by Simons and Richardson (1966) and need not be considered here.

In addition, there were important differences between the flume and field data for dune bed configurations. The longer records from Atrisco Lateral reflected the influence of a meandering thalweg and of accompanying large alternate bars that generally were not present in the flumes. Simons and Richardson (1966) have noted that alternate bars do form in flumes, but for the flume data analyzed here, the width-to-depth ratio was not great enough to permit the bars to develop significantly.

A second important implication arises in the developments leading to Figures 30 through 33 of the dimensionless spectra. These figures show that the spectral representations of the processes

can be determined as unique functions of the flow, fluid and sediment properties. It was fortunate for these studies that the water temperatures and sediment sizes varied over rather narrow ranges, for this permitted expressing the dimensionless spectra in extremely simple form. On the other hand, because of this limited range of conditions, it was not possible to define adequately the shapes of the spectra. But the results, so far as they were carried, are encouraging, and they point the way to future experimental studies that will permit a better definition of the spectra.

However, the most important result, by far, is the demonstration in Figures 6-9 and 15-17 that the properties of the profiles can be estimated by theoretical considerations of fairly simple models. Certainly, the assumption that the processes $y(x)$ and $y(t)$ are Gaussian is a crude approximation, but the results obtained using this model are reasonable and consistent.

In one important aspect, this study was unsuccessful. It was not possible to relate uniquely the statistical properties of the bed profiles to the characteristics of the flow. However, some simple empirical relations were considered that will permit predicting approximately many of the properties of interest. The most important relations in this regard are shown in Figure 44, which gives σ_y as a function of either depth or unit water discharge,

and Figure 25 from Nordin and Algert (1966, p. 109) which shows values of the correlation function at zero, one and two lag intervals as functions of unit water discharge. These values, along with the length of profile record permit calculations of most of the factors considered in the zero and h-level crossing analysis and the approximations of ℓ_h^+/ℓ_0^+ , as given by Equations 15 and 16. However, the relations of Figure 25 apply only if the lag interval is selected so that it bears a constant ratio to the standard deviation, σ_y.

Conclusions

In this study statistical properties of streambed profiles from four different size channels are compared by the techniques of time-series analyses and by considering the mean values and distributions of zero and h-level crossings, the durations of upward excursions of the records y(x) and y(t) above a fixed level h, and the distribution of maximum y values between successive zero crossings. The principal conclusions drawn from the study are the following:

1. No appreciable differences in the statistical properties of the profiles from the flumes could be attributed to flume size or to whether the bed forms were ripples or dunes, provided that the raw data were standardized to zero mean and unit variance and that the length scales were expressed as ratios of the mean length

between zero crossings. In addition, only minor differences were noted between the properties of the longitudinal profiles, $y = y(x)$, and the properties of the profiles, $y = y(t)$, obtained by sounding continuously in time at a fixed point. Longer records of both types, particularly the time records, are required to establish if the differences are real or apparent.

2. Spectra of the longer records from Atrisco Lateral appeared to reflect the influences of a meandering thalweg and large alternate bars that were not present in the flume data.

3. By dimensional analyses, forms of dimensionless spectra were derived which describe reasonably well the observed forms in the higher frequency and wave number regions. The peak values of the dimensionless spectral ordinates for the process $y = y(x)$ correlated with the squares of the mean velocity. From the equations of the dimensionless spectra, it was established that for constant flow conditions, the celerities of the individual wavelength components vary directly as the square root of the wave numbers.

4. From the mean spectral moments, it was shown that the mean wave celerity varied inversely as the mean wave number for the different flow conditions considered. This relation, together with the relation for celerity of wave-number components under constant flow conditions permits determining the properties of the process, $y(t)$, from the properties of the longitudinal profiles, $y(x)$.

5. The techniques of cross-spectral analysis were found useful for defining the mean rate of shifting of ripples and dunes and investigating their three-dimensional properties.

6. Values of the bed elevation follow an approximate Gaussian distribution. For a Gaussian process of known covariance function, the expected number of zero or h-level crossings, the expected length between crossings and the mean duration of upward excursions of the process y(t) above the fixed level h can be computed. The comparison of observed and computed values show good agreement for positive values of h and indicate systematic deviations for values of h below the mean bed elevation. The mean duration of upward excursions of the process y(t) is the mean rest period of a particle at the level h.

7. The distributions of the distances between zero crossings, ℓ_0, are approximately exponential. Values of the durations of upward excursions of y above the level h follow a gamma distribution with parameters that relate to h, as shown in Figures 10 through 13.

8. The distributions of maximum values of y between zero crossings represent the distributions of scour and fill associated with the formation and migration of sand waves. The sand waves are not symmetric about the mean bed elevation. The positive maximums, (a+), are distributed exponentially and the negative maximums, (a-),

are distributed according to a Gaussian distribution. For both cases, the distributions are functions of the standard deviation of the bed elevation, σ_y, which relates approximately to mean flow depth or unit water discharge, Figure 44.

9. Finally, the results of this study show that some of the distributions entering the two-dimensional model of sediment transport (Sayre and Conover, 1967), and most properties of the dune profiles that are of interest can be determined from theoretical considerations of fairly simple models.

Recommendations for Future Studies

The results of this study suggest a number of areas for future investigations. Four, in particular, appear especially promising. These are:

1. Studies should be undertaken to include fluid and sediment properties in the dimensionless spectra and to determine more accurately the dimensionless wave numbers at which the peak spectral ordinates occur.

2. The possibility of incorporating the distribution of wave height and length and the relation of wave celerity to wavelength components (Figure 37) into a continuity-type bedload transport relation based on size and rate of shifting of the sand waves should be investigated.

3. Experiments should be designed to obtain longer records of $y = y(t)$ so that the probability distributions of particle rest periods (the durations of upward excursions) can be adequately defined.

4. Models other than the simple Gaussian model should be investigated as possible representations of the processes $y(x)$ and $y(t)$ to see if more accurate predictions of the properties of the bed profiles can be obtained theoretically. In addition, it should be possible to investigate some models by simulation techniques. One such possibility would be a process of the form $y(t) = \rho \cos(\lambda y + \Theta)$, where ρ, λ, and Θ are all random variables of some specified distribution.

In addition to the above studies, it is necessary to obtain reliable field records of bed profiles to permit extending these studies to a greater range of flow conditions. Records of the process $y = y(t)$ are especially lacking, and many existing longitudinal profiles suffer from inadequate horizontal control.

As noted in Chapter 3, reliable relations between the statistical properties of the profiles and the characteristics of the flow still remain to be developed. Empirical relations exist, but they are far from satisfactory for predictive purposes.

Finally, detailed descriptions of bed profiles are of value only if they lead ultimately to a better understanding of sediment transport processes. Hopefully, the results of this study and of future studies along the lines outlined above will contribute to such an understanding.

REFERENCES

REFERENCES

Algert, J. H., 1965, A statistical study of bed forms in alluvial channels: Report CER65JHA26, Colorado State Univ., Fort Collins, Colorado, 31 p.

Ashida, K., and Tanaka, V., 1967, A statistical study of sand waves: Proc., 12th Congress, Intern. Assoc. for Hydr. Research, V. 2, p. 103-110.

Bendat, J. S., and Piersol, A. G., 1966, Measurement and analysis of random data: John Wiley and Sons, Inc., New York, 390 p.

Blackman, R. B., and Tukey, J. W., 1958, The measurement of power spectra: Dover, New York, 190 p.

Cartwright, D. E., and Longuet-Higgins, M.S., 1956, The statistical distribution of the maxima of a random function: Proc. Royal Soc. (London), Ser. A, V. 237, p. 212-232.

Colby, B. R., 1964, Discharge of sands and mean-velocity relationships in sand-bed streams: U.S. Geol. Survey Prof. Paper 462-A, 47 p.

Cramer, H., 1964, Model building with the aid of stochastic processes: Technometrics, V. 6, No. 2, p. 133-159.

Cramer, H., and Leadbetter, M. R., 1967, Stationary and related stochastic processes: John Wiley and Sons, Inc., New York, 348 p.

Granger, C. W. J., and Hatanaka, M., 1964, Spectral analysis of economic time series: Princeton Univ. Press, Princeton, New Jersey, 299 p.

Karaki, S. S., Gray, E. E., and Collins, J., 1961, Dual channel stream monitor: Proc. Amer. Soc. Civil Engineers, V. 87, No. HY6, p. 1-16.

Longuet-Higgins, M. S., 1958, On the intervals between successive zeros of a random function: Proc. Royal Soc. (London), Ser. A, V. 246, p. 99-118.

Longuet-Higgins, M. S., 1962, The distribution of intervals between zeros of a stationary random function: Phil. Trans. Royal Soc. (London), Ser. A, V. 254, p. 557-599.

Longuet-Higgins, M. S., 1963, Bounding approximations to the distribution of intervals between zeros of a stationary Gaussian process: in "Time Series Analysis", Ed. M. Rosenblatt, John Wiley and Sons, New York, p. 63-88.

Nordin, C. F., Simons, D. B., and Richardson, E. V., 1965, Interpreting depositional environments of sedimentary structures: Colo. State Univ., Civil Engineering Report No. CER65CFN-DBS-EVR15, 17 p.

Nordin, C. F., and Algert, J. H., 1966, Spectral analysis of sand waves: Proc. Am. Soc. Civil Engineers, V. 92, No. HY5, p. 95-114.

O'Loughlin, E. M., and Squarer, D., 1967, Areal variations of bed-form characteristics in meandering streams: Proc. 12th Congress, Intern. Assoc. for Hydr. Research, V. 2, p. 118-127.

Plate, E. J., 1967, Discussion of "Spectral analysis of sand waves": by C. F. Nordin, Jr. and J. H. Algert: Proc. Am. Soc. Civil Engineers, V. 93, No. HY4, p. 310-316.

Rathbun, R. E., and Guy, H. P., 1967, Measurement of hydraulic and sediment transport variables in a small recirculating flume: Water Resources Research, V. 3, No. 1, p. 107-122.

Rice, S. O., 1954, Mathematical analysis of random noise: In "Selected papers on noise and stochastic processes," ed. N. Wax, Dover, New York, p. 133-294.

Rodriguez-Iturbe, I., 1967, The application of cross-spectral analysis to hydrologic time series: Colo. State Univ. Hydrology Paper No. 24, 46 p.

Sayre, W. W., and Conover, W. J., 1967, General two-dimensional stochastic model for the transport and dispersion of bed-material sediment particles: Proc., 12th Congress, Intern. Assoc. for Hydr. Research, V. 2, p. 88-95.

Siddiqui, M. M., 1962, Some statistical theory for the analysis of radio propagation data: Journal of Research, Natl. Bur. of Standards, U.S. Dept. of Commerce, Washington, D.C., V. 66D, No. 5, p. 571-580.

Simons, D. B., and Richardson, E. V., 1966, Resistance to flow in alluvial channels: U.S. Geol. Survey Prof. Paper 422-J, 61 p.

Simons, D. B., Richardson, E. V., and Albertson, M. L., 1961, Flume studies using medium sand (0.45 mm): U.S. Geol. Survey Water Supply Paper 1498-A, 76 p.

Simons, D. B., Richardson, E. V., and Nordin, C. F., 1965, Bedload equation for ripples and dunes: U.S. Geol. Survey Prof. Paper 462-H, 9 p.

Squarer, D., 1968, Discussion of "Relation between bed forms and friction in streams" by V. A. Vanoni and L. S. Hwang: Proc. Am. Soc. Civil Engineers, V. 94, No. HY1, p. 327-330.

Taylor, R. H., and Brooks, N. H., 1961, Discussion of "Resistance to flow in alluvial channels": Proc. Am. Soc. Civil Engineers, V. 87, No. HY1, p. 246-256.

Tick, L. J., and Shaman, P., 1966, Sampling rates and appearance of stationary Gaussian processes: Technometrics, V. 8, no. 1, p. 91-106.

Yaglom, A. M., 1962, An introduction to the theory of stationary random functions: Prentice-Hall, Inc., Englewood Cliffs, New Jersey, 235 p.

APPENDIX I

TABLES

TABLE 1. SUMMARY OF BASIC DATA

Run No.	Channel		Date	Time	Time or station	Transverse station [1]	No. of data points	Lag interval (ft.) or (min.)	Mean depth (ft.)	Mean velocity (ft. /sec.)	Slope	Water temperature (°C)	Median diam. of bed mtl. (mm)
1	Atrisco	Lateral	6/23/66	--	0 - 4000	$\mathbb{C}_L$	12,924	0.333	2.20	2.16	0.00055	19	0.23
2	↓	↓	6/22/66	--	0 - 4000	$\mathbb{C}_L$	13,116	.333	2.30	2.11	0.00055	20	23
3			6/21/66	--	1000 - 4000	$\mathbb{C}_L$	9,864	.333	2.29	2.08	0.00058	20	23
4	8 ft.	Flume	3/15/66	--	936 min.	$\mathbb{C}_L$	936	1.00	2.80	2.09	.00063	20	.24
5			3/17/66	1115	60 - 180	2	924	.130					
6			3/17/66	1115	180 - 60	4	924	.130					
7			3/17/66	1115	60 - 180	6	912	.132					
8			3/17/66	1255	60 - 120	4	432	.139					
9			3/17/66	1300	60 - 120	4	444	.135					
10			3/17/66	1305	60 - 120	4	432	.139					
11			3/17/66	1310	60 - 120	4	432	.139					
12			3/17/66	1315	60 - 120	4	444	.135					
13			3/17/66	1320	60 - 120	4	444	135					
14			3/17/66	1325	60 - 120	4	456	.131					
15			3/17/66	1330	60 - 120	4	444	.135					
16			3/17/66	1530	60 - 180	2	876	.137					
17			3/17/66	1536	60 - 180	4	900	.133					
18			3/17/66	1540	60 - 180	6	900	.137					
19			3/17/66	--	888 min.	$\mathbb{C}_L$	888	1.0					
20			7/12/66	1732	60 - 180	4	468	.256	2.36	2.01	.00056	24	24
21			7/11/66	2114	60 - 180	4	736	.163					
22			7/12/66	0930	60 - 180	4	984	.122					
23			7/12/66	0924	60 - 180	4	720	.167					
24			7/12/66	0935	60 - 180	4	876	.137					
25			7/12/66	0946	60 - 180	4	612	.196					
26			7/12/66	0950	60 - 180	4	480	.250					
27			7/12/66	0953	60 - 180	4	528	.228					
28			7/12/66	1113	60 - 180	4	480	.250					
29			7/12/66	1308	60 - 180	4	468	.256					
30			7/12/66	1328	60 - 170	4	792	.152					
31			7/12/66	1329	170 - 60	4	969	0.158			.00056	24	.24
32			7/12/66	1727	60 - 180	4	852	.141					
33			7/12/66	1735	505 min.	4	672	.750					
34			7/13/66	0907	60 - 180	4	864	.139			.00053	25	
35			7/13/66	0912	60 - 180	4	480	.250					
36			7/13/66	1012	60 - 180	4	864	.134					
37			7/13/66	1016	60 - 180	4	480	.250					
38			7/14/66	0810	60 - 180	4	1188	.101			.00045	25	
39			7/14/66	1435	60 - 180	4	1176	.102			.00045	↓	
40	2 ft.		2/23/67		395 min.	$\mathbb{C}_L$	395	1.0	.518	1.10	.00088	20	.35
41			2/21/67	1110	5 - 55	$\mathbb{C}_L$	668	.075					
42			2/22/67	2350	5 - 55	L	667	.075					
43			2/23/67	1412	5 - 55	R	766	.070					
44			3/23/67		532 min.	$\mathbb{C}_L$	532	1.0	.522	1.07	.00088	20	35
45			3/21/67	1720	5 - 55	$\mathbb{C}_L$	640	.078					
46			3/22/67	0908	5 - 55	$\mathbb{C}_L$	696	.072					
47			3/22/67	2156	5 - 55	L	640	.078					
48			4/12/67	1640	1160 min.	$\mathbb{C}_L$	776	1.50	.521	1.62	.00212	20	35
49			4/11/67	1400	5 - 55	$\mathbb{C}_L$	416	.120					
50			4/12/67	1403	5 - 55	L	407	.123					
51			4/12/67	1536	5 - 55	L	393	.127					
52	0.67 ft.		11/30/65	1000	0 - 7.2	L	306	.0208	.174	.508	.00148	20	.30
53	0.67 ft.		11/30/65	1000	9 - 16	L	348	.0208	.174	.508	.00148	20	.30
54	0.67 ft.	↓	12/1/65	1000	0 - 7.2	L	318	.0208	.174	.508	.00148	20	.30
55	Atrisco	Lateral	6/22/66		0 - 2000	$\mathbb{C}_L$	6000	.333	2.30	2.11	.00055	20	.23
56	↓	↓	6/22/66		0 - 200	$\mathbb{C}_L$	600	.333	2.30	2.11	.00055	20	.23
57			6/22/66		200 - 400	$\mathbb{C}_L$	600	.333	2.30	2.11	.00055	20	.23

[1] $\mathbb{C}_L$ is centerline, L and R are left and right third points of the channel, 2, 4, and 6 are stations from the left wall of the 8-foot flume.

TABLE 2. STATISTICAL PROPERTIES OF RAW DATA

Run	Variance	Standard Deviation	Skewness	Excess of Kurtosis
1	6.70×10^{-2}	2.59×10^{-1}	6.38×10^{-1}	1.07×10^{0}
2	7.63×10^{-2}	2.76×10^{-1}	5.09×10^{-1}	9.47×10^{-1}
3	7.28×10^{-2}	2.70×10^{-1}	2.77×10^{-1}	3.35×10^{-1}
4	4.00×10^{-2}	2.00×10^{-1}	1.71×10^{0}	9.91×10^{0}
5	2.09×10^{-2}	1.44×10^{-1}	4.04×10^{-1}	-8.12×10^{-3}
6	1.58×10^{-2}	1.26×10^{-1}	4.92×10^{-1}	6.45×10^{-2}
7	1.77×10^{-2}	1.33×10^{-1}	1.48×10^{-1}	-2.87×10^{-1}
8	2.62×10^{-2}	1.62×10^{-1}	6.06×10^{-2}	-2.03×10^{-1}
9	1.90×10^{-2}	1.38×10^{-1}	2.59×10^{-1}	-5.62×10^{-1}
10	3.12×10^{-2}	1.77×10^{-1}	5.70×10^{-1}	3.35×10^{-1}
11	3.59×10^{-2}	1.89×10^{-1}	4.12×10^{-1}	-3.15×10^{-1}
12	3.38×10^{-2}	1.84×10^{-1}	3.38×10^{-1}	-2.58×10^{-1}
13	2.96×10^{-2}	1.72×10^{-1}	5.20×10^{-1}	-1.49×10^{-1}
14	3.80×10^{-2}	1.95×10^{-1}	6.07×10^{-1}	-3.23×10^{-1}
15	3.83×10^{-2}	1.96×10^{-1}	5.57×10^{-1}	-4.36×10^{-1}
16	3.22×10^{-2}	1.79×10^{-1}	8.66×10^{-1}	2.32×10^{0}
17	4.68×10^{-2}	2.16×10^{-1}	1.65×10^{-1}	-5.84×10^{-1}
18	3.37×10^{-2}	1.84×10^{-1}	2.06×10^{-1}	-1.53×10^{-1}
19	1.14×10^{-2}	1.07×10^{-1}	1.29×10^{-1}	-1.67×10^{-1}
20	2.16×10^{-2}	1.47×10^{-1}	4.50×10^{-1}	5.03×10^{-1}
21	1.23×10^{-2}	1.11×10^{-1}	2.28×10^{-1}	4.46×10^{-1}
22	1.94×10^{-2}	1.39×10^{-1}	3.17×10^{-1}	-2.21×10^{-1}
23	1.88×10^{-2}	1.37×10^{-1}	1.47×10^{-1}	-2.20×10^{-1}
24	1.96×10^{-2}	1.40×10^{-1}	5.09×10^{-1}	-8.21×10^{-2}
25	2.61×10^{-2}	1.62×10^{-1}	8.33×10^{-1}	8.11×10^{-1}
26	2.77×10^{-2}	1.67×10^{-1}	6.97×10^{-1}	4.20×10^{-1}
27	2.98×10^{-2}	1.73×10^{-1}	6.91×10^{-1}	4.41×10^{-1}
28	1.76×10^{-2}	1.33×10^{-1}	4.06×10^{-1}	7.06×10^{-1}
29	1.44×10^{-2}	1.20×10^{-1}	5.37×10^{-1}	1.66×10^{0}
30	1.07×10^{-2}	1.03×10^{-1}	9.84×10^{-2}	8.41×10^{-3}
31	1.17×10^{-2}	1.08×10^{-1}	-9.77×10^{-2}	5.49×10^{-1}
32	2.11×10^{-2}	1.45×10^{-1}	8.07×10^{-1}	1.55×10^{0}
33	1.45×10^{-2}	1.20×10^{-1}	1.75×10^{-1}	2.57×10^{-1}
34	1.22×10^{-2}	1.10×10^{-1}	2.04×10^{-1}	-1.79×10^{-1}
35	1.23×10^{-2}	1.11×10^{-1}	1.16×10^{0}	9.00×10^{0}
36	1.03×10^{-2}	1.01×10^{-1}	1.60×10^{-1}	2.91×10^{-1}
37	1.04×10^{-2}	1.02×10^{-1}	-2.71×10^{-2}	-4.17×10^{-2}
38	1.25×10^{-2}	1.12×10^{-1}	7.66×10^{-1}	1.12×10^{0}
39	8.52×10^{-3}	9.23×10^{-2}	1.03×10^{0}	1.71×10^{0}
40	1.29×10^{-3}	3.60×10^{-2}	6.78×10^{-1}	4.76×10^{-1}
41	1.91×10^{-3}	4.37×10^{-2}	2.81×10^{-1}	1.98×10^{-1}
42	2.25×10^{-3}	4.74×10^{-2}	-1.85×10^{-1}	-7.54×10^{-3}
43	2.09×10^{-3}	4.57×10^{-2}	3.33×10^{-1}	-4.25×10^{-1}
44	1.20×10^{-3}	3.46×10^{-2}	-2.29×10^{-1}	-4.87×10^{-1}
45	1.64×10^{-3}	4.04×10^{-2}	7.92×10^{-2}	-5.28×10^{-1}
46	1.50×10^{-3}	3.87×10^{-2}	2.15×10^{-1}	-4.16×10^{-1}
47	1.79×10^{-3}	4.23×10^{-2}	2.40×10^{-1}	-1.78×10^{-1}
48	5.62×10^{-3}	7.50×10^{-2}	9.27×10^{-1}	6.70×10^{-1}
49	5.48×10^{-3}	7.39×10^{-2}	1.03×10^{0}	1.64×10^{0}
50	5.54×10^{-3}	7.44×10^{-2}	3.60×10^{-1}	2.68×10^{0}
51	3.23×10^{-3}	5.68×10^{-2}	1.46×10^{-1}	-8.08×10^{-1}
52	2.16×10^{-3}	4.64×10^{-2}	4.44×10^{-1}	-4.99×10^{-1}
53	1.19×10^{-3}	3.44×10^{-2}	2.84×10^{-1}	-4.33×10^{-1}
54	- Not Used -			
55	8.09×10^{-2}	2.84×10^{-1}	5.41×10^{-1}	3.83×10^{0}
56	8.72×10^{-2}	2.96×10^{-1}	1.16×10^{0}	2.49×10^{0}
57	3.95×10^{-2}	1.99×10^{-1}	4.81×10^{-2}	-5.73×10^{-2}

TABLE 3. SUMMARY OF FLOW CHARACTERISTICS FOR DIMENSIONLESS SPECTRA

Run No.	Mean velocity ft/sec	Mean depth ft	Median particle diameter mm	Froude No.	Maximum G'	ϵ' for maximum G'
53	0.508	0.174	0.30	0.214	1800	0.006
46	1.07	.522	0.35	.262	220	.012
43	1.10	.518	0.35	.270	320	.004
49	1.62	.521	0.35	.396	150	.023
32	2.01	2.36	0.24	.230	120	.015
17	2.09	2.80	0.24	.220	150	.009

TABLE 4. COMPARISON OF WAVE CELERITIES

Run number		From zero crossing			From Equation 8		
y(x)	y(t)	L ft	T min	c=L/T ft/min	$L=1/\overline{\varepsilon}$ ft	$T=1/\overline{f}$ min	$c=\overline{f}/\overline{\varepsilon}$ ft/min
17	19	8.45	29.3	0.288	7.62	42.5	0.179
32	33	4.78	16.6	.288	5.45	26.8	.204
43	40	1.36	14.3	.0952	1.75	29.7	.0590
46	44	1.01	27.4	.0368	1.24	38.8	.0320
49	48	2.56	25.5	.100	3.00	32.4	.0926

TABLE 5. AVERAGE VALUES OF OBSERVED VARIABLES

Channel	V ft/sec	D ft	W ft	S	T °C	d_{50} mm	σ_y ft	Ave a^+ ft	ℓ_o ft	Remarks
Atrisco	2.16	2.20	55	0.00057	19	0.23	0.259	0.277	4.48	Dunes
Atrisco	2.11	2.30	55	.00055	20	.23	.276	.287	4.61	Dunes
Atrisco	2.08	2.29	55	.00058	20	.23	.270	.302	3.90	Dunes
8-ft flume	2.09	2.80	8	.00063	20	.24	.169	.214	2.95	Dunes-Recir. system
8-ft flume	2.01	2.36	8	.00056	24	.24	.127	.146	2.28	Dunes-Recir. system
2-ft flume	1.62	.521	2	.00212	20	.25	.0700	.0806	1.42	Dunes-Recir. system
2-ft flume	1.10	.518	2	.00088	20	.35	.0432	.0416	.58	Ripples-Recir. system
2-ft flume	1.07	.522	2	.00088	20	.35	.0390	.0408	.54	Ripples-Recir. system
0.67-ft flume	.80	.197	0.67	.00148	20	.30	.0404	.0400	.36	Ripples-Sand feed system
		From Nordin and Algert, (1966)								
Bernardo	3.62	2.60	70	.00058	8.34	0.23	.647	--	--	Dunes
Bernardo	2.48	4.15	70	.00058	8.34	.23	.745	--	--	Dunes
8-ft flume	2.11	1.05	8	.00134	16.7	.28	.175	--	--	Dunes-Recir. system
8-ft flume	1.91	.670	8	.00136	17.8	.28	.115	--	--	Dunes-Recir. system
0.4-ft flume	1.81	.580	0.4	.0044	18.4	.34	.0478	--	--	Sand feed system
0.4-ft flume	1.78	.485	.4	.0038	15.6	.34	.0330	--	--	Sand feed system
0.4-ft flume	1.74	.400	.4	.0037	17.8	.34	.270	--	--	Sand feed system

TABLE 6. SUMMARY OF WAVE PROPERTIES

Run Number	[1] Length in feet or Period in minutes		[2] Height in feet		Ripple Index	
	Average	Coefficient of Variation	Average	Coefficient of Variation	Average	Coefficient of Variation
1	6.06	.533	.370	.643	22.8	.857
2	6.14	.535	.368	.655	22.7	.815
3	5.28	.535	.408	.597	17.2	.764
4*	25.9	.763	.214	1.43	163.	.786
5	5.07	.658	.225	.571	25.7	.678
6	3.73	.700	.184	.377	21.6	.733
7	4.24	.604	.201	.388	22.2	.575
8	5.16	.408	.341	.514	22.3	.870
9	4.66	.553	.269	.535	21.7	.772
10	3.89	.742	.268	.509	17.5	1.05
11	5.13	.524	.305	.482	20.5	.722
12	3.89	.757	.251	.477	18.8	.916
13	6.44	.340	.384	.468	19.4	.590
14	4.49	.812	.264	.616	21.7	.979
15	6.18	.462	.364	.483	18.3	.513
16	5.06	.575	.315	.915	23.7	.739
17	4.84	.779	.265	.547	25.0	1.23
18	4.54	.698	.297	.483	17.8	.821
19*	25.6	.664	.149	.229	175.	.674
20	4.31	.475	.261	.473	18.6	.429
21	3.55	.502	.221	.506	18.4	.671
22	3.49	.564	.265	.476	16.2	.826
23	3.67	.574	.257	.524	16.0	.584
24	4.40	.471	.296	.578	19.2	.770
25	4.31	.595	.316	.484	15.8	.627
26	4.34	.532	.300	.546	19.0	.897
27	4.89	.489	.367	.506	16.5	.668
28	4.55	.515	.276	.538	18.7	.536
29	4.77	.528	.253	.494	23.9	.704
30	3.85	.649	.165	.347	25.6	.727
31	4.12	.754	.161	.450	27.5	.868
32	4.72	.445	.260	.506	21.3	.577
33*	16.3	.941	.133	.216	127.	.929
34	4.36	.521	.200	.411	27.4	.735
35	4.59	.562	.255	.645	25.5	.783
36	3.27	.538	.173	.381	21.6	.647
37	4.64	.428	.204	.446	26.7	.576
38	4.28	.510	.175	.380	26.5	.559
39	3.78	.545	.185	.457	21.6	.549
40*	30.2	.426	.0783	.277	399.	.426
41	1.20	.484	.0922	.328	14.7	.648
42	1.15	.568	.0902	.288	13.4	.579
43	1.24	.606	.0913	.307	14.3	.679
44*	40.4	.744	.0750	.353	577.	.802
45	1.24	.534	.0856	.268	14.9	.545
46	1.34	.542	.0827	.216	15.9	.422
47	1.28	.518	.0874	.318	15.7	.583
48*	17.7	.514	.111	.491	183.	.574
49	2.73	.408	.167	.454	18.7	.642
50	2.75	.424	.149	.482	24.4	.836
51	3.15	.630	.114	.369	27.4	.589
52	.498	.353	.0609	.752	13.7	1.08
53	.440	.485	.0520	.752	14.3	.697

* Wave period. [1] Length is trough-to-trough distance. [2] Height is difference in elevation, crest to trough.

TABLE 7. MISCELLANEOUS PROPERTIES FROM THE ZERO-CROSSING AND SPECTRAL ANALYSIS

Run No.	1/ Length		2/ Amplitude		3/	4/	5/	Type of Profile
	L_o	C_v	$\bar{\alpha}_+$ ft	C_v	σ_y ft	δ^2	$1/m_1$	
1	8.96	0.577	0.277	0.850	0.259	---	---	y(x)
2	9.22	.589	.287	.913	.276	---	---	y(x)
3	7.79	.560	.302	.782	.270	---	---	y(x)
4	57.3	.504	.386	1.46	.200	0.933	26.0	y(t)
5	4.97	.599	.164	.868	.144	.978	6.38	y(x)
6	4.94	.681	.158	.886	.126	.968	4.91	
7	5.37	.618	.156	.673	.133	.973	5.75	
8	5.24	.631	.180	.712	.162	.964	4.46	
9	6.13	.379	.225	.573	.138	.952	3.85	
10	5.78	.511	.221	.687	.177	.966	5.11	
11	6.59	.596	.223	.684	.189	.972	5.56	
12	3.39	.877	.119	1.21	.184	.975	5.31	
13	6.39	.481	.243	.690	.172	.970	4.91	
14	4.74	.789	.192	1.02	.195	.982	6.37	
15	7.38	.186	.306	.467	.196	.977	6.24	
16	6.21	.512	.256	1.09	.176	.960	4.52	
17	8.45	.384	.274	.747	.216	.983	7.59	
18	6.96	.358	.226	.555	.184	.979	6.48	y(x)
19	29.3	.591	.099	.885	.107	.974	42.5	y(t)
20	4.68	.448	.169	.800	.147	.931	5.35	y(x)
21	4.34	.648	.138	.834	.111	.946	4.01	
22	4.21	.575	.189	.648	.139	.974	4.47	
23	4.19	.623	.167	.708	.137	.946	4.07	
24	5.04	.416	.190	.705	.140	.966	4.43	
25	5.61	.412	.201	.843	.162	.952	5.15	
26	5.62	.598	.212	.836	.167	.938	5.85	
27	5.79	.530	.227	.702	.173	.944	5.68	
28	3.70	.635	.137	.928	.133	.909	4.72	
29	4.04	.706	.144	1.00	.120	.876	3.48	
30	3.98	.620	.091	.899	.103	.968	5.37	
31	5.69	.576	.129	.716	.108	.966	5.86	
32	4.78	.644	.157	.853	.145	.970	5.44	y(x)
33	16.6	.817	.103	.815	.120	.961	26.8	y(t)
34	4.67	.662	.132	.732	.110	.965	4.95	y(x)
35	5.78	.453	.179	1.06	.111	.830	3.02	
36	3.20	.709	.093	.836	.101	.961	4.31	
37	4.12	.756	.106	.755	.102	.923	5.25	
38	4.20	.552	.072	1.01	.112	.983	6.21	
39	2.79	.757	.088	1.23	.0923	.962	3.32	y(x)
40	14.3	.989	.0237	1.16	.0360	.958	29.7	y(t)
41	.968	.635	.0432	.857	.0437	.886	1.36	y(x)
42	1.16	.666	.0483	.666	.0474	.895	1.61	y(x)
43	1.36	.542	.0512	.680	.0457	.921	1.75	y(x)
44	27.4	.630	.0279	.963	.0346	.970	38.8	y(t)
45	1.14	.546	.0493	.619	.0404	.874	1.33	y(x)
46	1.01	.515	.0430	.652	.0387	.881	1.24	y(x)
47	1.13	.679	.0431	.820	.0423	.904	1.58	y(x)
48	25.5	.562	.0885	.817	.0750	.927	32.4	y(t)
49	2.56	.472	.0952	.901	.0739	.948	3.00	y(x)
50	2.77	.610	.0734	1.03	.0744	.927	2.37	
51	3.16	.665	.0653	.687	.0568	.956	3.56	
52	.636	.534	.0384	.920	.0464	.980	1.08	
53	.782	.460	.0416	.449	.0344	.964	.81	

1/ L_o is the average distance in feet or time in minutes between successive up crossings of y = 0. C_v is the coefficient of variation.

2/ $\bar{\alpha}_+$ is the average of maximum y values between successive zeros.

3/ From eq. 5. 4/ From eq. 20. 5/ Mean wave length in feet, or wave period in minutes from the spectra, eq. 8.

APPENDIX II

FIGURES

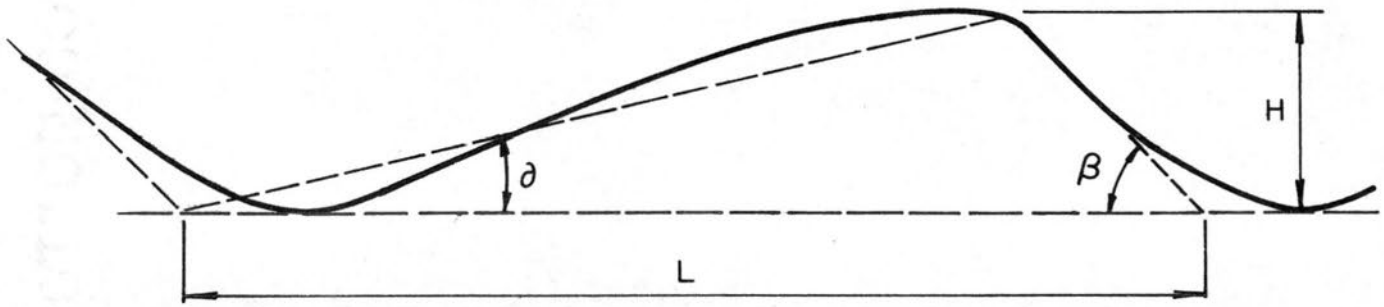

Figure 1. Idealized dune shape.

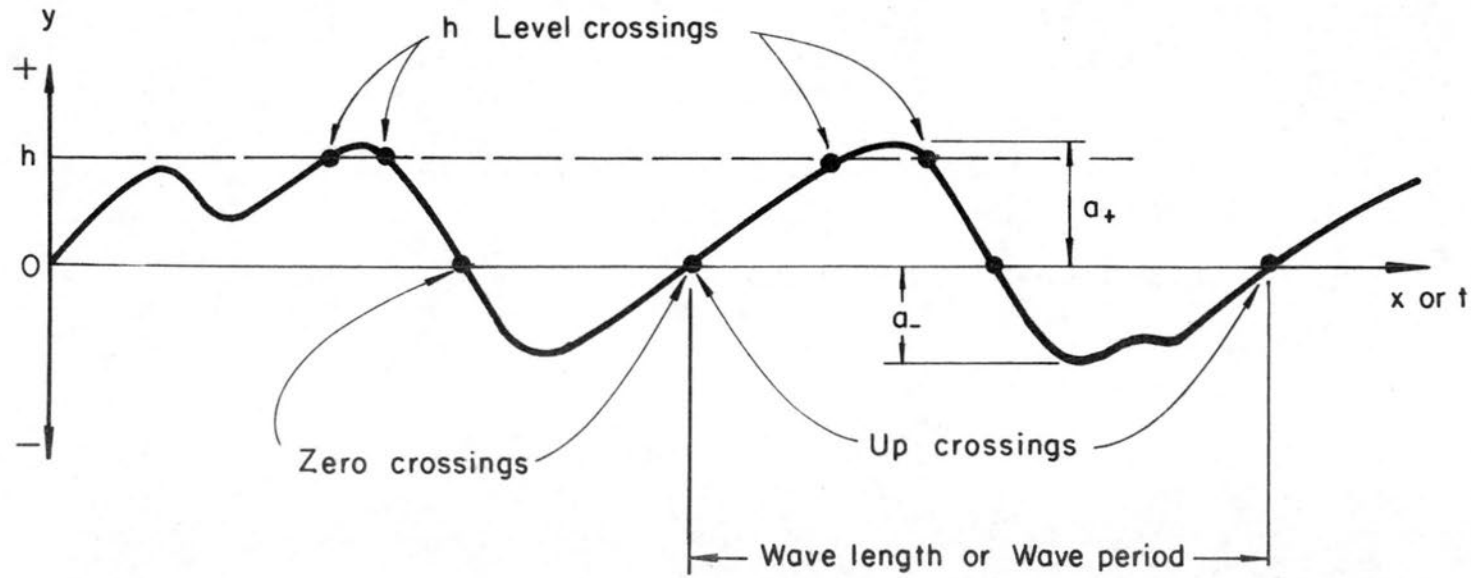

Figure 2. Definition sketch of bed profile.

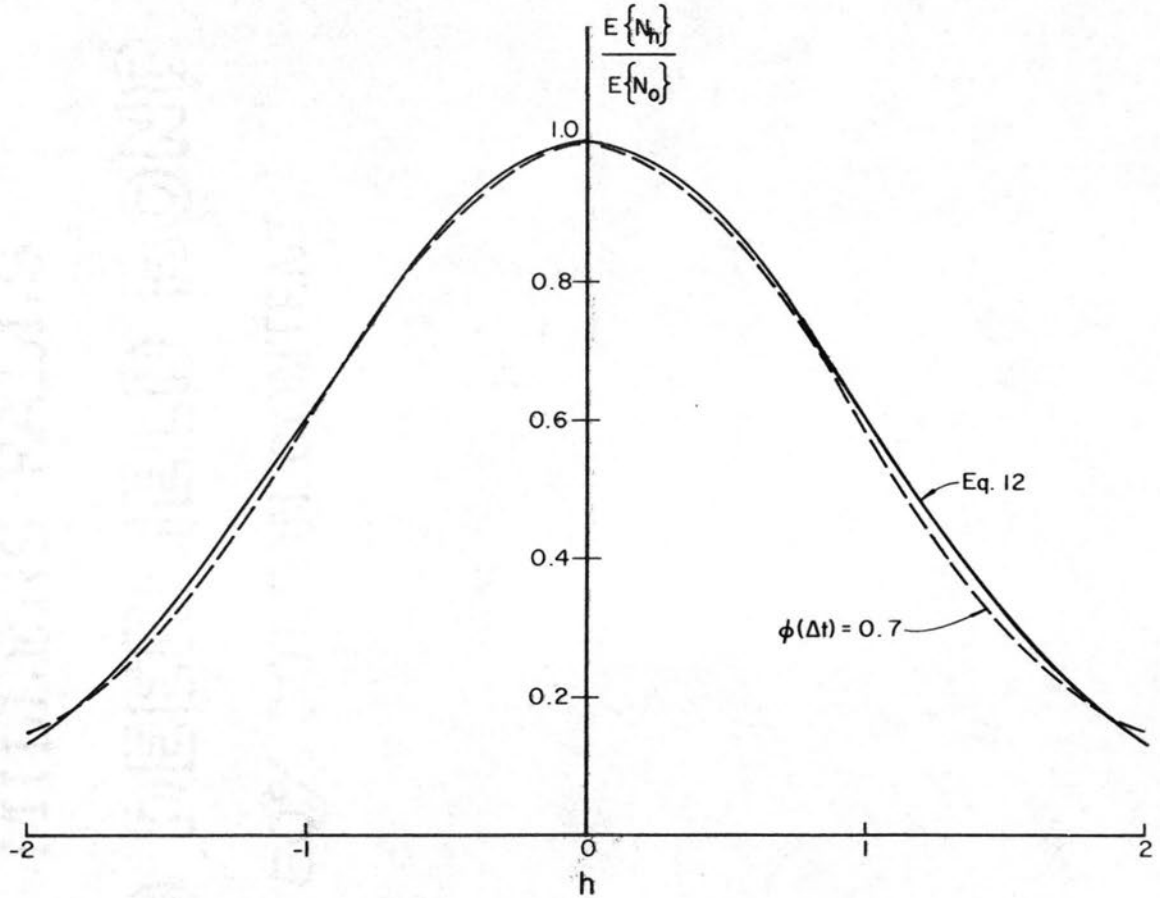

Figure 3. Ratio of the expected number of h-level crossings to the expected number of zero crossings, $E\{N_h\}/E\{N_0\}$, as a function of h.

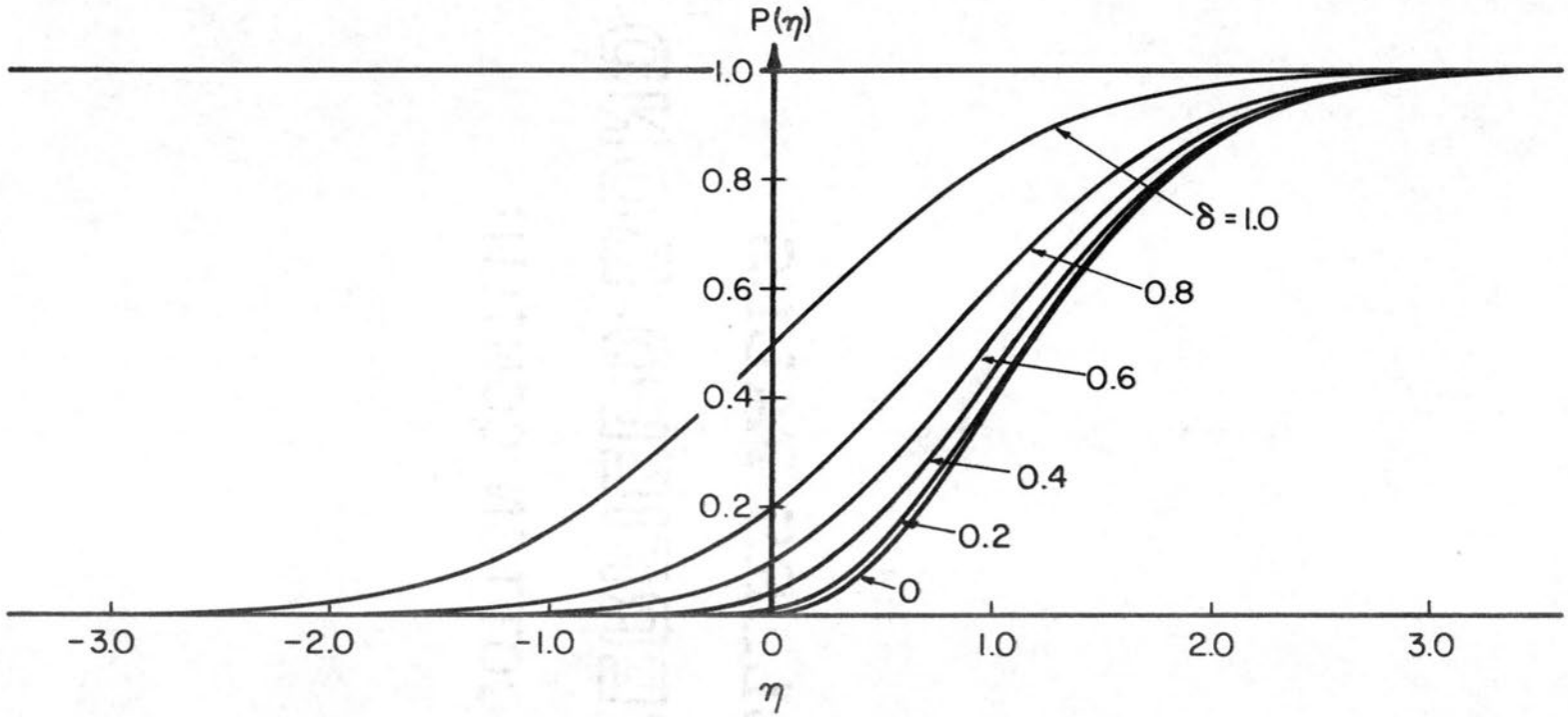

Figure 4. Cumulative probability distribution functions for dimensionless maxima, η, as a function of δ.

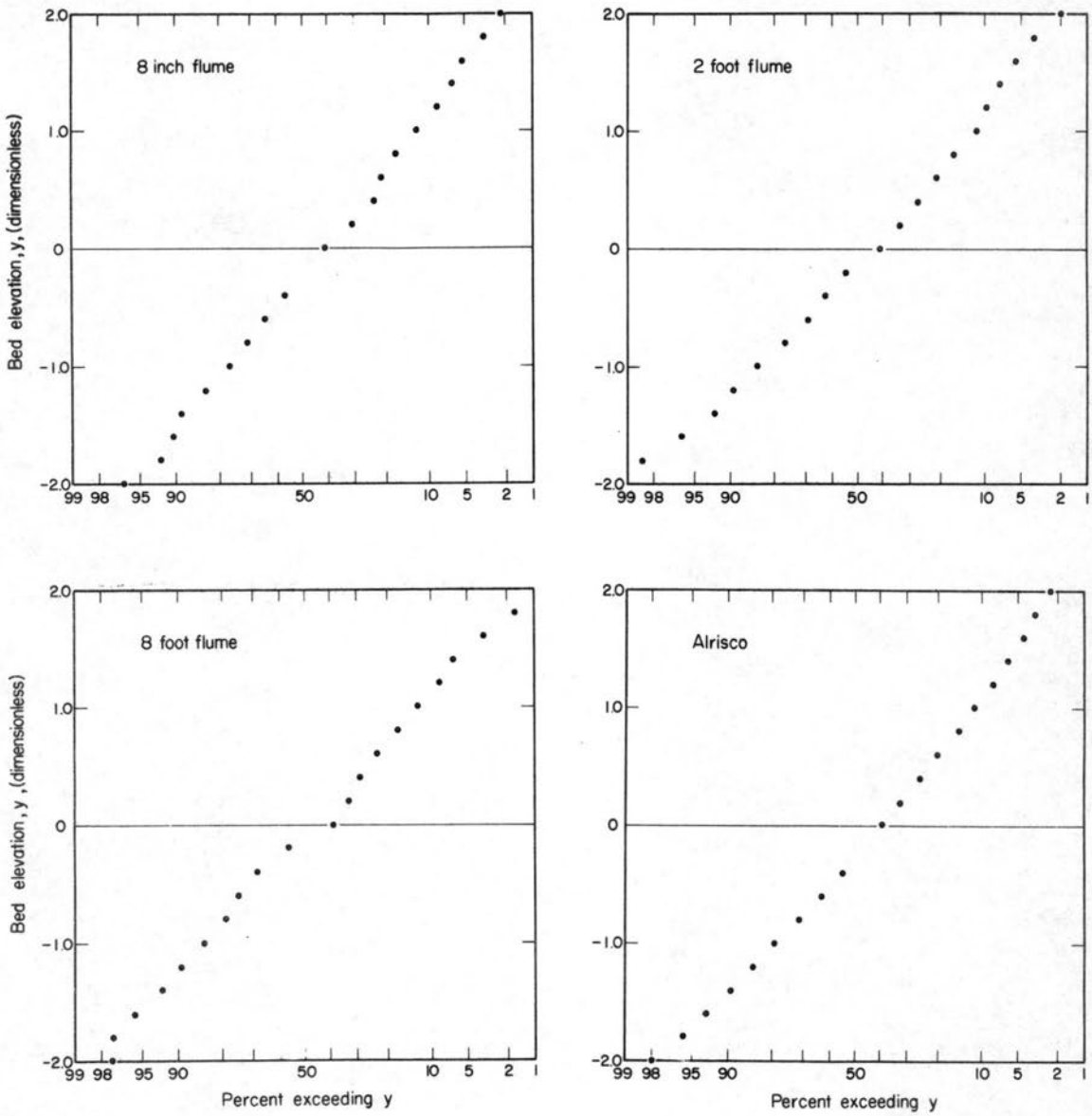

Figure 5. Distributions of bed elevations.

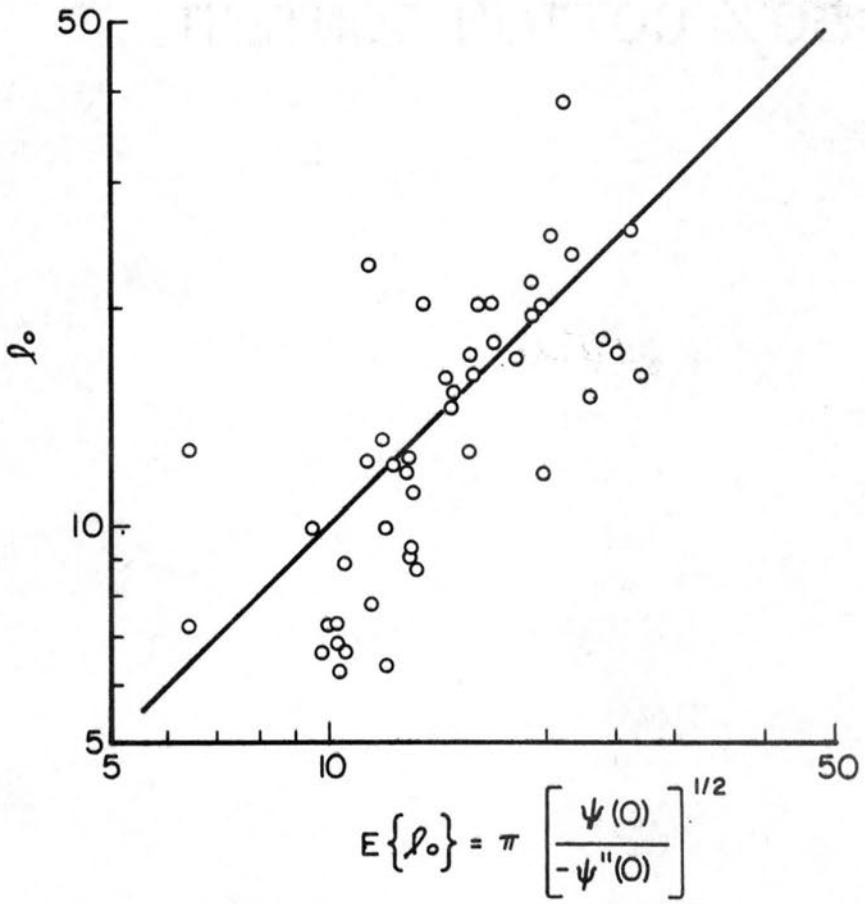

Figure 6. Comparison of the expected length or duration between zero crossings for a Gaussian process, $E\{\ell_0\}$, with the observed values, ℓ_0.

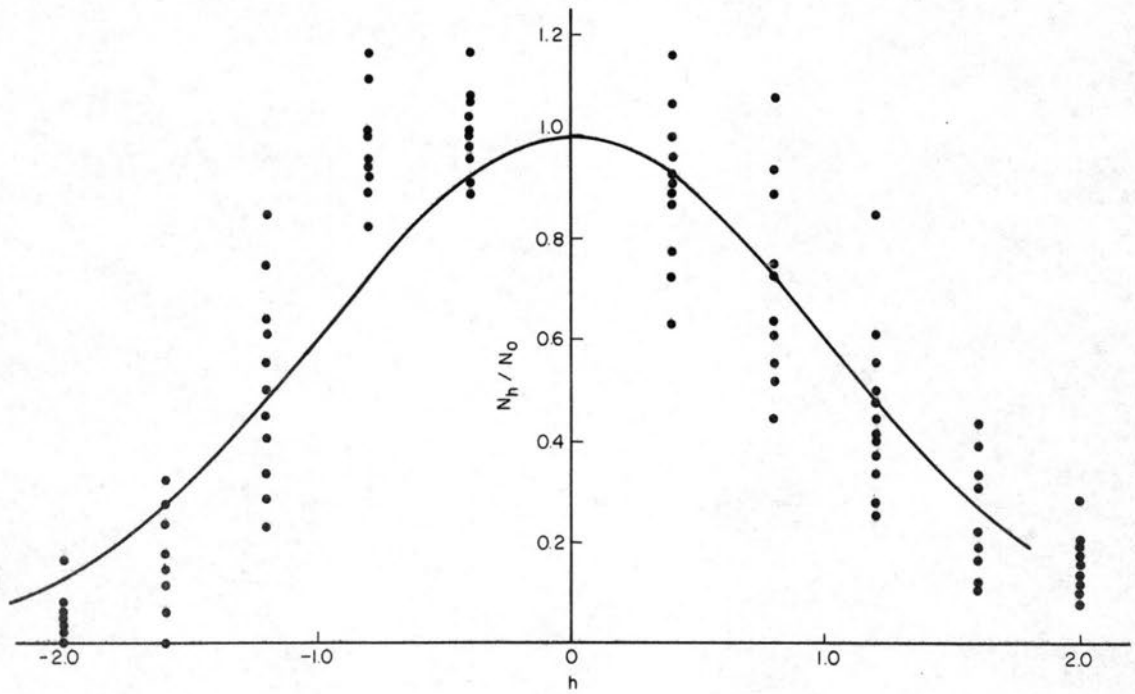

Figure 7. Observed values of N_h/N_0 as a function of h.

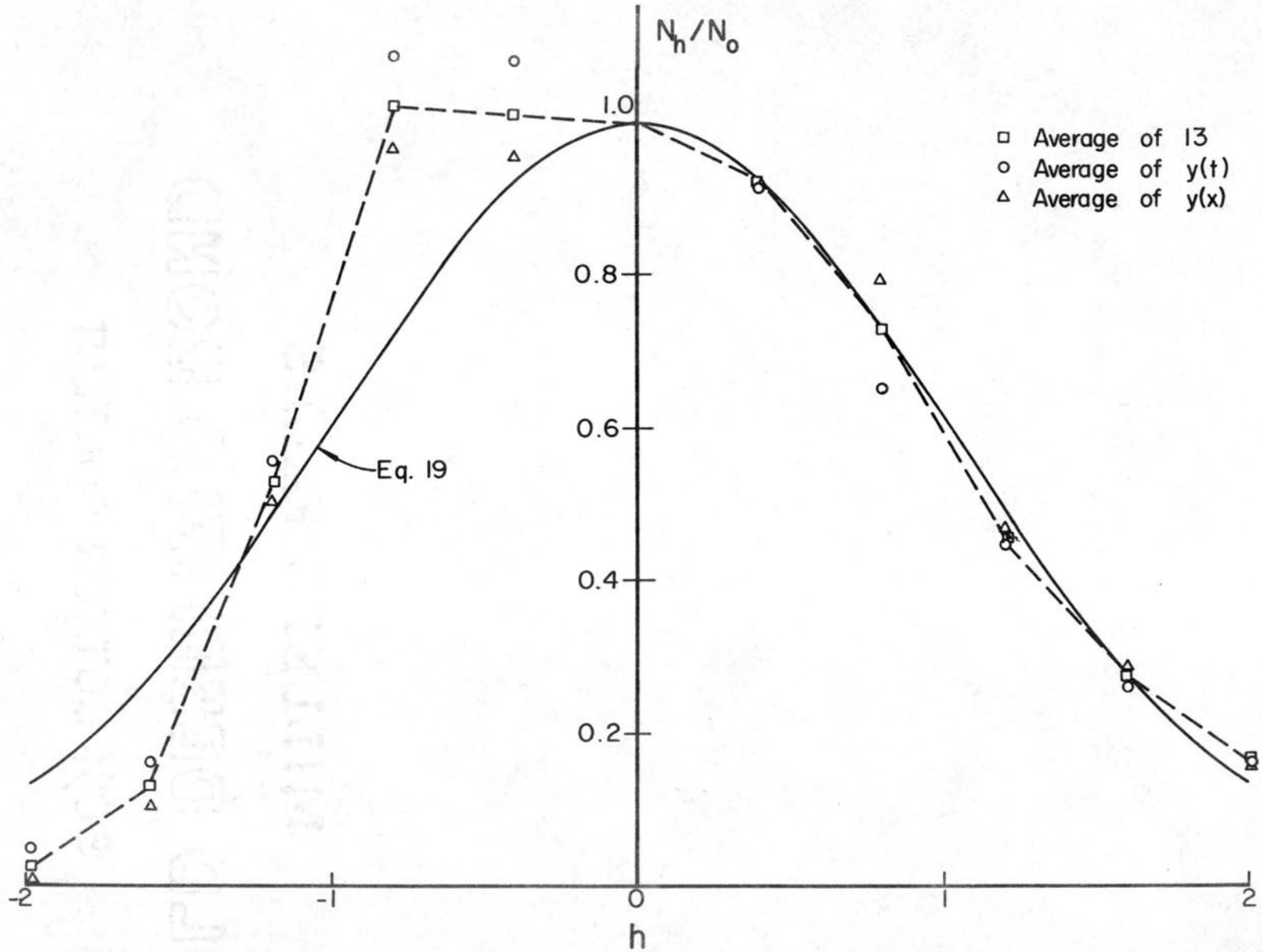

Figure 8. Average values of N_h/N_0 as a function of h.

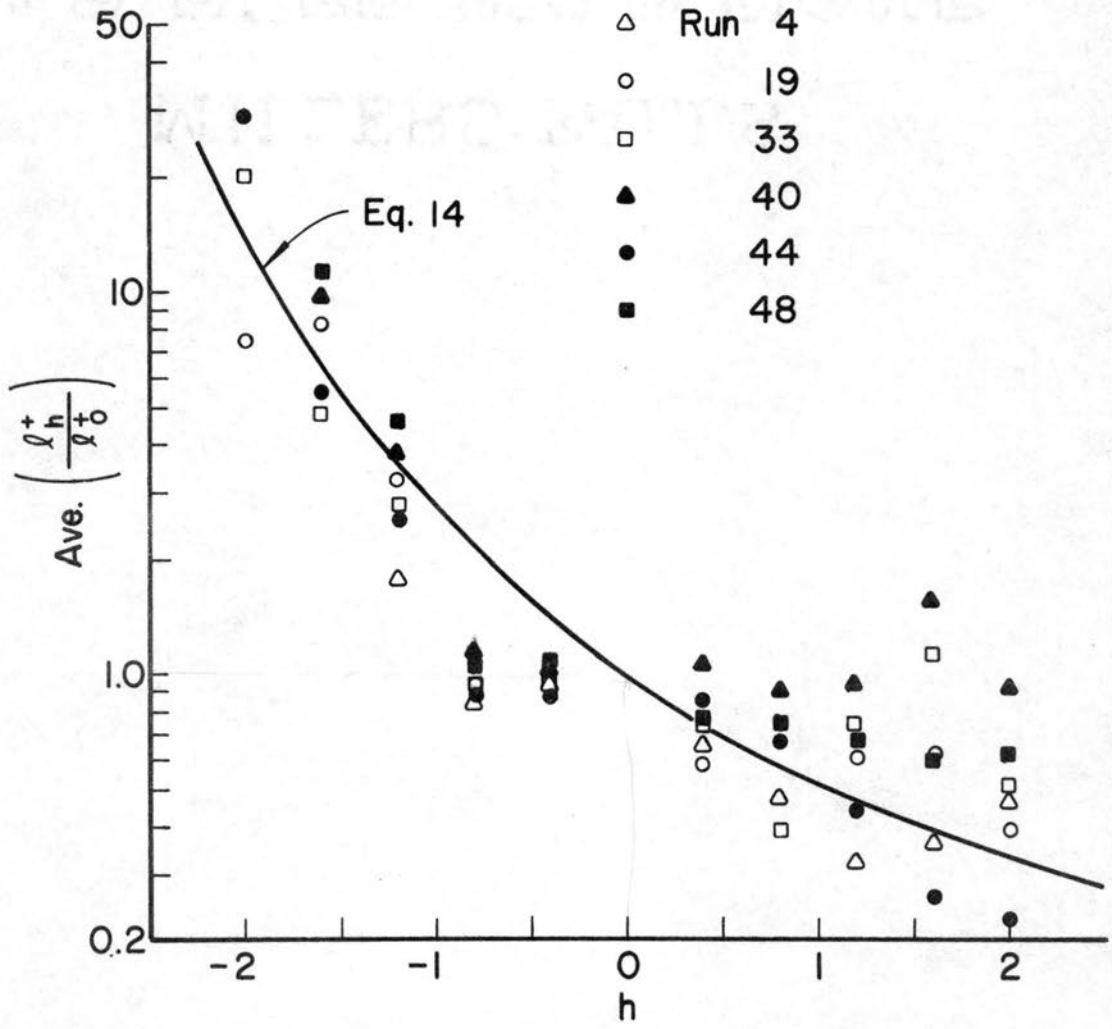

Figure 9. Observed values of the ratio ℓ_h^+/ℓ_0^+ plotted against h. The solid curve represents Equation 14.

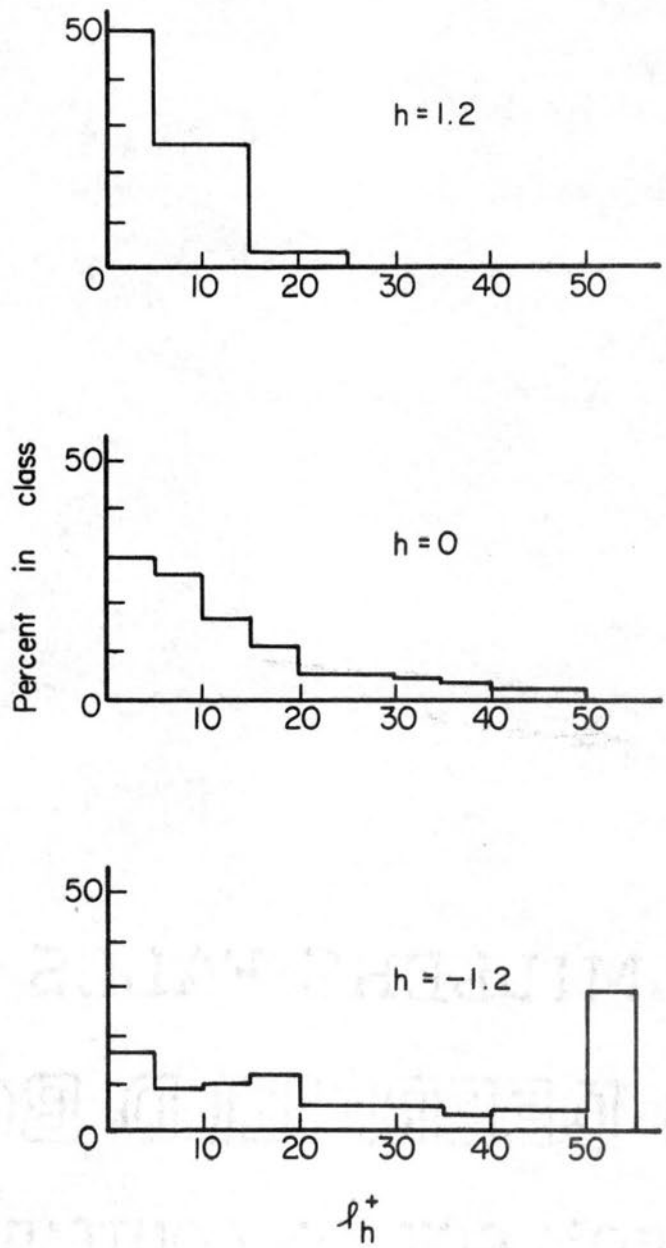

Figure 10. Bar graph showing the observed distributions of ℓ_h^+ for run 1.

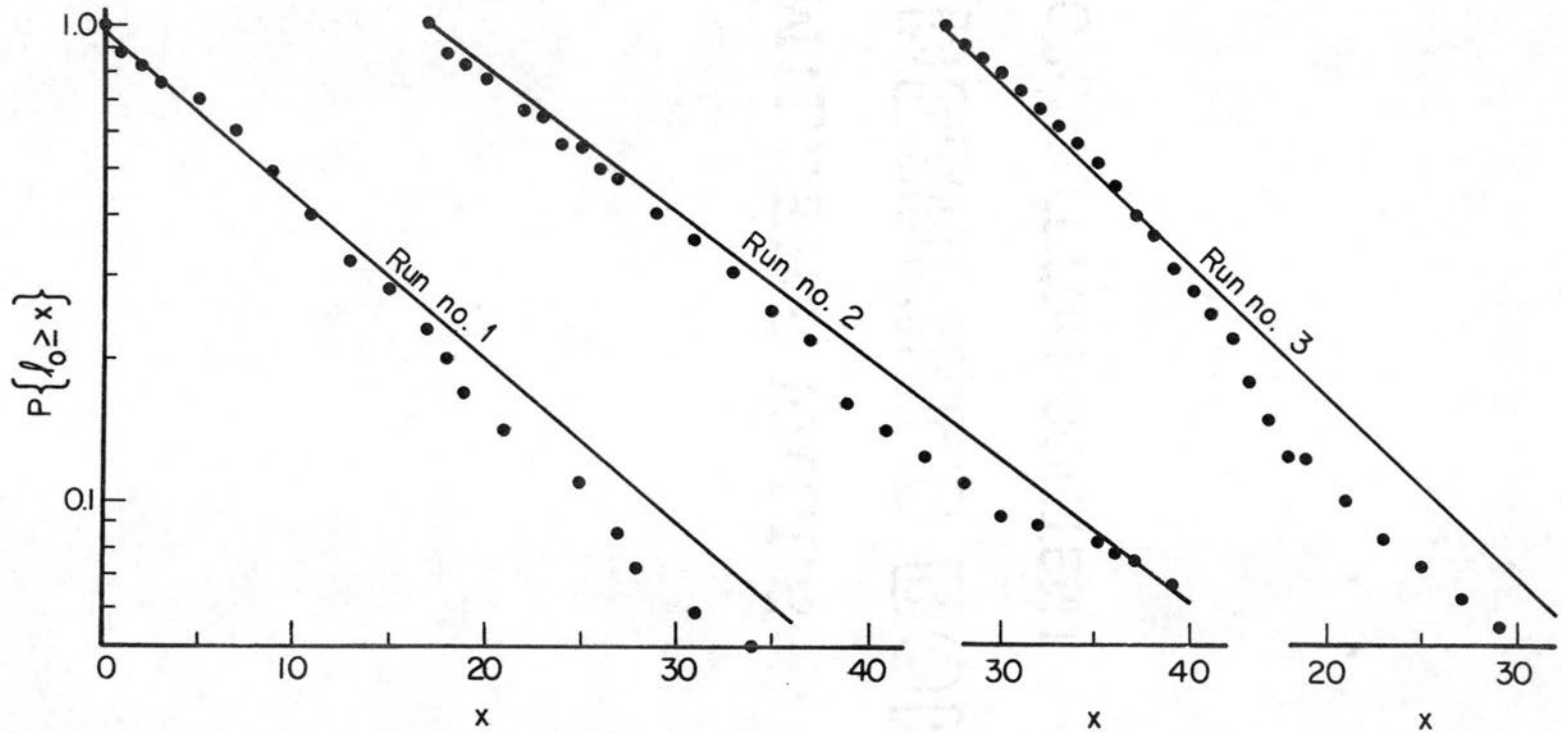

Figure 11. Observed distributions of ℓ_0^+ for runs 1, 2, 3. Solid lines are exponential distributions with the same mean values as the observed means.

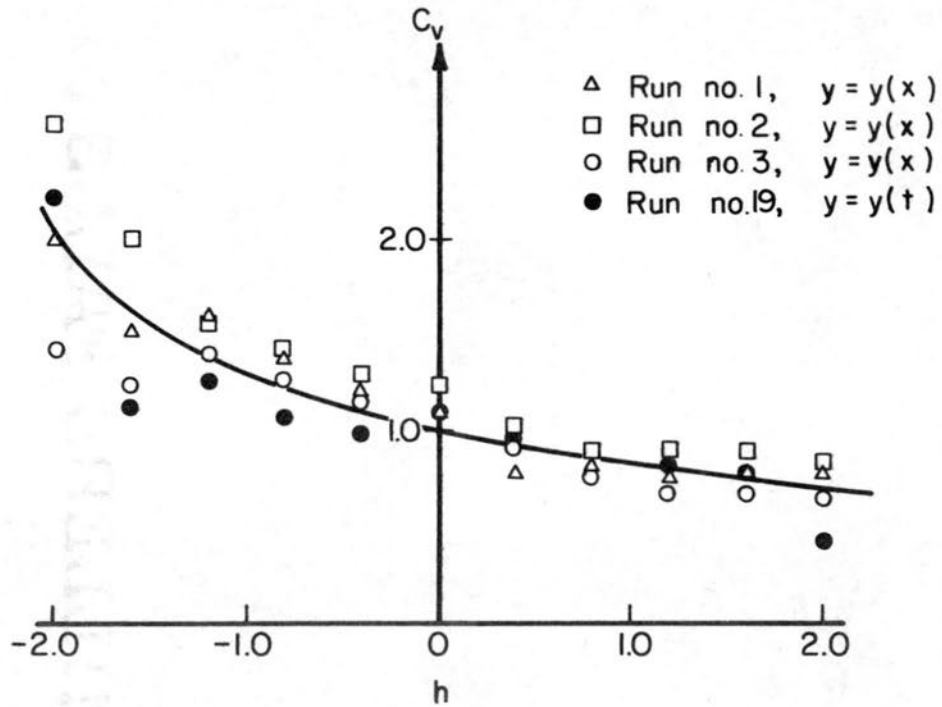

Figure 12. Observed values of the coefficient of variation, C_v, for the distributions of ℓ_h^+ plotted as functions of h.

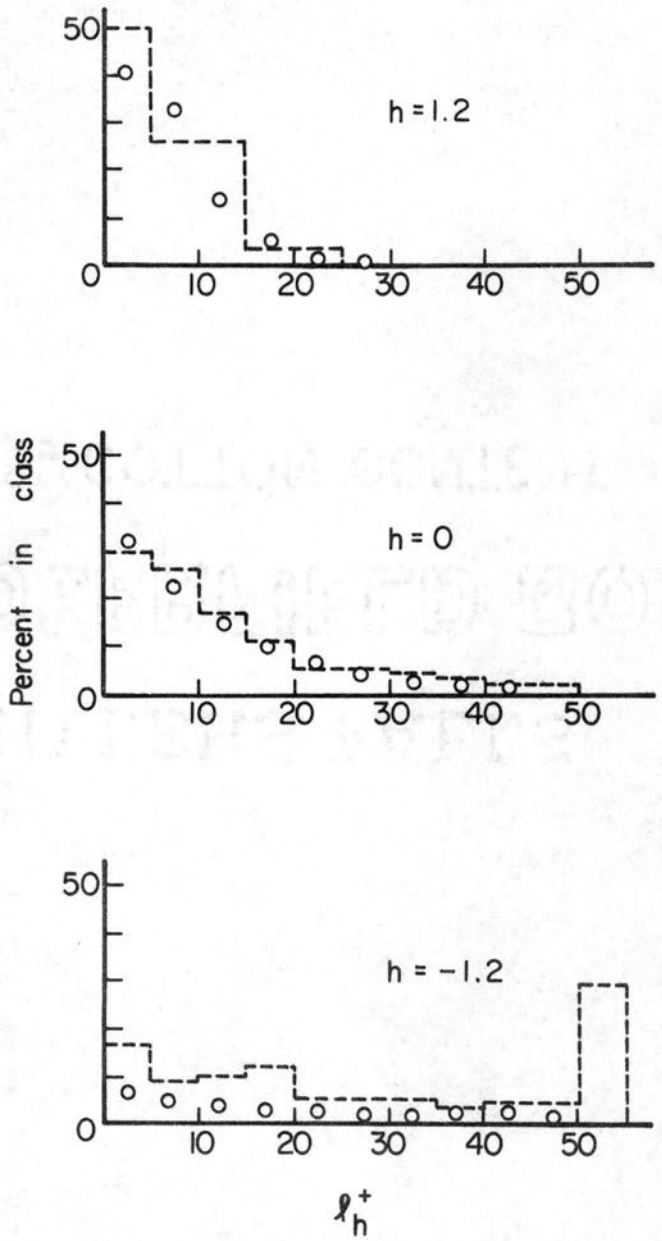

Figure 13. Comparison of observed ℓ_h^+ distributions with the theoretical class frequencies from a gamma distribution. The plotted points are from the theoretical distribution.

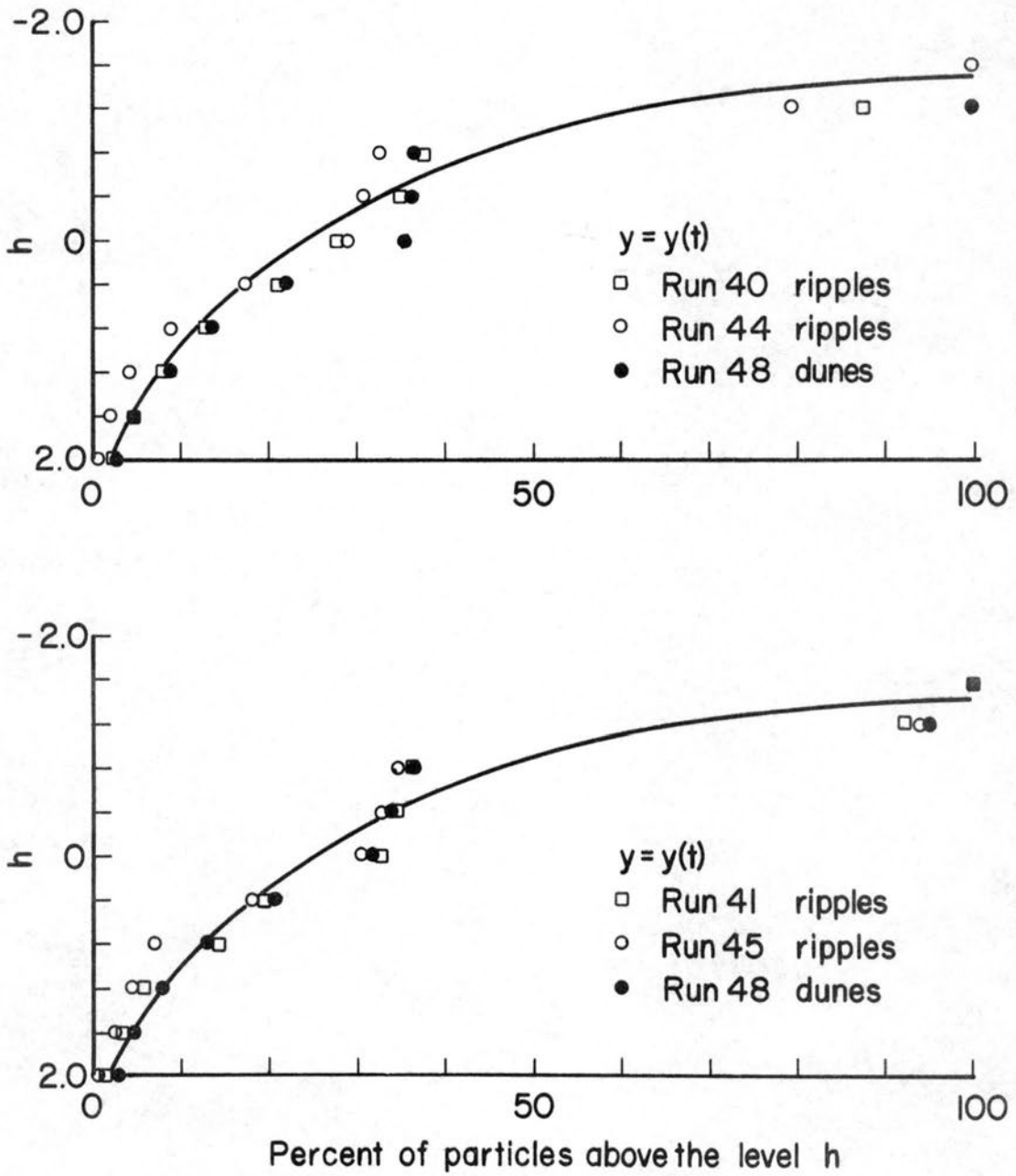

Figure 14. Graphs showing the percent of particles in the bed above the level h.

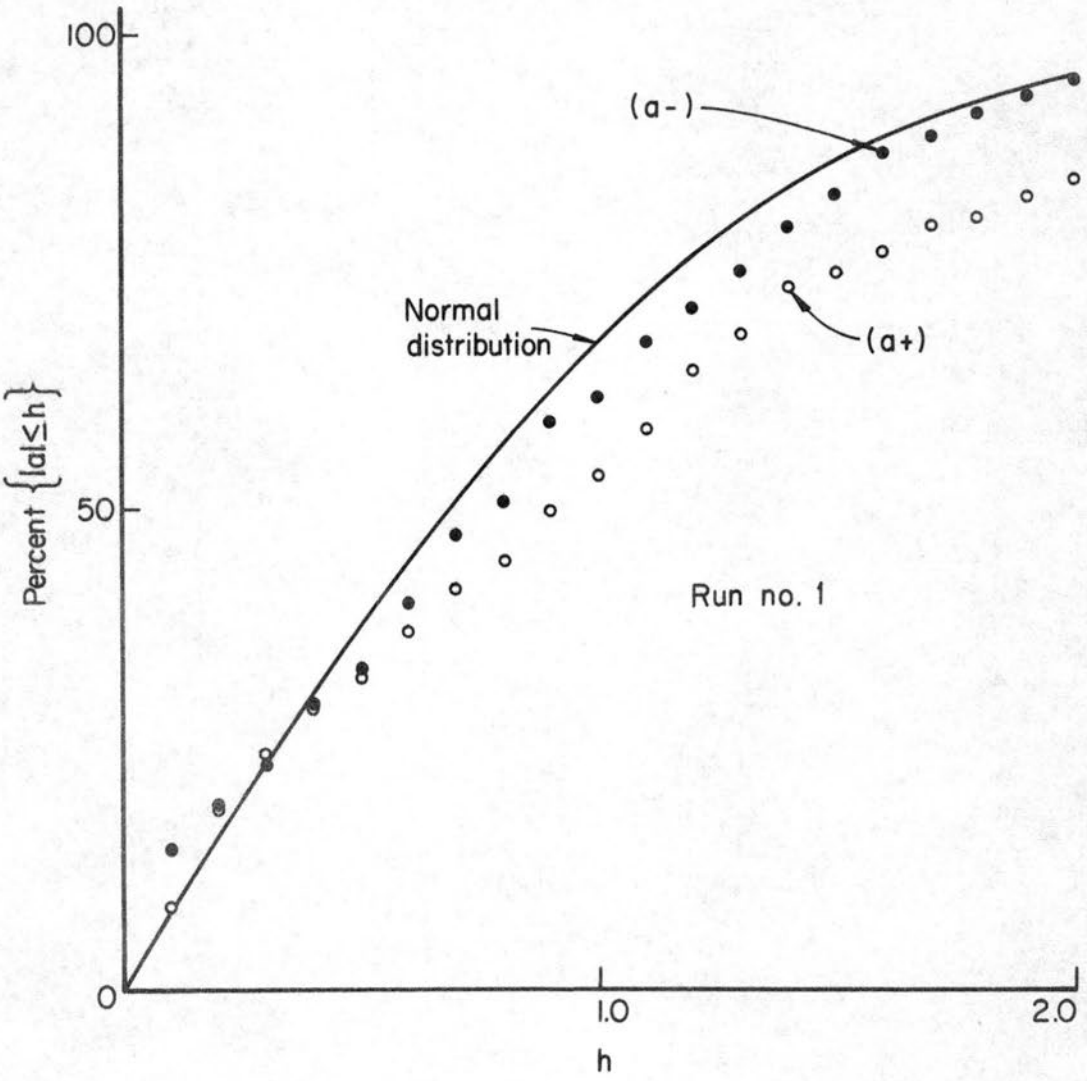

Figure 15. Distribution of positive and negative a values for run 1.

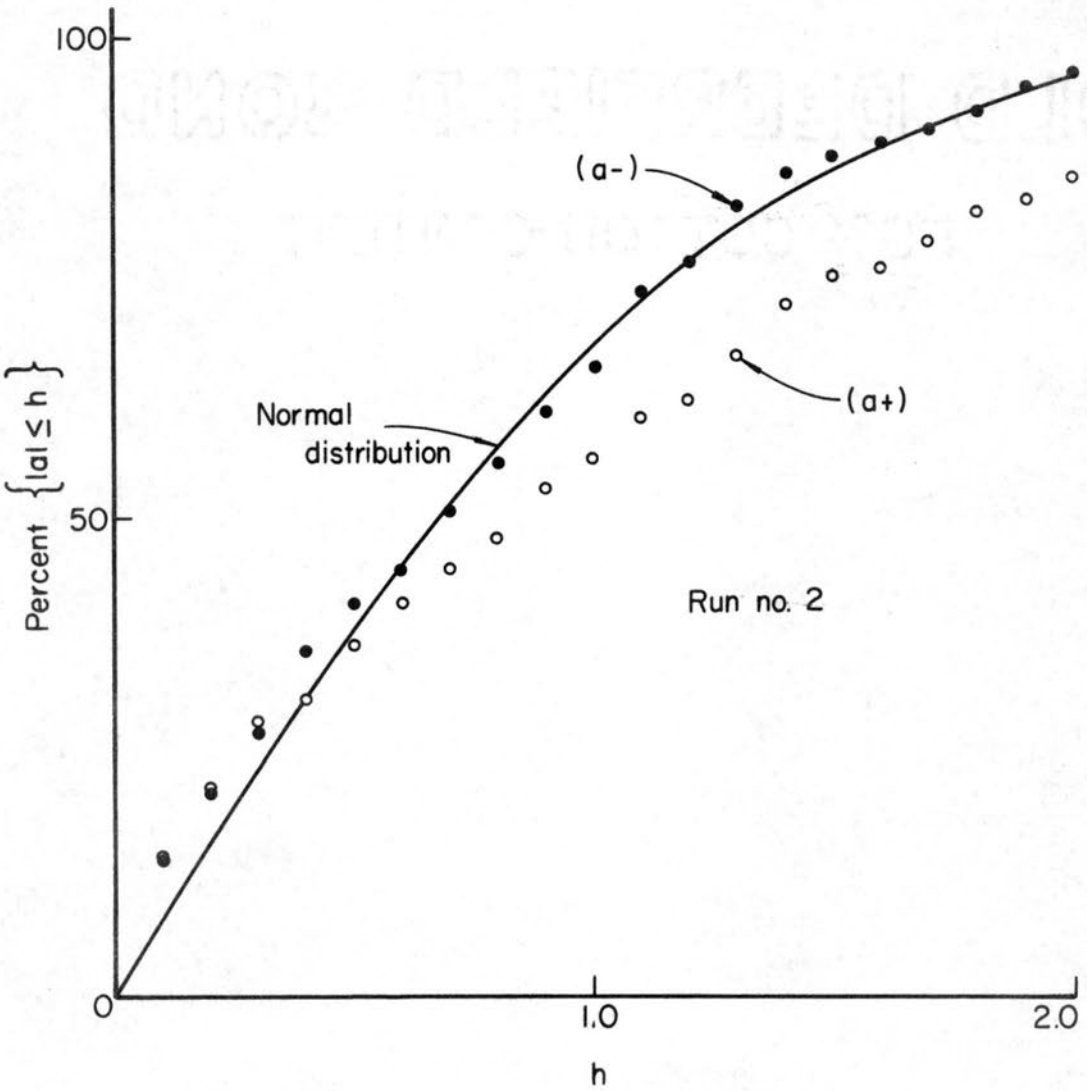

Figure 16. Distribution of positive and negative a values for run 2.

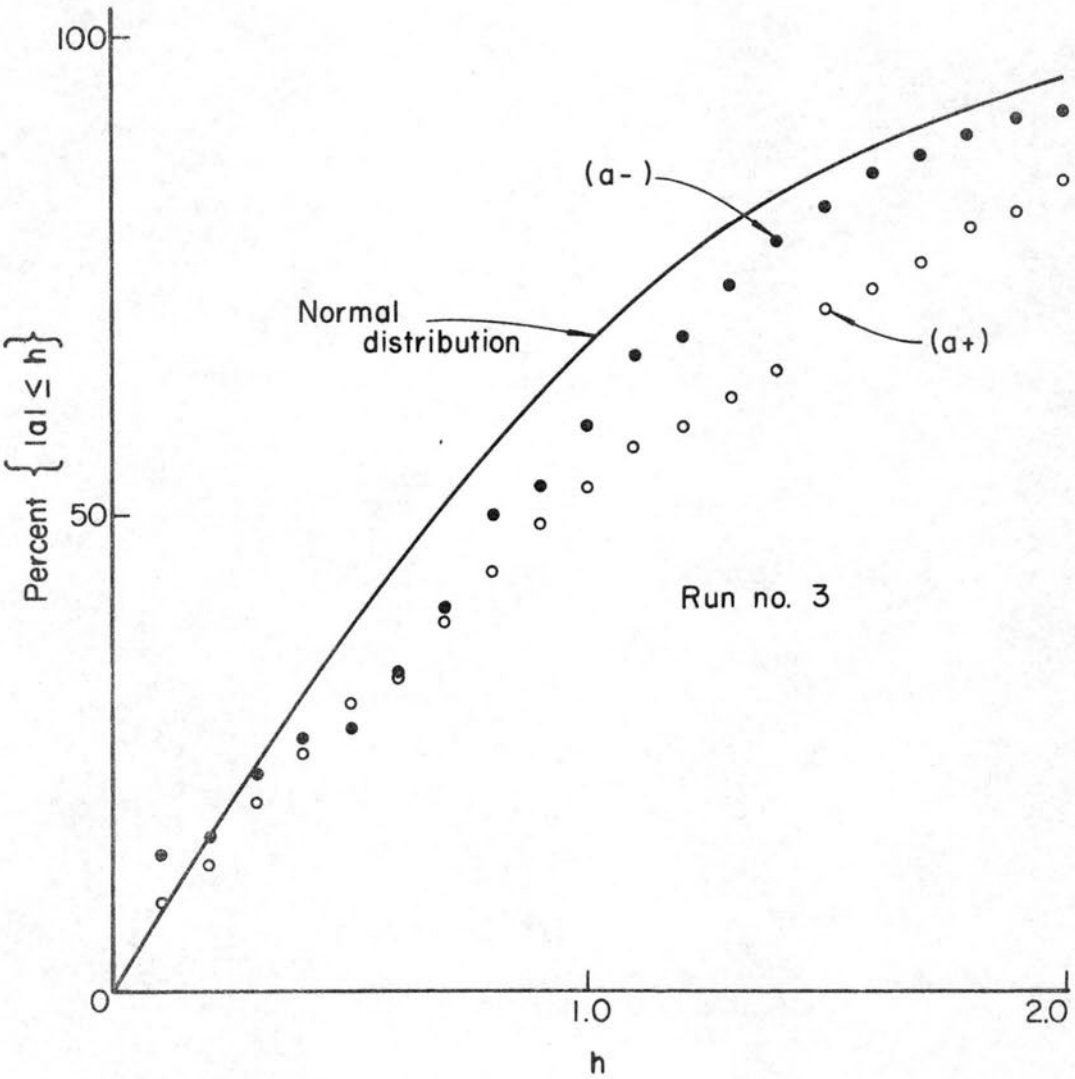

Figure 17. Distribution of positive and negative a values for run 3.

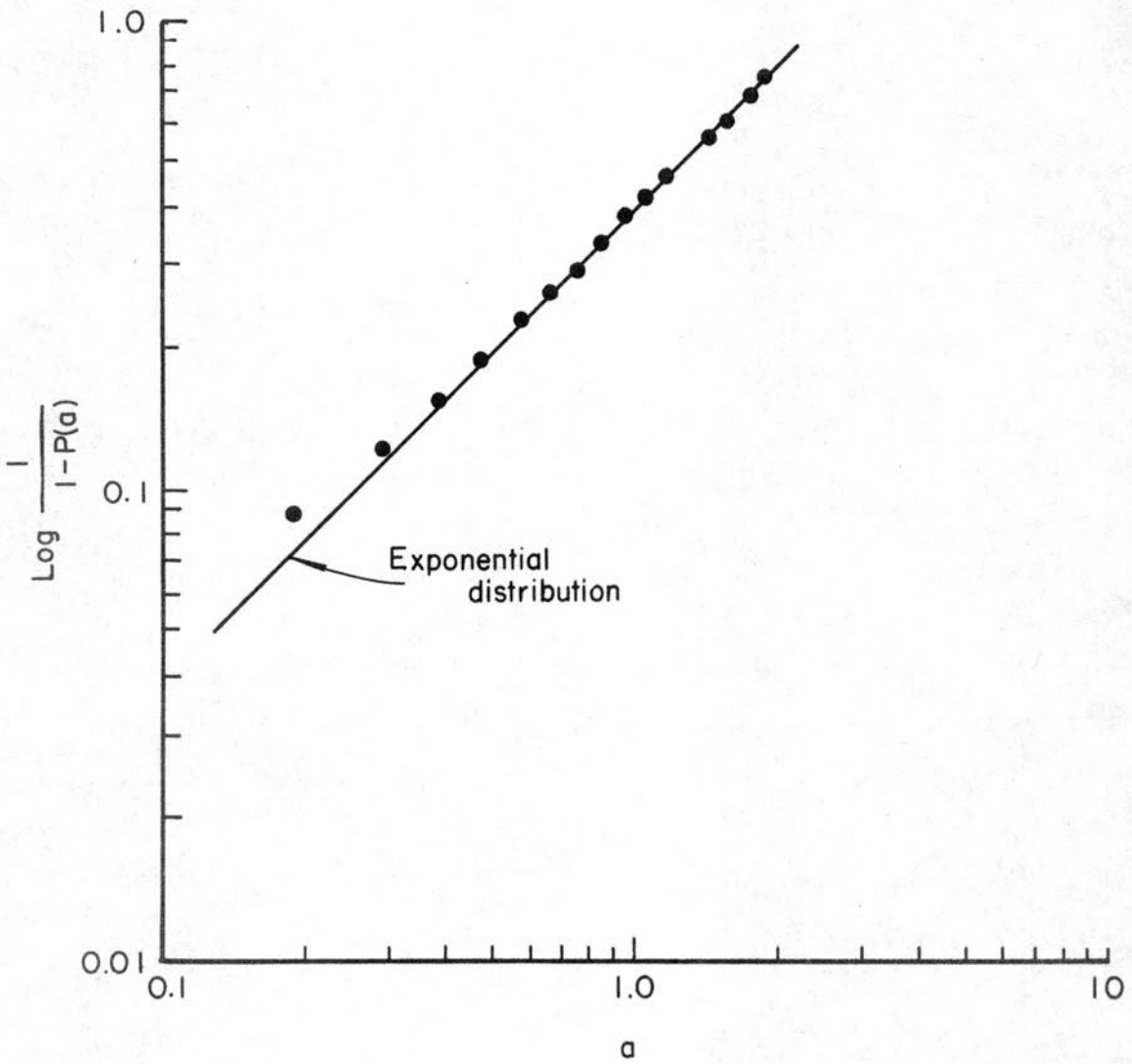

Figure 18. Approximate exponential distribution of positive a values for run 55.

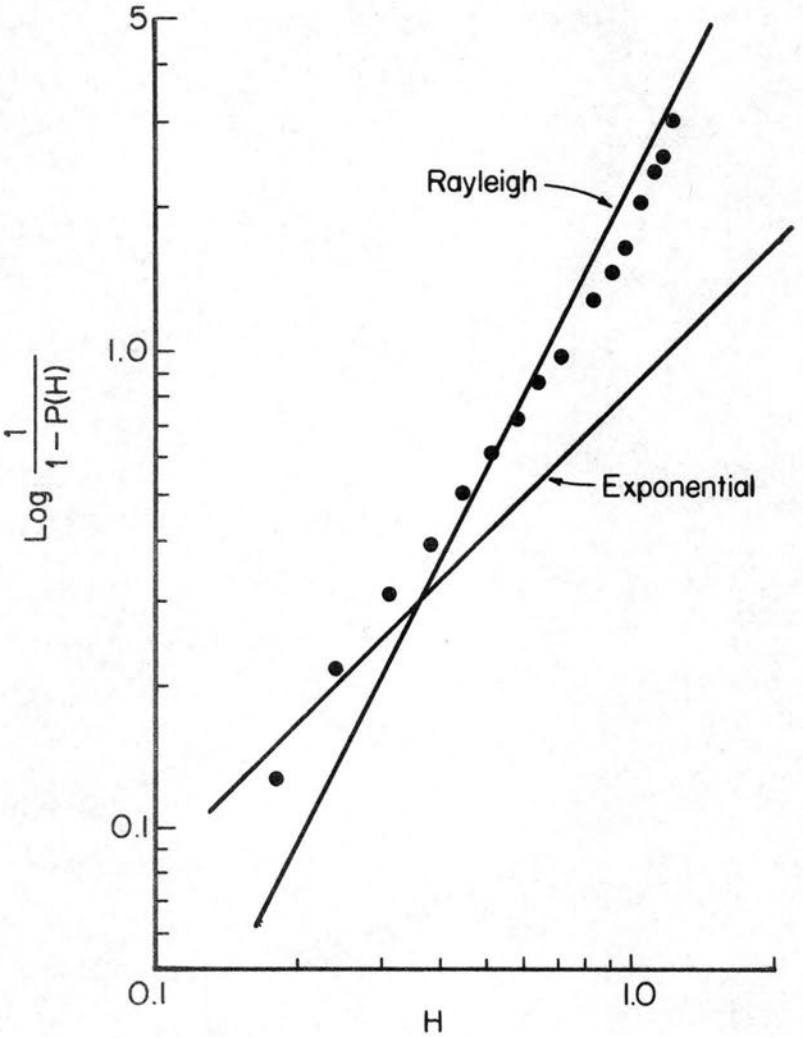

Figure 19. Distribution of wave heights, H, for run 55.

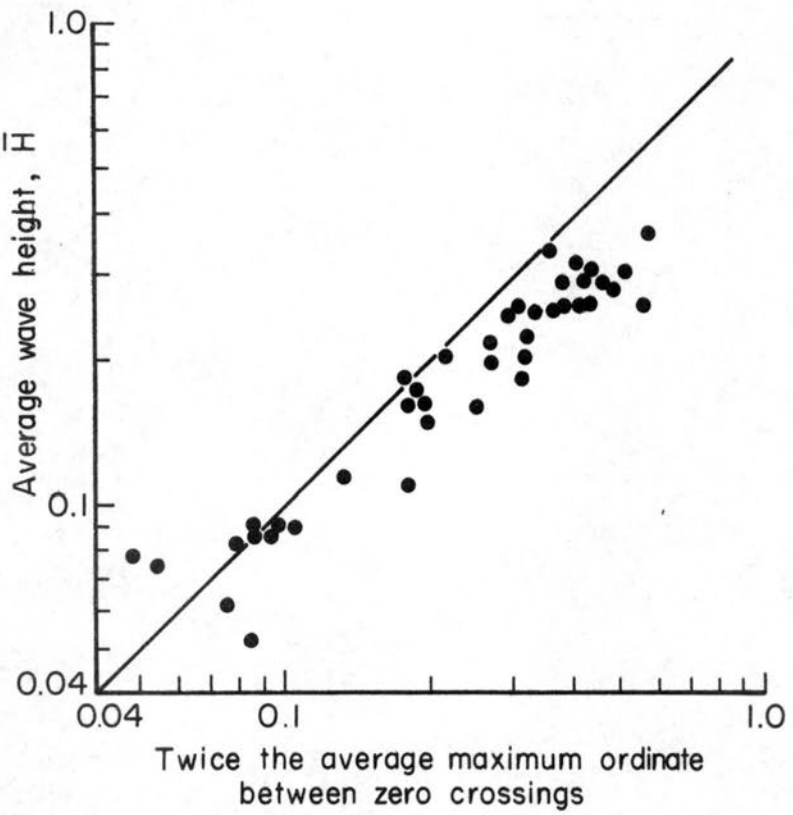

Figure 20. Relation between twice the average maximum ordinate between zero crossings, 2 a_+, and $\overline{H}$.

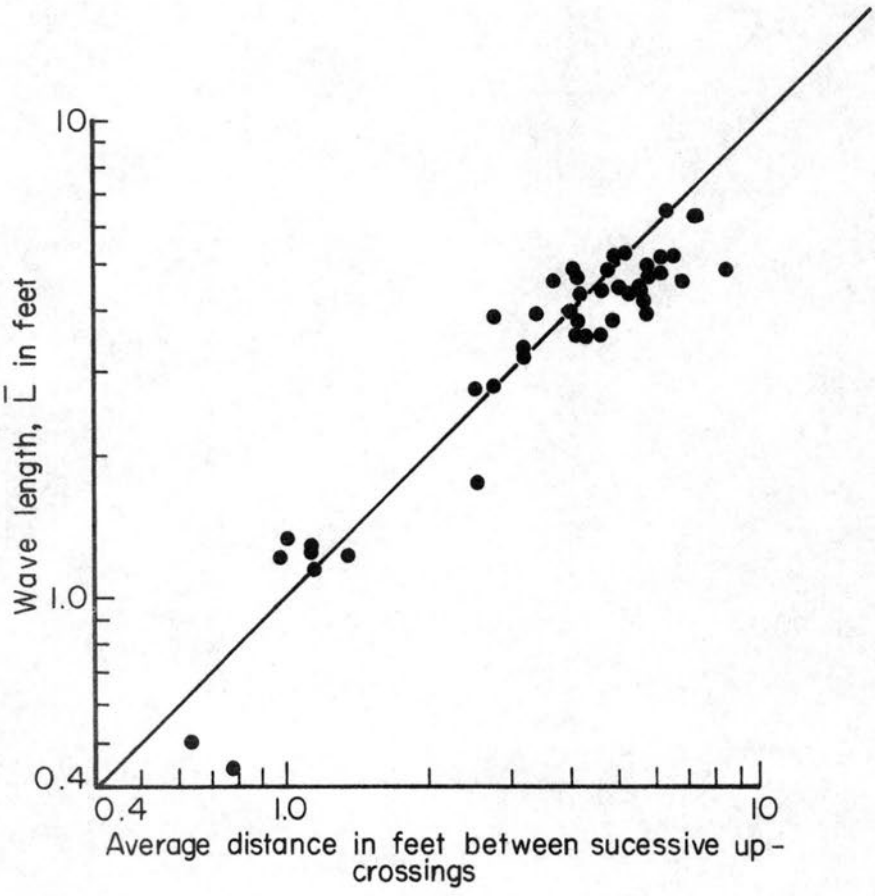

Figure 21. Relation between mean values of the distances between successive zero upcrossings of y and the mean dune length, $\bar{L}$.

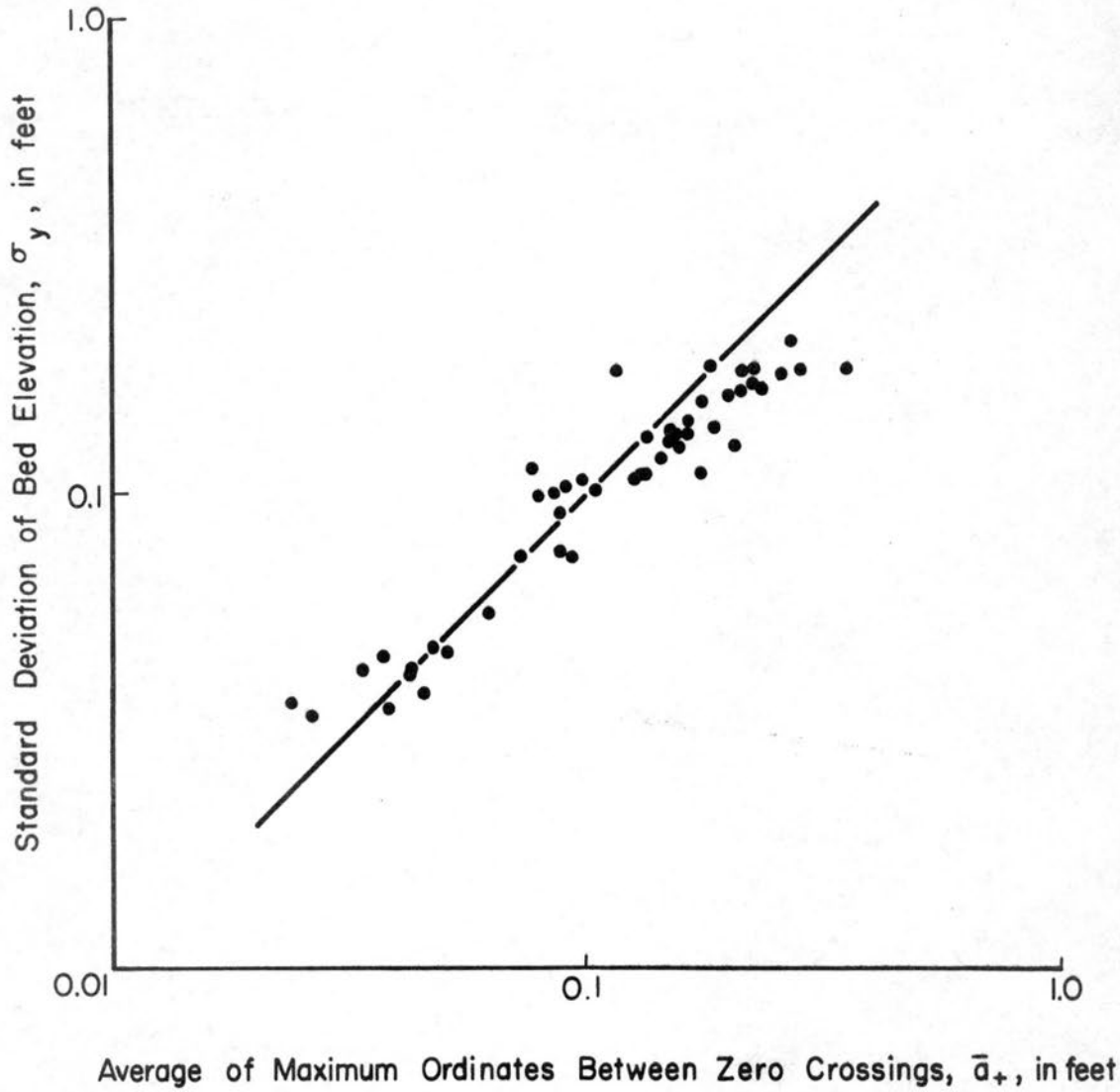

Figure 22. Relation between average of maximum ordinates between zero crossing, $\bar{a}_+$, and standard deviation, of bed elevation, σ_y .

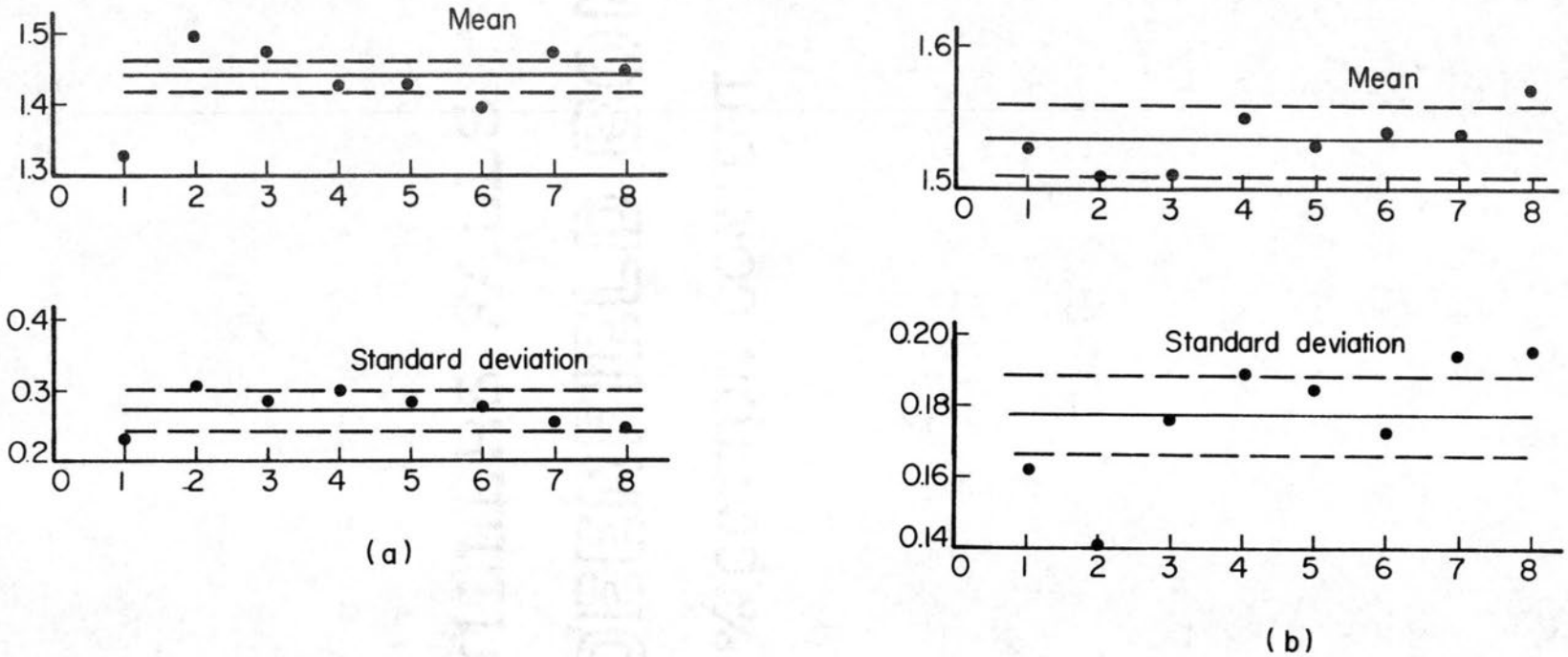

Figure 23. Comparisons of means and standard deviations, in feet, (a) for eight short segments of the record of run 3, Atrisco Lateral; (b) for eight longitudinal profiles during equilibrium flow in the 8-ft flume, runs 8 through 15. The solid line represents the average value and the dashed linesindicate a 90 percent significance level.

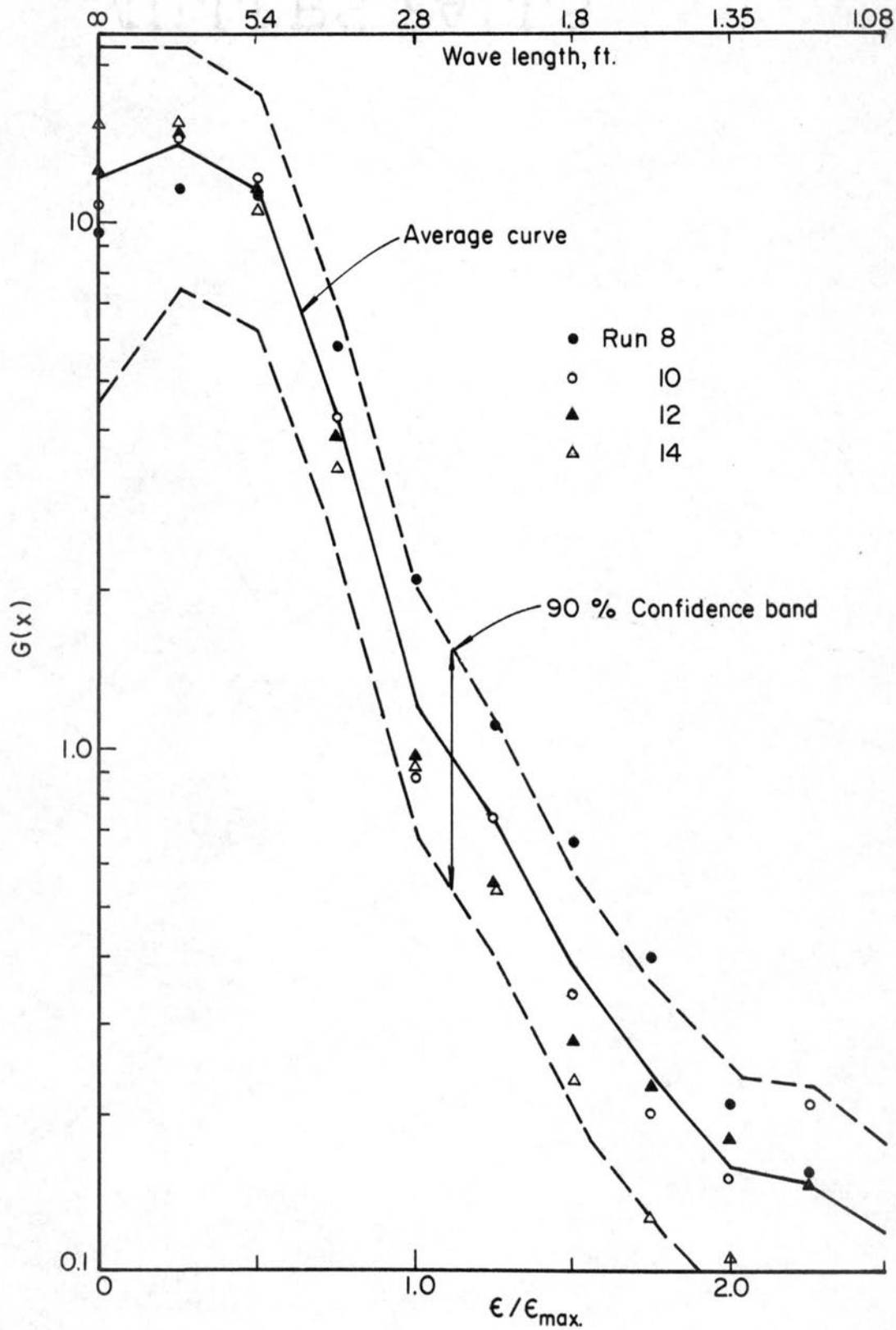

Figure 24. Spectra for indicated flume records.

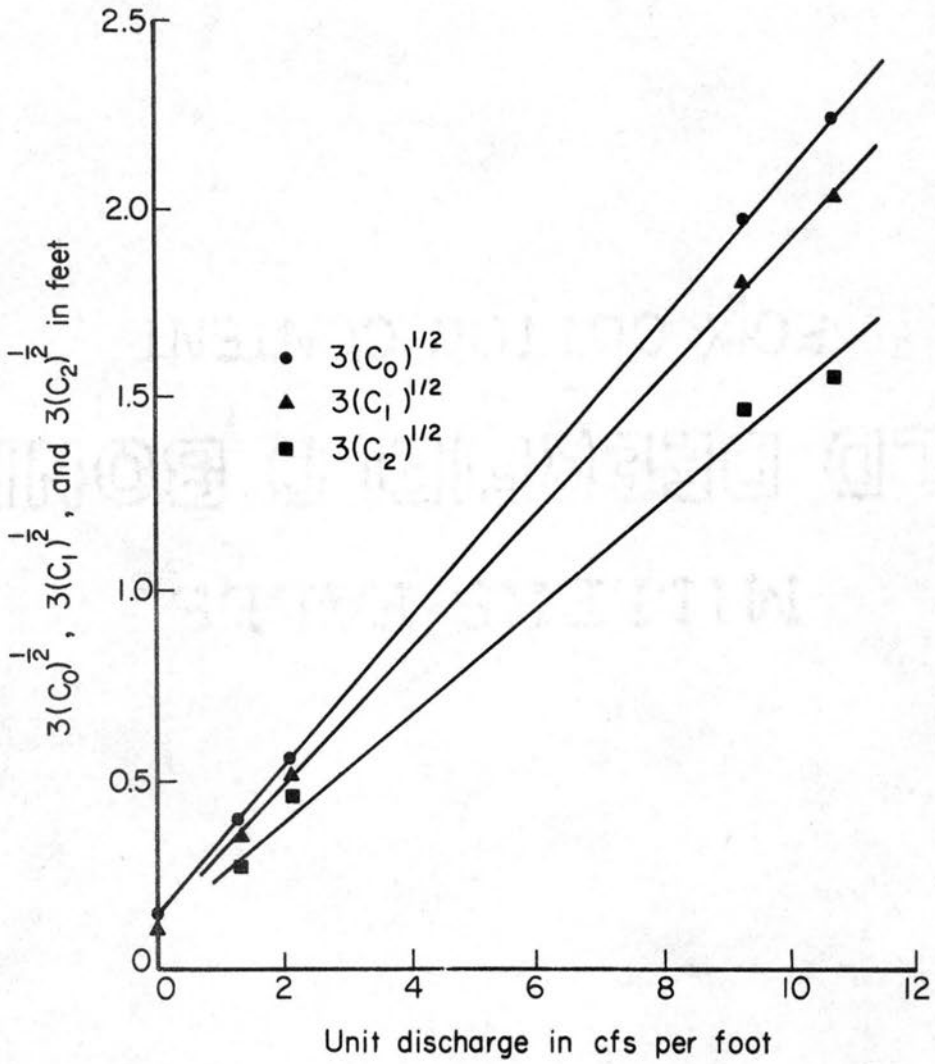

Figure 25. Relation of C_0, C_1, and C_2 to unit water discharge (after Nordin and Algert, 1966).

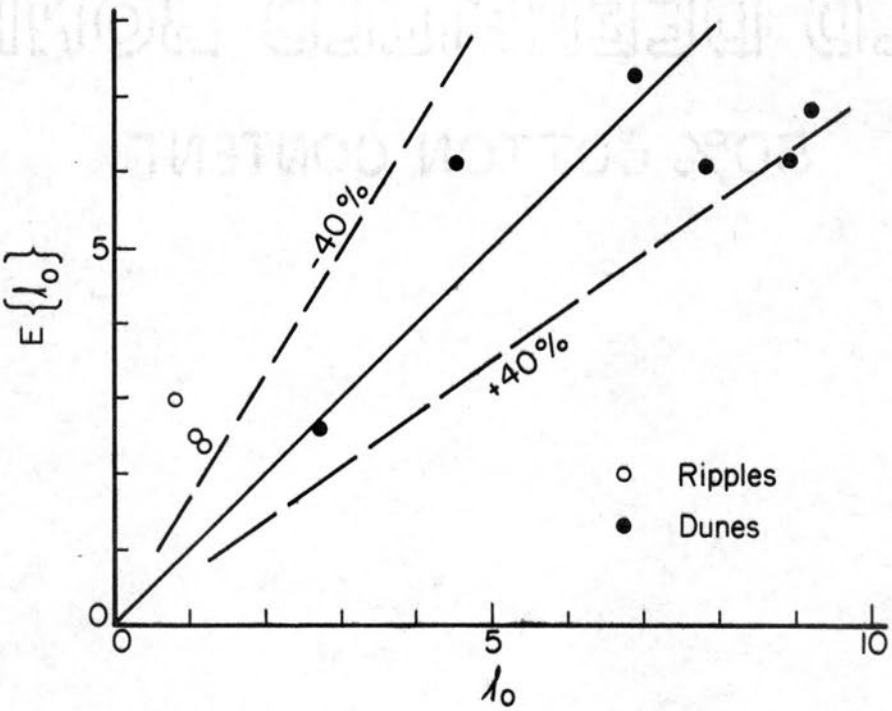

Figure 26. Comparison of estimated and observed average distance in feet between zero crossings.

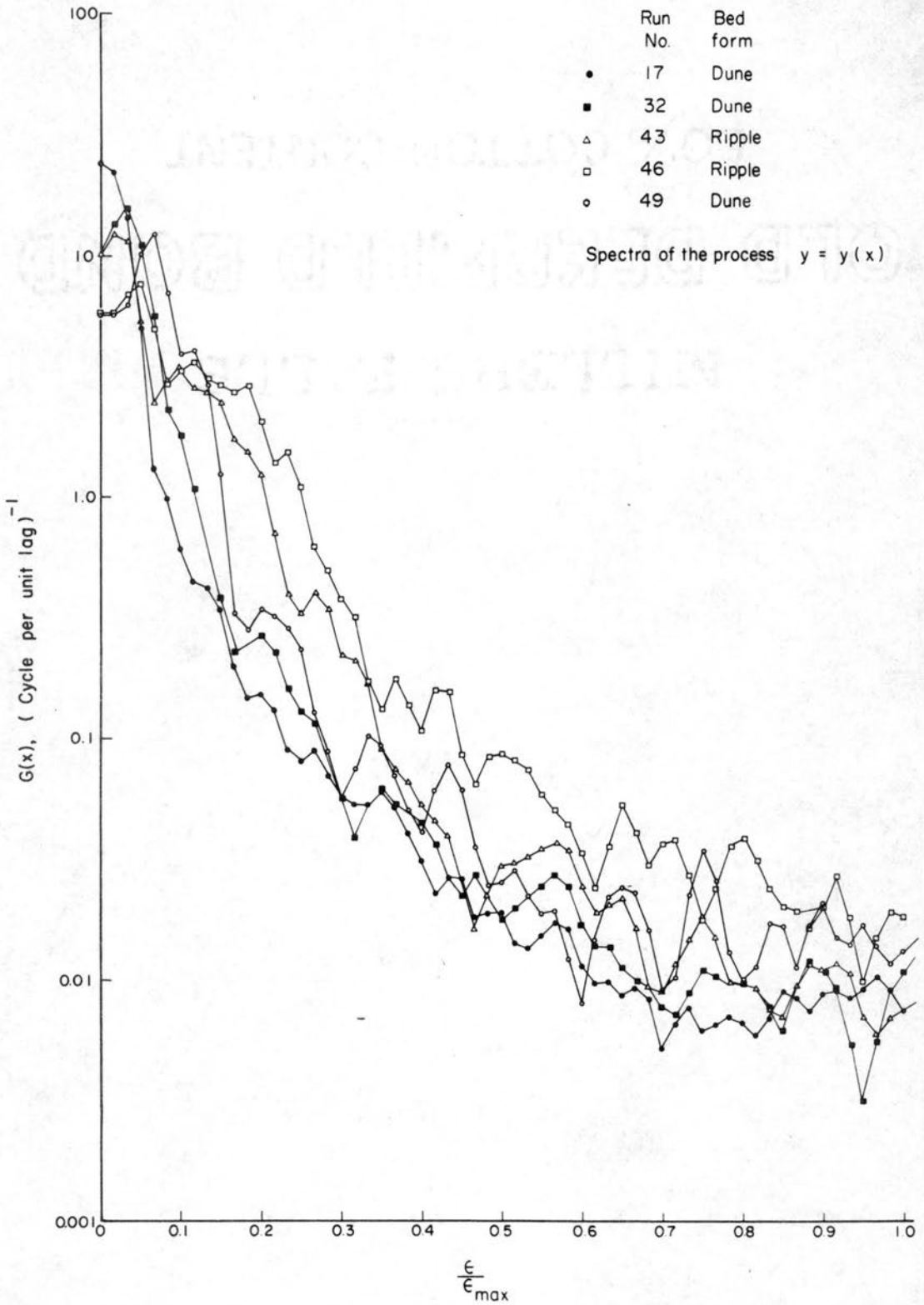

Figure 27. Spectra of the processes, y = y(x).

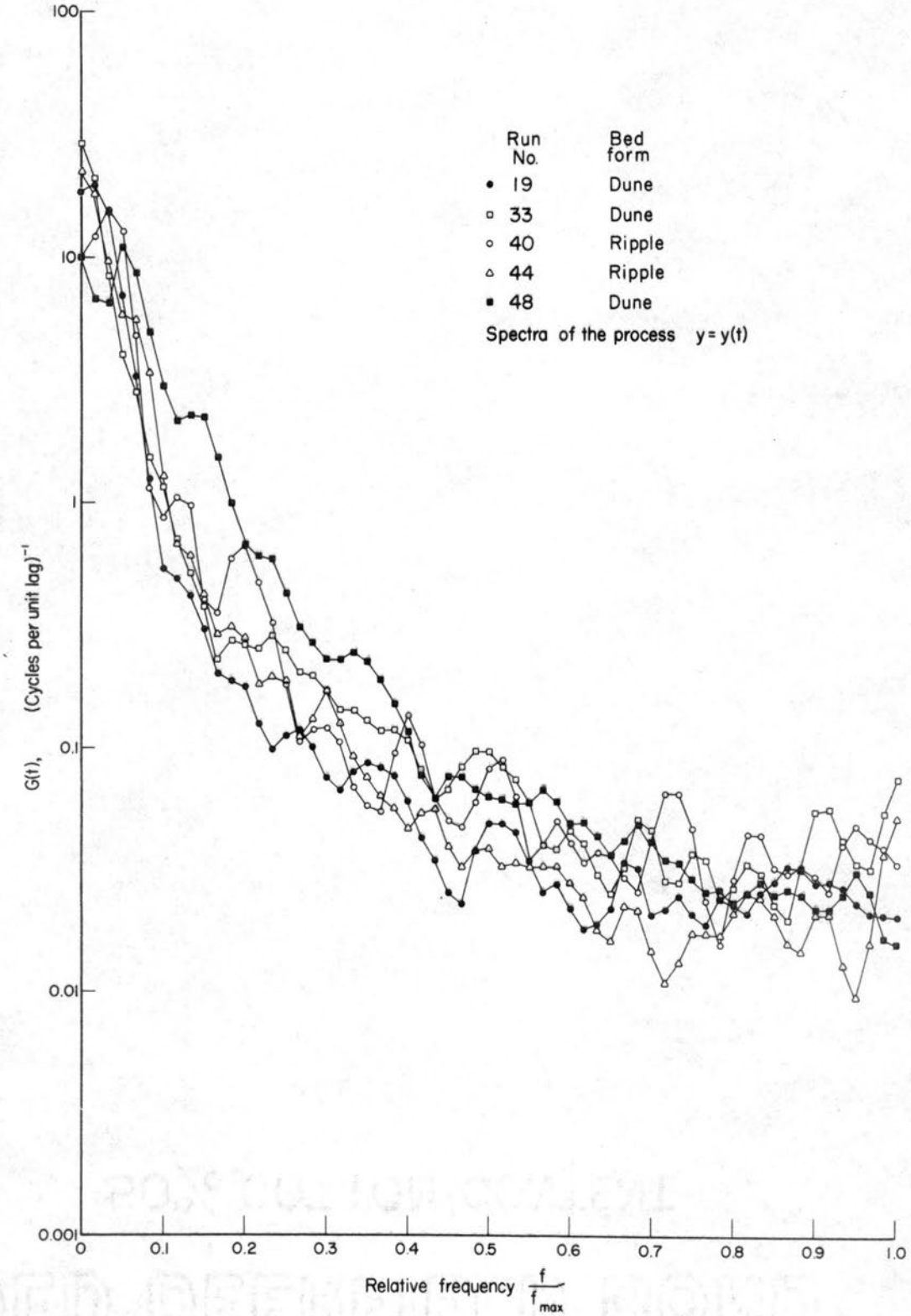

Figure 28. Spectra of the processes, y = y(t).

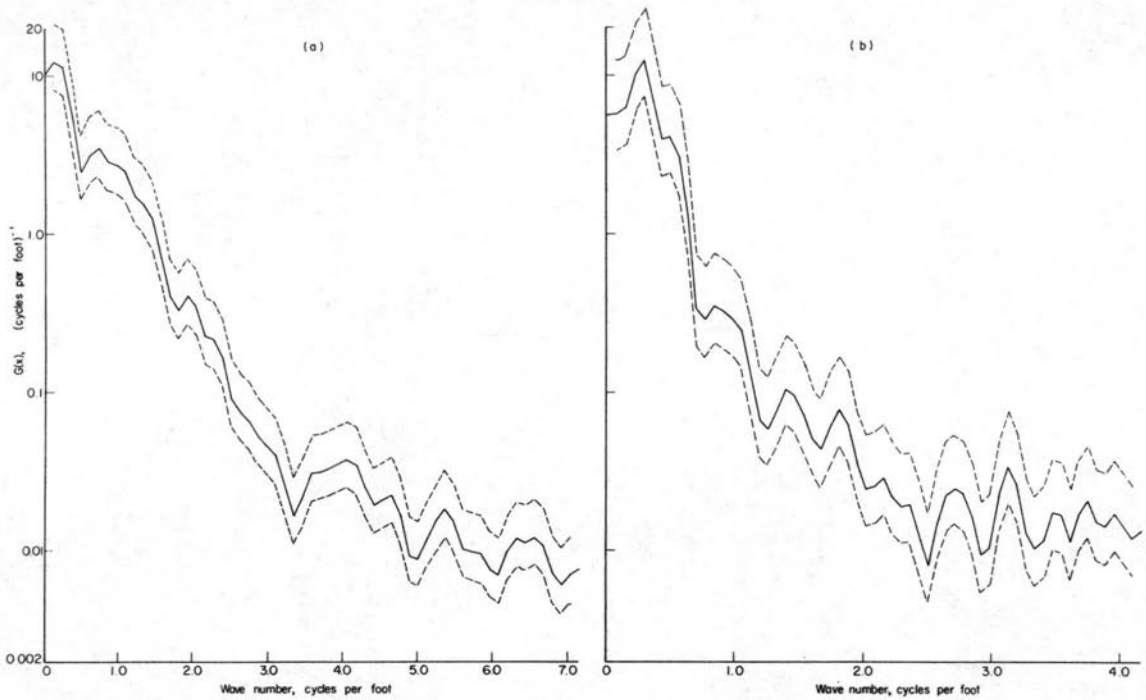

Figure 29. Comparison of ripple and dune spectra, 2-ft flume. (a) ripple, (b) dunes.

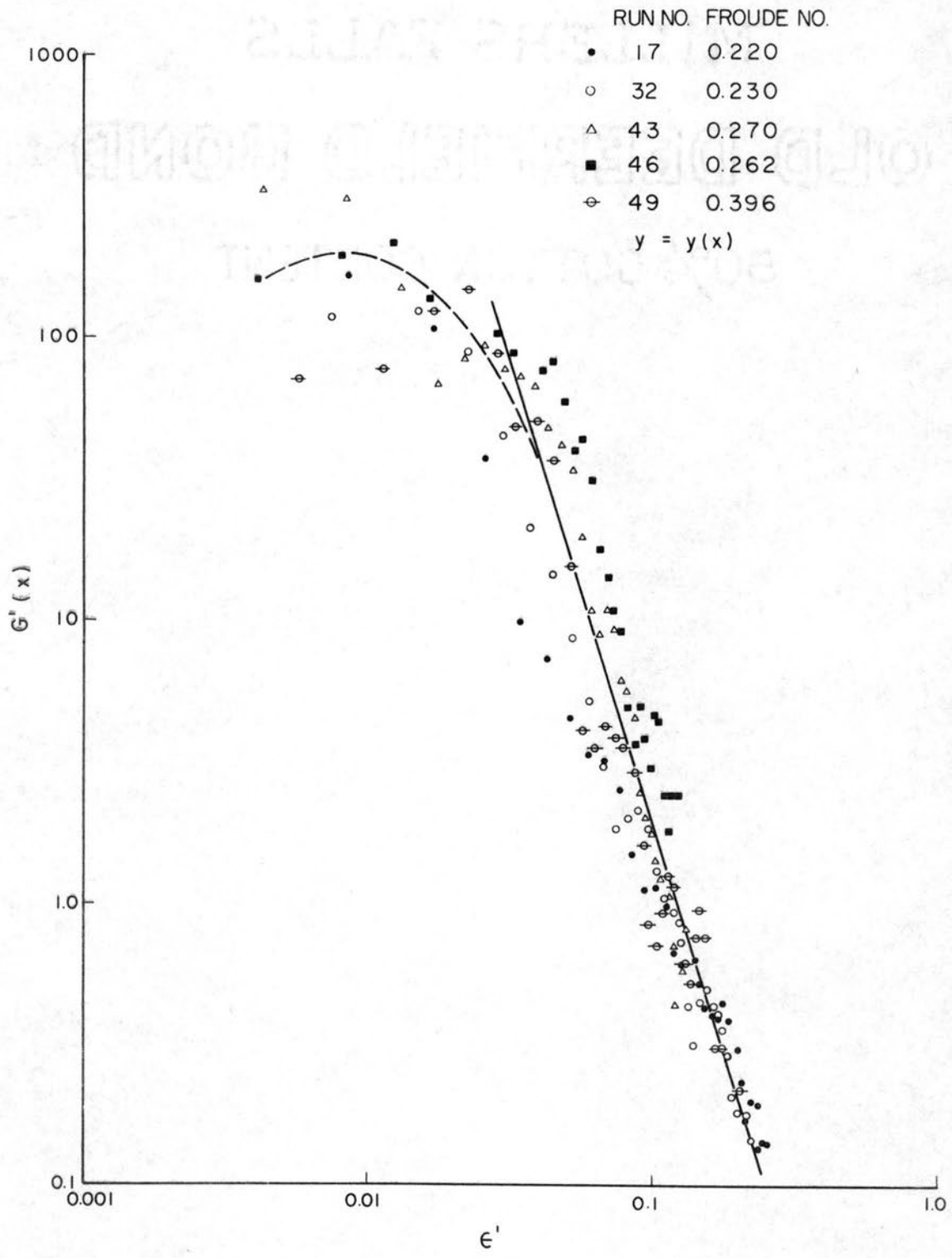

Figure 30. Dimensionless spectra for the process y = y(x).

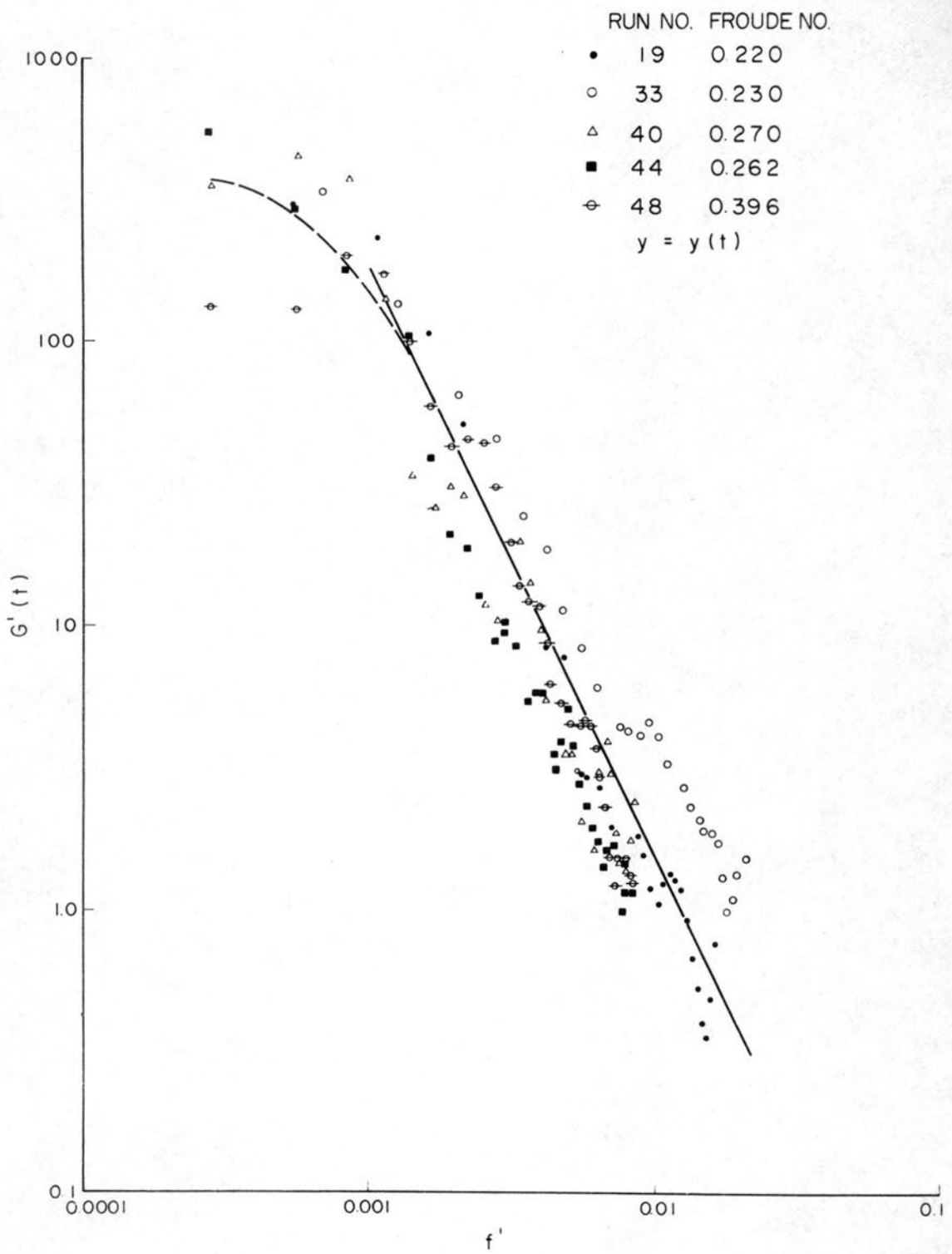

Figure 31. Dimensionless spectra for the process y = y(t).

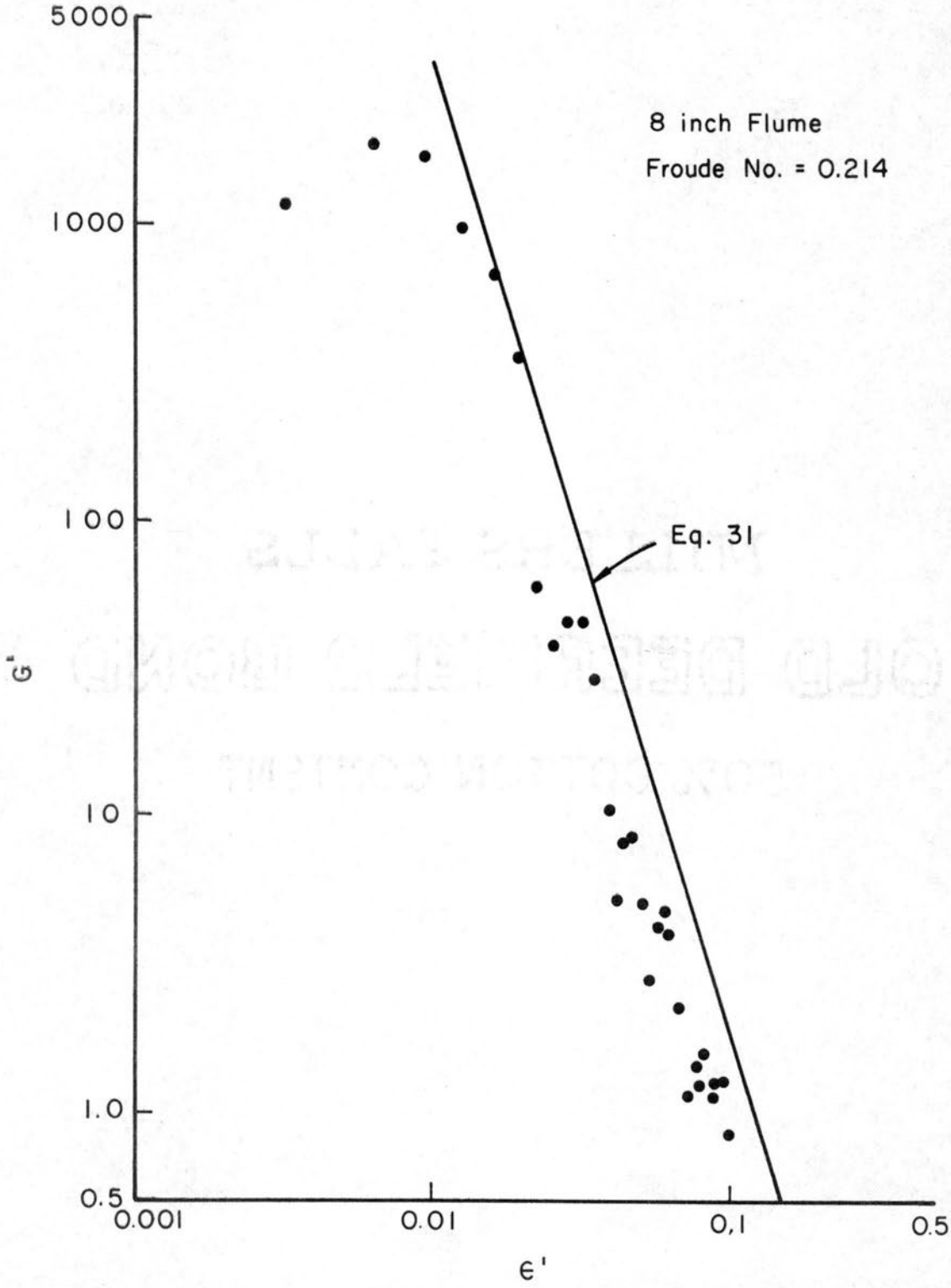

Figure 32. Dimensionless spectrum for y = y(x), 8-inch flume.

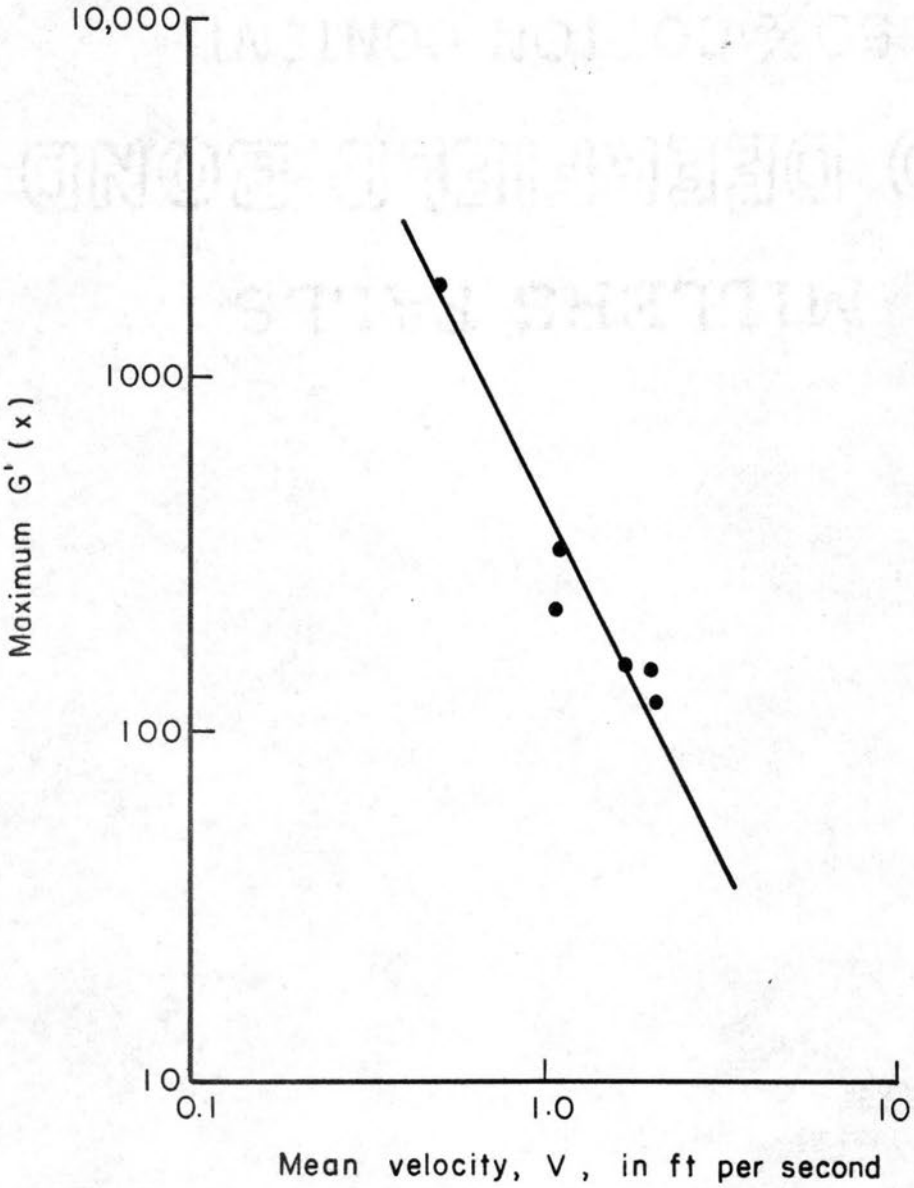

Figure 33. Relation of maximum value of G'(x) to mean velocity.

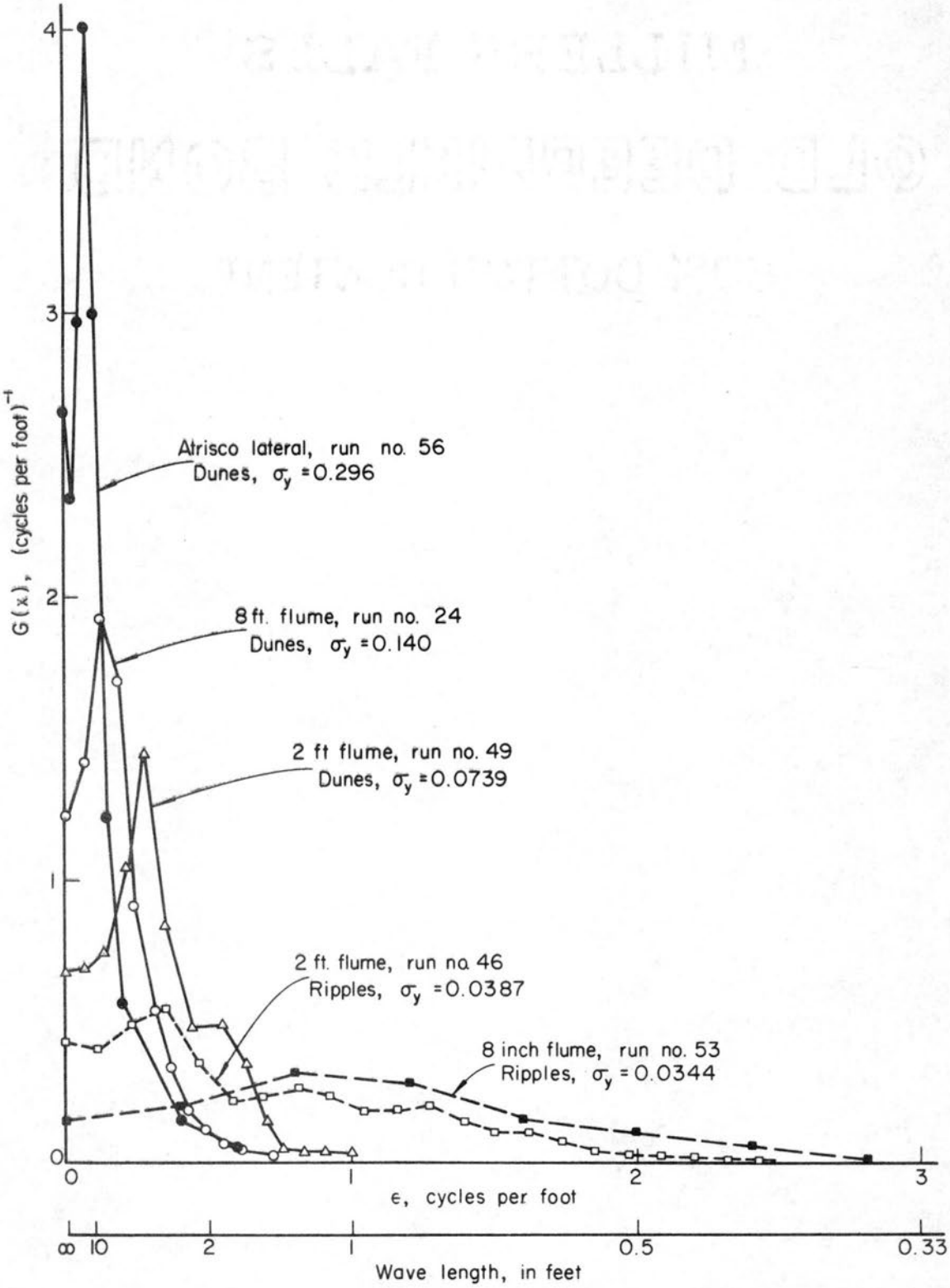

Figure 34. Spectra of longitudinal profiles, y = y(x), showing effect of channel size and bed configuration.

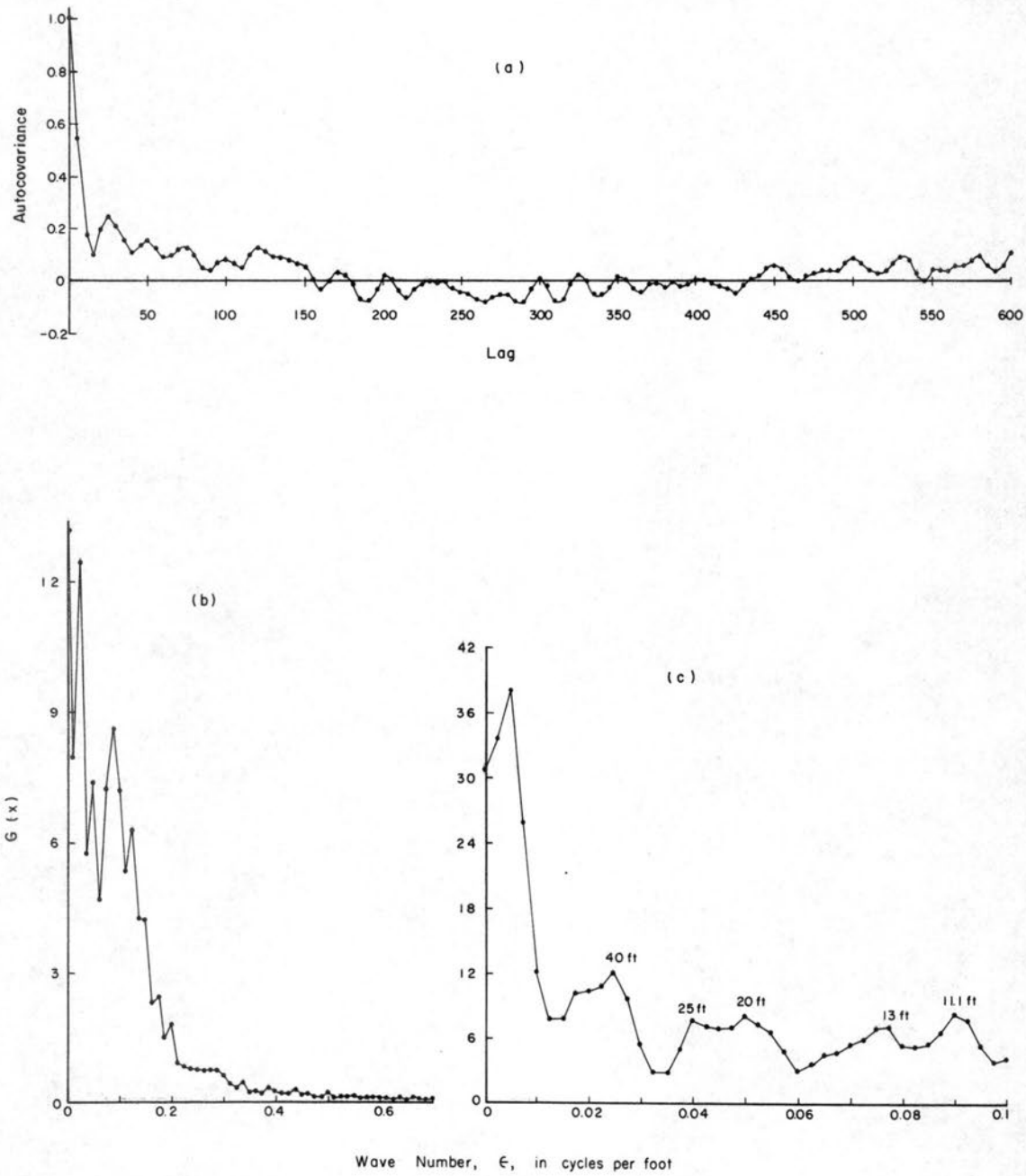

Figure 35. Autocovariance function and spectrum for run 3, Atrisco Lateral.

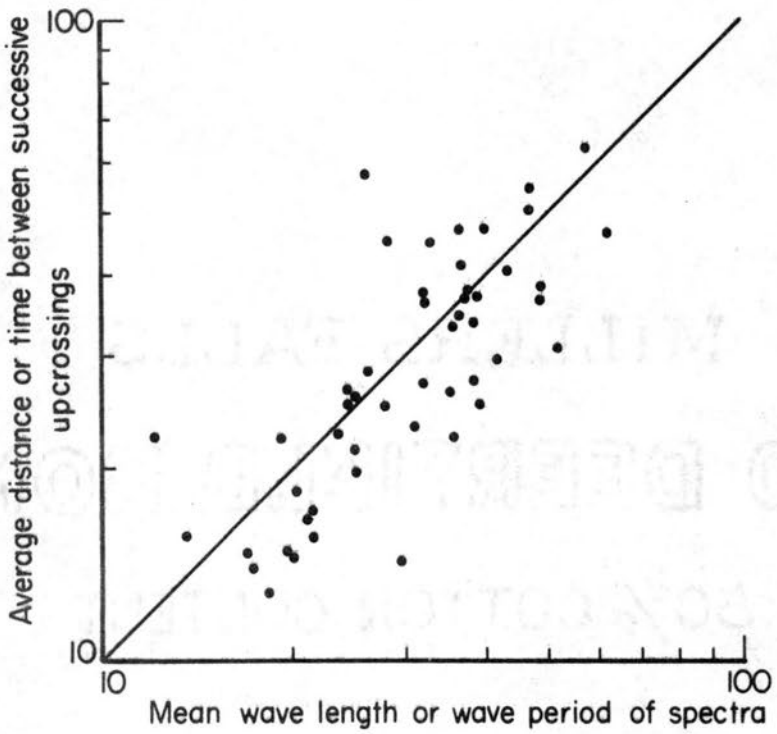

Figure 36. Relation between average distance or time between successive zero upcrossings and the mean wave length or period of spectra from Equation 8. Dimensions are in units of lag intervals.

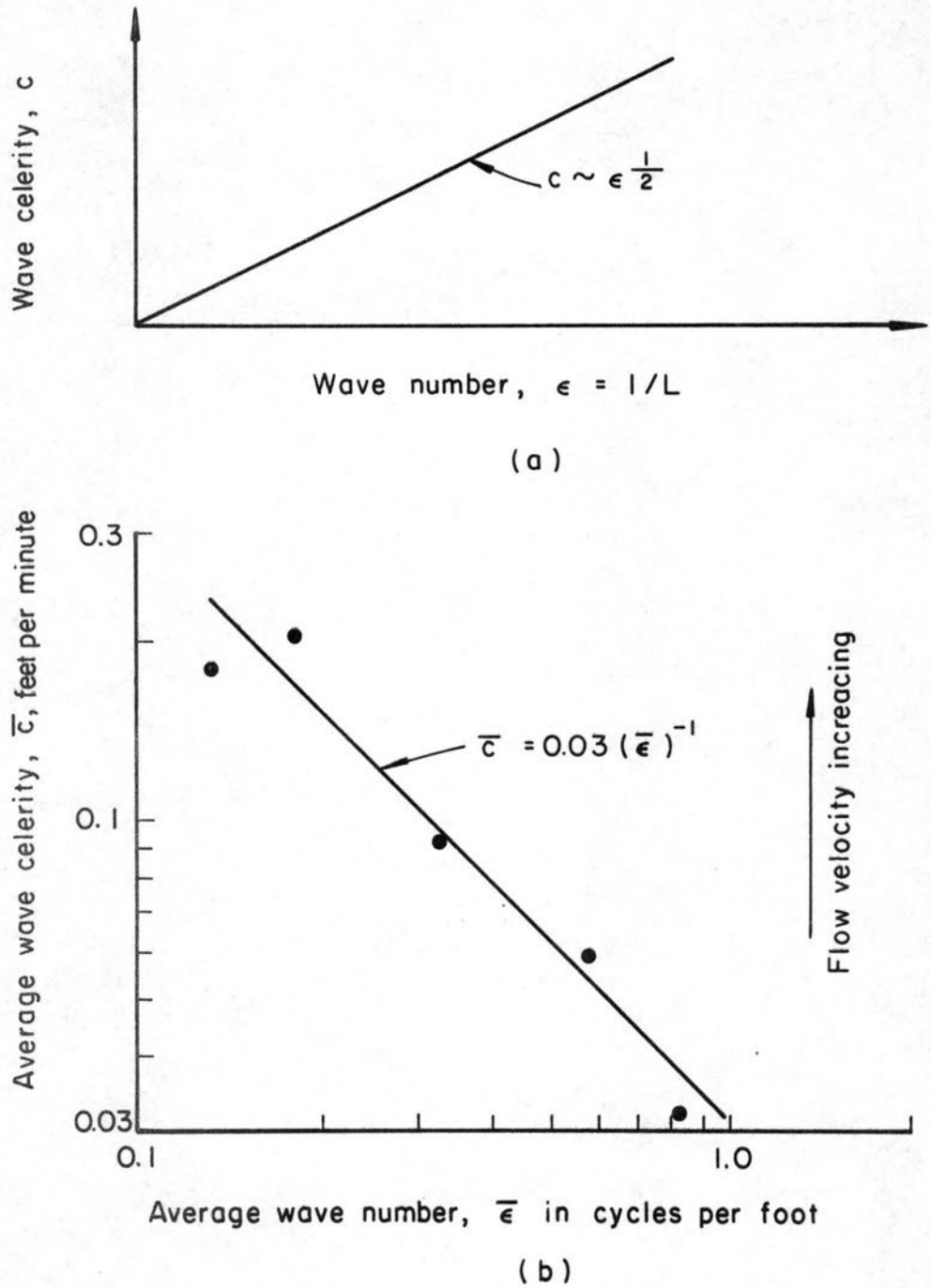

Figure 37. Relation of wave celerity, c, to wave number, ε, (a) for various wave-number components of a single record, flow conditions constant, (b) for average wave numbers from the spectral moments of records obtained under different flow conditions.

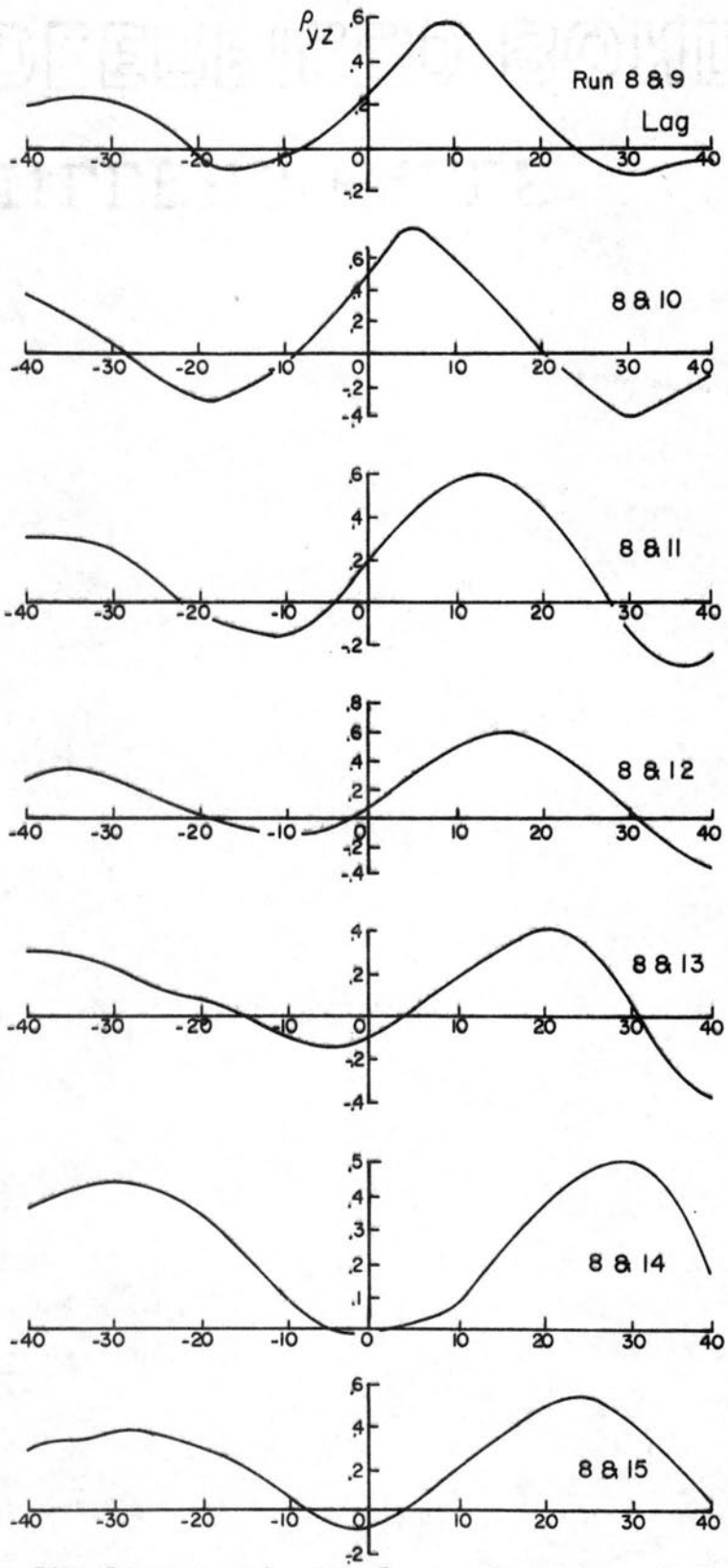

Figure 38. Cross-correlograms for run 8 with runs 9 through 15.

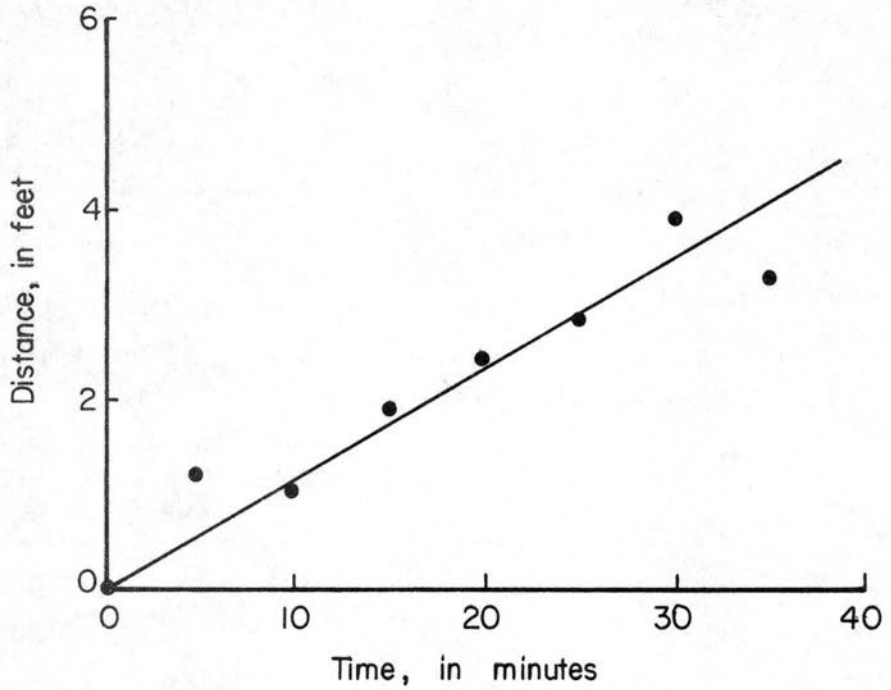

(a)

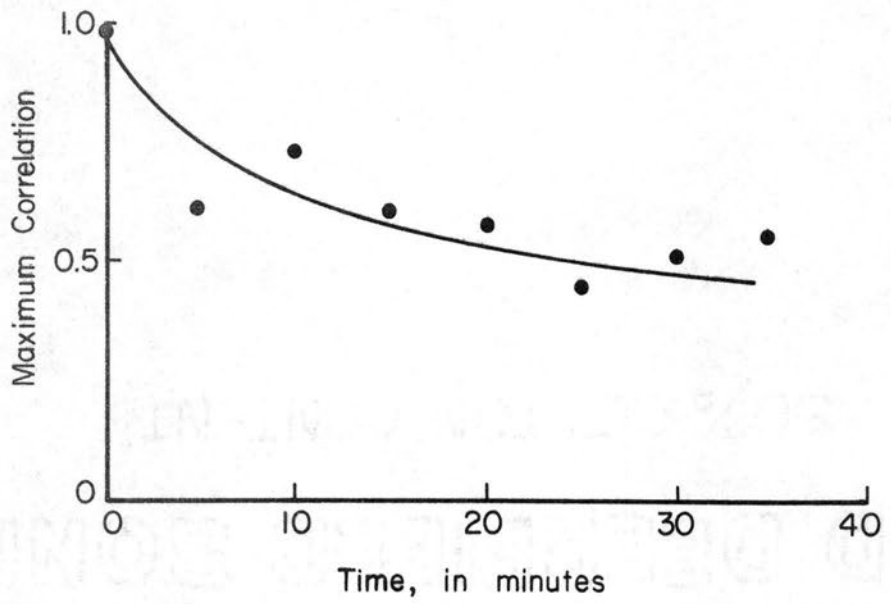

(b)

Figure 39. (a) Distance from the origin of the maximum cross-correlation as a function of time;
(b) Change in maximum correlation with time.

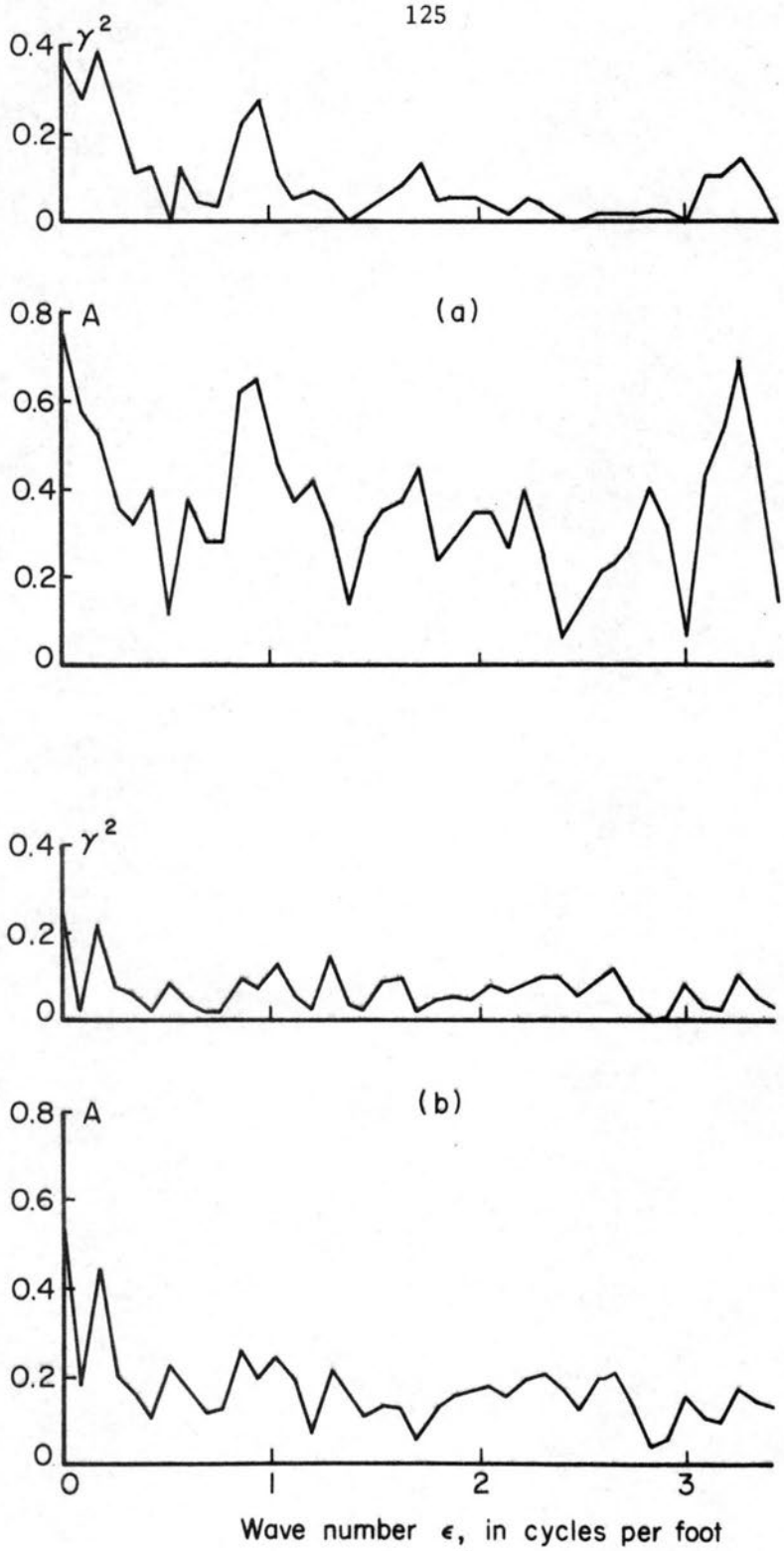

Figure 40. Coherence, γ^2, and gain functions, A, (a) for runs 8 and 9, (b) for runs 9 and 15.

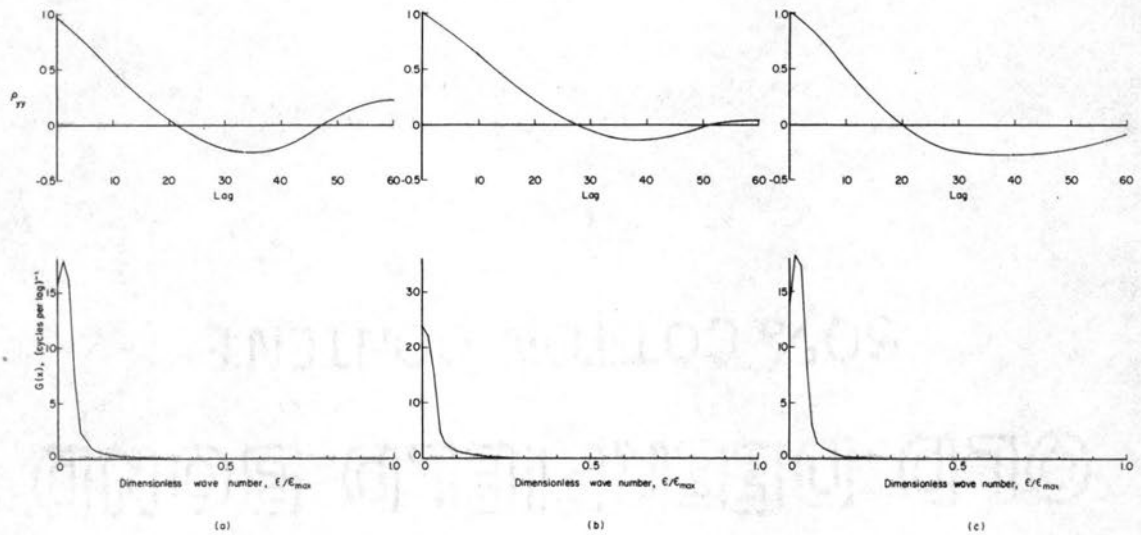

Figure 41. Correlograms and spectra for y = y(x), (a) run 16, two feet left of centerline; (b) run 17, centerline; (c) run 18, two feet right of centerline.

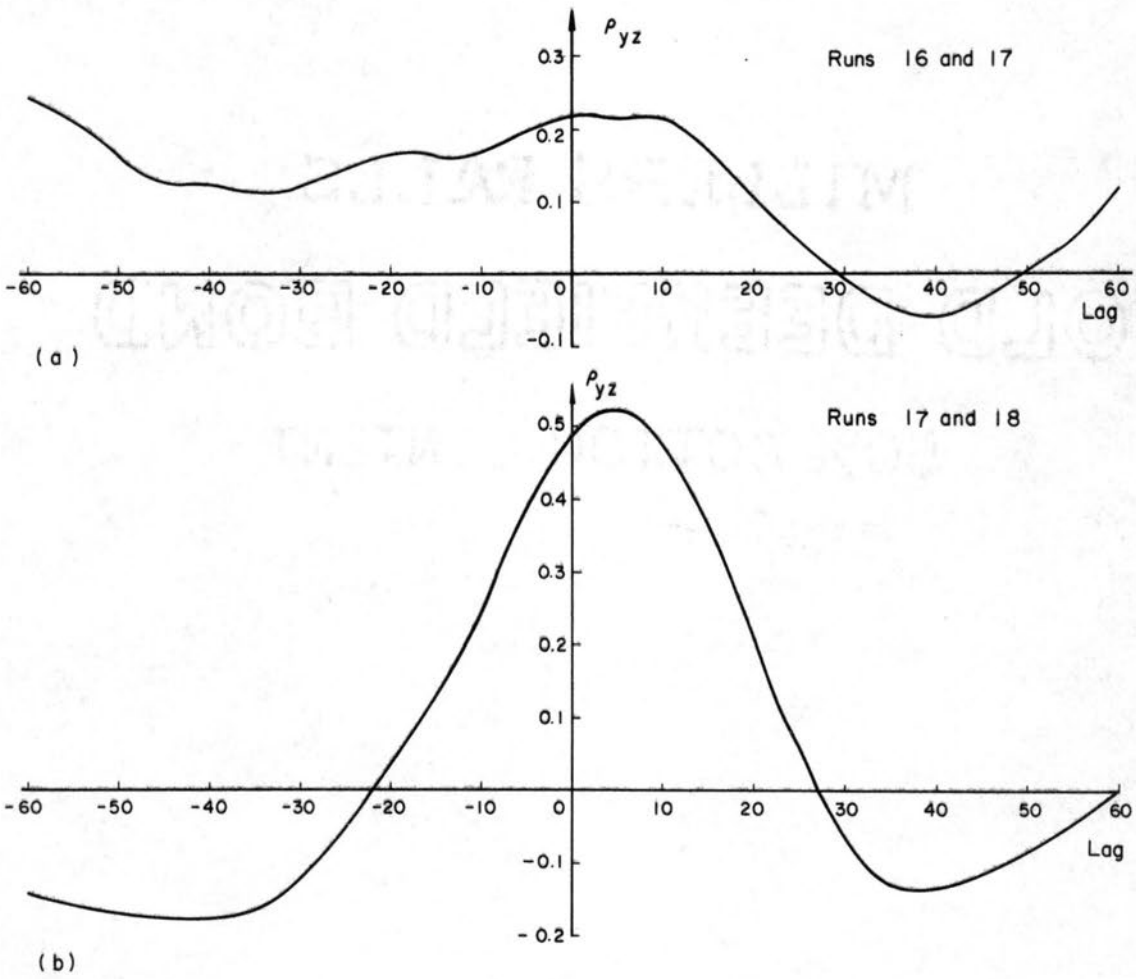

Figure 42. Cross-correlograms (a) runs 16 and 17, (b) runs 17 and 18.

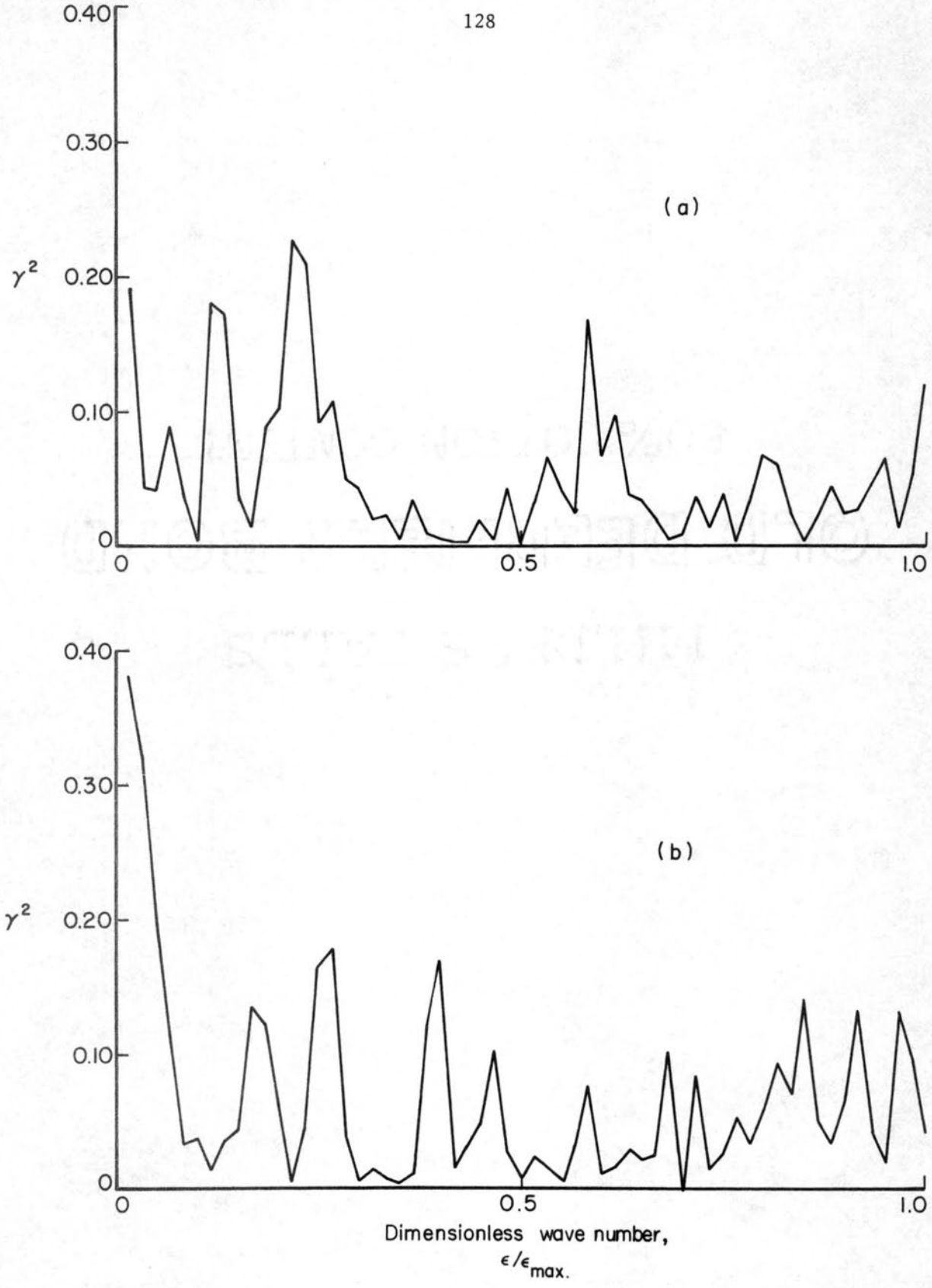

Figure 43. Coherence diagrams (a) runs 16 and 17, (b) runs 17 and 18.

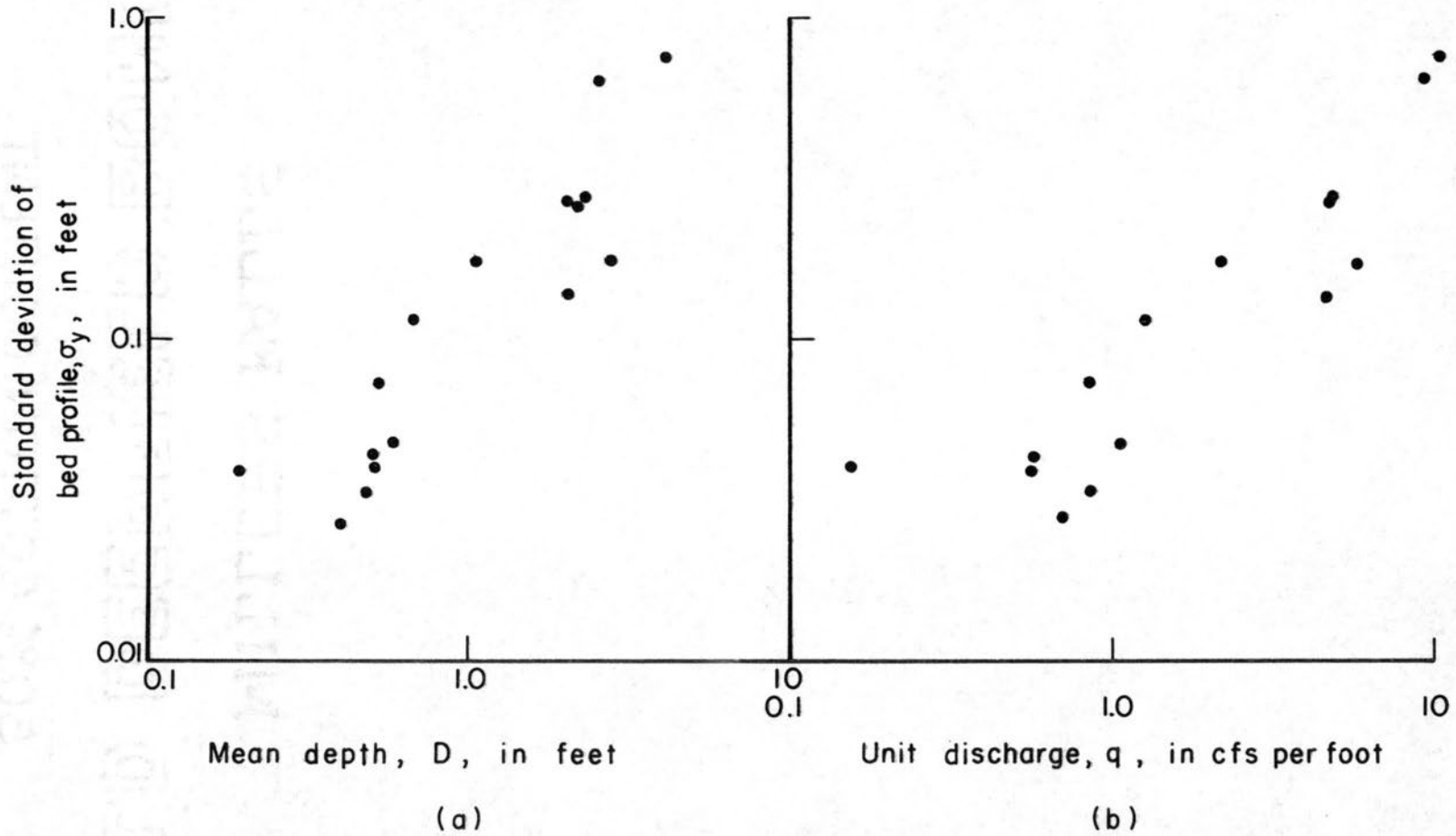

Figure 44. (a) Relation of standard deviation of bed profiles, σ_y, to mean flow depth, D;
(b) Relation of standard deviation of bed profiles, σ_y, to unit water discharge, q.

APPENDIX III

PLANNING OF DATA REQUIREMENTS

APPENDIX III

PLANNING OF DATA REQUIREMENTS

This appendix gives some approximate guidelines for planning the length of records required for the various analyses considered in the text. The statistical basis for determining record length and the computational procedures are given by Bendat and Piersol (1966, p. 278-320), and will not be repeated here. The computer programs used in this study are available from the writer or from Mrs. Lois Niemann, Civil Engineering Department, Colorado State University.

The computational procedures used in this study can be applied to any continuous record of streambed elevation, provided that the record meets the necessary conditions for stationarity. From a practical point of view, this means that for longitudinal profiles, the channel cross section should not vary appreciably along the channel and that for either longitudinal or time records, the flow and sediment transport rates should be approximately constant during the period of observation.

We consider here only flow conditions where well-defined sand waves are known to be present at the streambed, that is, only lower regime flow. The bed configurations for lower regime flow are ripples, dunes, bars, and combinations of these features (Simons and Richardson, 1966). In the following discussion the computational procedures for spectral analysis of a single

record first are outlined. Next, some rough guidelines for determining the length of record and the spacing of observations for converting a continuous record to discrete data points for spectral analysis are given. Finally, the record length and spacing of data points for other types of analysis, such as estimating the mean lengths between zero and h-level crossings, are considered.

Computational Procedures

A continuous record of bed profile, $y = y(x)$ of length L_r is converted to discrete data points by sampling the continuous record at intervals $\Delta x = h$ ft, so that the sampling rate is $1/h$ samples per ft. The entire record is converted to N discrete data points, y_i, $i = 1,2, \ldots, N$. We consider the entire sequence of y_i values to have zero mean and unit variance. The covariance function corresponding to Equation 2 of the text is computed by the formula

$$\phi_{yy}(s) = \frac{1}{N - s} \sum_{n=1}^{N-s} y_n \, y_{n+s} \tag{3-1}$$

for $s = 0, 1, \ldots, m$, where m is the maximum number of lags.

Next, the finite cosine series transform function of the auto-covariances is computed from

$$\tilde{G}(s) = \sum_{J=0}^{m} \hat{\phi}(J) \cos \frac{Js\pi}{m} \tag{3-2}$$

for s = 0, 1, 2, ..., m. In the above,

$$\hat{\phi}(0) = \phi_{yy}(0)$$

$$\hat{\phi}(i) = 2\phi_{yy}(i),\ i = 1,2,\ \ldots,\ m-1 \qquad (3\text{-}3)$$

$$\hat{\phi}(m) = \phi_{yy}(m)\ .$$

The spectrum is computed from the equations

$$G(0) = 0.5\ \tilde{G}(0) + 0.5\ \tilde{G}(1)$$

$$G(i) = 0.25\ \tilde{G}(i-1) + 0.5\ \tilde{G}(i) + 0.25\ \tilde{G}(i+1) \qquad (3\text{-}4)$$

$$\text{for } i = 1, 2, \ldots, m-1$$

$$G(m) = 0.5\ \tilde{G}(m-1) + 0.5\ \tilde{G}(m).$$

These computations yield m+1 values for the spectrum at each of the lags s = 0, 1, ..., m, corresponding to the wave numbers $\varepsilon_s = s/2mh$ or to wave lengths $L_s = 2mh/s$.

Length of Record and Spacing of Data Points

The computational procedures outlined above show that in selecting a length of continuous record for spectral analysis by digital techniques, three quantities must be considered: the record length, L_r, the sampling (digitizing) rate, h, and the maximum lag, m. The smallest wave length for which spectral estimates are computed is 2h and the largest wave length for which the spectral estimates are computed is 2mh.

As a general rule, we should select a sampling rate such that $2h \leq L_{min}$, where L_{min} is the smallest wave-length component of interest, and a maximum lag m such that $2mh \simeq L_{max}$, where L_{max} is the largest wave-length component of interest. The record length, L_r, should be no less than 10mh for the percentage error of the estimated spectrum to be of reasonable size (Parzen, 1967).

For a given bed form, say dunes, quite satisfactory results have been obtained by selecting mh approximately equal to the mean dune length, by sampling at an interval h so that the average dune length is represented by 20 to 30 data points, and by selecting a length of record 10 to 20 times the mean dune length. For the case where ripples are superposed on the backs of dunes, a sampling interval h of about one-fourth the mean ripple length is recommended. Generally, the contribution to the total variance of wave-number components greater than four cycles per foot was negligible in the case of ripples. For dunes, the contribution to the variance from components greater than one cycle per foot was negligible.

Where large alternate bars with smaller bed forms superposed are known to exist in a channel, a somewhat different procedure is called for. The record should be sufficiently long to cover ten or a dozen of the bars if the properties of the bars are of interest. However, to investigate the properties of the smaller features, it is suggested that short segments of the longer record be analyzed after trend removal. Methods for removing trends are given in Bendat and Piersol (1966) and Parzen (1967).

Records for Zero and H-Level Crossing Analysis

It has been shown by Tick and Shaman (1966) that the expected number of maximums and minimums of y and the expected number of zero and h-level crossings determined from the discrete approximation to a continuous Gaussian process in a given length of record is always less than the expected number determined from the continuous record. If the sampling interval h is selected such that $4h \leq L_{min}$, the estimated number of crossings from the discrete process will be at least 90 percent of the number in the continuous process for any level h within two standard deviations of the mean. Therefore, a sampling rate at least twice that recommended for spectral analysis is required for determining the average number of zero or h-level crossings.

Much longer records are required to determine the probability distributions of maximum and minimum y values between zero crossings, of the lengths between zero crossings, and of the durations of the positive excursions of y above the level h, than are required for the spectral analysis. The writer recommends at least one hundred observations of these values to obtain reasonable estimates of the distributions. As a rule of thumb, the records should be ten times as long as the records for spectral analysis, and if consideration is to be given to h-level crossings at levels beyond one and one-half times the standard deviation from the mean, for ripples or dunes, the record should be of the order of 300 times the mean

ripple or dune length. Because the ripples and dunes are not symmetric about the mean bed elevation, and because the y values are not strictly Gaussian in distribution, no hard and fast rules can be established for the record lengths to determine the distributions of the h-level crossings. The probability distributions of maximum and minimum y values between zero crossings, Figures 15-17 of the text, are the logical starting place to estimate record length requirements for a given number of observations of these extreme events.

REFERENCES FOR APPENDIX III

Bendat, J. S., and Piersol, A. G., 1966, Measurement and analysis of random data: John Wiley and Sons, Inc., New York, 390 p.

Parzen, E., 1967, Time series analysis papers: Holden-Day, San Francisco, 565 p.

Simons, D. B., and Richardson, E. V., 1966, Resistance to flow in alluvial channels: U.S. Geol. Survey Prof. Paper 422-J, 61 p.

Tick, L. J., and Shaman, P., 1966, Sampling rates and appearance of stationary Gaussian processes: Technometrics, V. 8, No. 1, p. 91-106.